

EFFECT OF FUEL PROPERTIES ON SPRAY CHARACTERISTICS AND
INJECTION BEHAVIOUR OF GTL-DIESEL FUEL BLENDS



A THESIS SUBMITTED IN PARTIAL FULFILLMENT
OF THE REQUIREMENT FOR THE DEGREE OF
MASTERS OF ENGINEERING IN AUTOMOTIVE ENGINEERING
(INTERNATIONAL PROGRAM)
INTERNATIONAL COLLEGE
KING MONGKUT'S INSTITUTE OF TECHNOLOGY LADKRABANG
2015

This material is reserved for educational use only, not allowed for commercial use.

KMITL-2015-IC-M-004-01

Forbidden to modify the content, and cite the document when use.



COPYRIGHT 2015

INTERNATIONAL COLLEGE

THE KING MONGKUT'S INSTITUTE OF TECHNOLOGY LADKRABANG commercial use.

NATIONAL SCIENCE AND TECHNOLOGY DEVELOPMENT AGENCY use.

THESIS TITLE	EFFECT OF FUEL PROPERTIES ON SPRAY CHARACTERISTICS AND INJECTION BEHAVIOUR OF GTL-DIESEL FUEL BLENDS
STUDENT	MR. SANTOSH PAUDEL
STUDENT ID	55600908
DEGREE	MASTER OF ENGINEERING
PROGRAM	AUTOMOTIVE ENGINEERING
YEAR	2015
THESIS ADVISOR	ASST. PROF DR. CHINDA CHAROENPHONPHANICH DR. PEERAWAT SAISIRIRAT PROF. DR. HIDENORI KOSAKA

ABSTRACT

With higher thermal efficiency, diesel engine has been considered in recent development of engine technology. On the related note, recent advanced fuel technology, e.g. Gas-To-Liquid (GTL) and Bio-Hydrogenated Diesel (BHD), has further unlocked performance potential while maintaining stringent emission regulation. To understand fundamental of the diesel fuel injection characteristics, the current study focuses on the effect of fuel properties on fuel injection in the common rail system. In this research GTL is blended with commercial diesel at the ratio of 20% (GTL 20), 40% (GTL40), 60% (GTL60) and 80% (GTL 80) of GTL fraction by weight and relevant physical and chemical properties were measured and compared. For each fuel blend along with neat GTL (GTL 100) and commercial diesel, Zeuch injection method has been used to study injection characteristics. In addition, a constant volume, high pressure chamber is chosen to study spray evolution at selected ambient conditions. A 2nd generation common rail, single cylindrical hole solenoid injector has been used throughout the investigation. The injection characteristic was investigated in terms of fuel mass flow rate, discharge coefficient and injection delay. Furthermore, spray characteristics were investigated in terms of spray tip penetration, spray cone angle and spray velocity. The injection pressure, energizing time for the injector and ambient pressure has been chosen to match modern commercial diesel vehicle operation.

However, the effect of multiple injection has not been included in this study. The goal of this research is to achieve a better understanding on how fuel properties effect on fuel injection characteristics of diesel engine.



This material is reserved for educational use only, not allowed for commercial use.

Forbidden to modify the content, and cite the document when use.

ACKNOWLEDGEMENTS

I feel utmost privileged to be guided by my advisor Assistant Professor Dr. Chinda Charoenphonphanich, Department of Mechanical Engineering King Mongkut's Institute of Technology Ladkrabang, co-advisor Dr. Peerawat Saisirirat, National Metal and Material Technology Center (MTEC), National Science and Technology Development Agency (NSTDA), and Professor Dr. Hidenori Kosaka, Department of Mechanical and Aerospace Engineering, Tokyo Institute of Technology, who have supported as well as motivated and encouraged me for my thesis works. Whose proficiency and invaluable suggestions has always been inspiration to me.

I would like to express my deepest thanks and gratitude to Dr. Preechar Karin, International College, KMITL and Dr. Nuwong Chollacoop, Lab head, Renewable energy laboratory, MTEC, who have motivated, provided their invaluable feedback and positive criticism which has led the successful completion of this thesis.

I would like to express my gratitude to Thailand Advanced Institute of Science and Technology, Tokyo Institute of Technology (TAIST-Tokyo Tech) and NSTDA for providing opportunity to study Automotive Engineering with full scholarship support. I would also like to extend my gratitude to MTEC for the financial support and lab facility, and PTT-RTI for GTL fuel. In addition, Combustion and Engine Research Laboratory (CERL), King Mongkut's University of Technology (KMUTT) and automotive lab KMITL for providing the opportunity to use equipment and laboratory facilities during completion of this research.

I also greatly appreciate the efforts put on by Mr. Prathan Srichai and Mr. Ronnachart Munsin in imparting me the knowledge they have gained in years of research and study regarding the fuel injection, spray and combustion. I will forever be in debt of the knowledge they have chosen to share with me.

Last but not the least I am thankful to my parents, my friends and colleagues for their constant motivation, support and for taking their time to discuss on various aspects during my study.

TABLE OF CONTENTS

ABSTRACT	I
ACKNOWLEDGEMENTS	III
TABLE OF CONTENTS	IV
LIST OF TABLES	VII
LIST OF FIGURES	VIII
CHAPTER 1.....	1
INTRODUCTION	1
1.1. Background.....	1
1.2. Objective.....	3
1.3. Scope of work.....	4
CHAPTER 2.....	5
BACKGROUND THEORY AND LITERATURE REVIEW	5
2.1. Diesel engine.....	5
2.2. Fuel injection system.....	6
2.3. Diesel engine combustion.....	8
2.4. Diesel engine characteristics.....	11
2.5. Diesel fuel and alternatives.....	14
2.5.1. Diesel fuel.....	14
2.5.2. Biodiesel.....	15
2.5.3. Synthetic fuel.....	15
2.6. Diesel fuel properties.....	16
2.6.1. Cetane number or cetane index.....	16
2.6.2. Boiling range.....	17
2.6.3. Cold flow properties.....	17
2.6.4. Flash point.....	17
2.6.5. Viscosity.....	18
2.6.6. Density.....	18
2.6.7. Heating value.....	18
2.6.8. Lubricity.....	18
2.6.9. Sulfur content.....	19

This material is reserved for educational use only, not allowed for commercial use.

Forbidden to modify the content, and cite the document when use.

2.7. Literature review	19
CHAPTER 3.....	24
EXPERIMENTAL EQUIPMENTS AND METHODS.....	24
3.1. Fuel properties test	24
3.1.1. Density meter.....	24
3.1.2. Kinematic viscosity measurement	25
3.1.3. Bomb calorimeter	26
3.1.4. CHNS analyzer.....	26
3.1.5. Flash point measurement	27
3.1.6. Cloud point and pour point measurement	28
3.2. Injection behavior analysis.....	28
3.2.1. Test fuels.....	28
3.2.2. Experimental conditions	29
3.2.3. Experimental setup.....	30
3.2.4. Data acquisition	31
3.2.5. Bulk modulus and Zeuch method	31
3.2.6. Injection characteristics analysis.....	32
3.3. Spray analysis.....	33
3.3.1. Experimental setup.....	34
3.3.2. Schlieren photography setup.....	35
3.3.3. Spray image analysis.....	36
CHAPTER 4.....	39
RESULTS AND DISCUSSION.....	39
4.1. Fuel properties results.....	39
4.1.1. Effects on density.....	39
4.1.2. Effect on heating value	40
4.1.3. Effect on viscosity.....	41
4.1.4. Effect on H-C ratio.....	43
4.1.5. Effect on bulk modulus	43
4.2. Injection characteristics.....	44
4.2.1. Injection rate profiles.....	44
4.2.2. Injection delay time.....	52

4.2.3. Fuel injection quantity (mass)	53
4.2.4. Coefficient of discharge.....	55
4.3. Spray analysis.....	56
4.3.1. Spray penetration.....	57
4.3.2. Spray angle	64
4.3.3. Spray velocity.....	70
4.3.4. Spray volume	76
4.4. Effect of GTL-Diesel fuel blends on Diesel combustion.....	78
CHAPTER 5.....	81
CONCLUSIONS.....	81
5.1. Conclusions	81
5.2. Recommendation for further work.....	82
REFERENCES	83
APPENDICES.....	88
Appendix-A. Standard required for diesel fuel oils.....	89
A.1 Requirements for Diesel Fuel Oils (ASTM D 975-97).....	89
A.2 Requirements for Diesel Fuel Oils (EN 590).....	90
Appendix-B. Specifications of measurement devices used.....	91
B.1 Dynamic pressure sensor.....	91
B.2 Static pressure sensor	92
B.3 High speed video camera.....	93
Appendix-C. Detail of control program/mechanism.....	95
C.1 Injector energizing and camera actuating.....	95
C.2 Injection pressure controlling.....	97
Appendix-D Proceedings.....	99
D.1 Burapha university international conference 2014.....	99
D.2 International conference on science, technology and innovation for sustainable well-being.....	107
BIOGRAPHY	115

LIST OF TABLES

Table 1.1 EU emission standards for commercial vehicles (diesel engine)	2
Table 3.1 Experimental test condition	29
Table 3.2 Fuel properties for spray analysis	34
Table 3.3 Experimental condition for spray analysis	34
Table 4.1 Fuel properties result for neat fuels	39



LIST OF FIGURES

Figure 1.1 Global petroleum (diesel and gasoline) demand	1
Figure 2.1 The p-V diagrams of two stroke and four stroke diesel engine	5
Figure 2.2: Operating concept of common rail injection system	8
Figure 2.3: Direct injection combustion chamber, air distributed, wall distributed.....	9
Figure 2.4: Indirect injection combustion chamber, a) pre chamber b) whirl chamber	9
Figure 2.5: Block diagram of diesel combustion (adapted from	10
Figure 2.6: Diesel engine characteristics	11
Figure 3.1 Density Meter DMA 4500.....	24
Figure 3.2 Viscometer.....	25
Figure 3.3 Bomb Calorimeter	26
Figure 3.4 CHN analyzer	27
Figure 3.5 Flash point measuring device	27
Figure 3.6 Cloud and pour point measuring device	28
Figure 3.7 Test fuels.....	29
Figure 3.8 Schematic diagram of experimental setup for injection analysis.....	30
Figure 3.9 Data acquisition (oscilloscope traces)	31
Figure 3.10 Schematic diagram for bulk modulus measurement.....	32
Figure 3.11 Definition of injection quantity and injection delay time	33
Figure 3.12 Schematic of experimental setup.....	35
Figure 3.13 Schematic of spray image capturing technique	36
Figure 3.14 Procedure involved in spray measurement.....	37
Figure 3.15 Definition of spray penetration and spray angle	38
Figure 4.1 Fuel type vs density.....	40
Figure 4.2 Fuel type vs heating value (a) by weight (b) by volume.....	41
Figure 4.3 Fuel type vs viscosity (a)kinematic (b) dynamic.....	42
Figure 4.5 Fuel type vs H/C ratio.....	43
Figure 4.6 Bulk modulus of test fuels at 45 bar.....	44
Figure 4.7 Injection rate profile at $P_i = 400$ bar, $T_e = 0.5$ ms, and $P_b = 45$ bar.....	45
Figure 4.8 Injection rate profile at $P_i = 800$ bar, $T_e = 0.5$ ms, and $P_b = 45$ bar.....	45
Figure 4.9 Injection rate profile at $P_i = 1200$ bar, $T_e = 0.5$ ms, and $P_b = 45$ bar.....	46

This material is reserved for educational use only, not allowed for commercial use.

Forbidden to modify the content, and cite the document when use.

Figure 4.10 Injection rate profile at $P_i = 1600$ bar, $T_e = 0.5$ ms, and $P_b = 45$ bar	46
Figure 4.11 Injection rate profile at $P_i = 400$ bar, $T_e = 1.0$ ms, and $P_b = 45$ bar.....	47
Figure 4.12 Injection rate profile at $P_i = 800$ bar, $T_e = 1.0$ ms, and $P_b = 45$ bar.....	48
Figure 4.13 Injection rate profile at $P_i = 1200$ bar, $T_e = 1.0$ ms, and $P_b = 45$ bar	48
Figure 4.14 Injection rate profile at $P_i = 1600$ bar, $T_e = 1.0$ ms, and $P_b = 45$ bar	49
Figure 4.15 Injection rate profile at $P_i = 400$ bar, $T_e = 2.5$ ms, and $P_b = 45$ bar.....	50
Figure 4.16 Injection rate profile at $P_i = 800$ bar, $T_e = 2.5$ ms, and $P_b = 45$ bar.....	50
Figure 4.17 Injection rate profile at $P_i = 1200$ bar, $T_e = 2.5$ ms, and $P_b = 45$ bar	51
Figure 4.18 Injection rate profile at $P_i = 1200$ bar, $T_e = 2.5$ ms, and $P_b = 45$ bar	51
Figure 4.19 Injection delay for set of test fuels at different injection pressure	52
Figure 4.20 Amount of fuel injection with different injection pressure at $T_e = 0.5$ ms	53
Figure 4.21 Amount of fuel injection with different injection pressure at $T_e = 1.0$ ms	54
Figure 4.22 Amount of fuel injection with different injection pressure at $T_e = 2.5$ ms	54
Figure 4.23 Coefficient of discharge vs GTL fraction.....	55
Fig.4.24 Spray images of GTL and diesel at different test condition	56
Figure 4.25 Spray penetration at $P_b = 19$ bar, $P_i = 800$ bar, and $T_e = 0.5$ ms.....	58
Figure 4.26 Spray penetration at $P_b = 19$ bar, $P_i = 1200$ bar, and $T_e = 0.5$ ms	58
Figure 4.27 Spray penetration at $P_b = 19$ bar, $P_i = 800$ bar, and $T_e = 1.0$ ms.....	59
Figure 4.28 Spray penetration at $P_b = 19$ bar, $P_i = 1200$ bar, and $T_e = 1.0$ ms.....	59
Figure 4.29 Spray penetration at $P_b = 45$ bar, $P_i = 400$ bar, and $T_e = 0.5$ ms.....	61
Figure 4.30 Spray penetration at $P_b = 45$ bar, $P_i = 800$ bar, and $T_e = 0.5$ ms.....	61
Figure 4.31 Spray penetration at $P_b = 45$ bar, $P_i = 1200$ bar, and $T_e = 0.5$ ms.....	62
Figure 4.32 Spray penetration at $P_b = 45$ bar, $P_i = 400$ bar, and $T_e = 1$ ms.....	62
Figure 4.33 Spray penetration at $P_b = 45$ bar, $P_i = 800$ bar, and $T_e = 1$ ms.....	63
Figure 4.34 Spray penetration at $P_b = 45$ bar, $P_i = 1200$ bar, and $T_e = 1$ ms.....	63
Figure 4.35 Spray penetration at $P_b = 45$ bar, $P_i = 1600$ bar, and $T_e = 1$ ms.....	64
Figure 4.36 Spray angle at $P_b = 19$ bar, $P_i = 800$ bar, and $T_e = 0.5$ ms	65
Figure 4.37 Spray angle at $P_b = 19$ bar, $P_i = 1200$ bar, and $T_e = 0.5$ ms	65
Figure 4.38 Spray angle at $P_b = 19$ bar, $P_i = 800$ bar, and $T_e = 1.0$ ms	66
Figure 4.39 Spray angle at $P_b = 19$ bar, $P_i = 1200$ bar, and $T_e = 1.0$ ms	66
Figure 4.40 Spray angle at $P_b = 45$ bar, $P_i = 400$ bar, and $T_e = 0.5$ ms	67
Figure 4.41 Spray angle at $P_b = 45$ bar, $P_i = 800$ bar, and $T_e = 0.5$ ms	67

Figure 4.42 Spray angle at $P_b = 45$ bar, $P_i = 1200$ bar, and $T_e = 0.5$ ms	68
Figure 4.43 Spray angle at $P_b = 45$ bar, $P_i = 400$ bar, and $T_e = 1.0$ ms	68
Figure 4.44 Spray angle at $P_b = 45$ bar, $P_i = 800$ bar, and $T_e = 1.0$ ms	69
Figure 4.45 Spray angle at $P_b = 45$ bar, $P_i = 1200$ bar, and $T_e = 1.0$ ms	69
Figure 4.46 Spray angle at $P_b = 45$ bar, $P_i = 1600$ bar, and $T_e = 1.0$ ms	70
Figure 4.47 Spray velocity at $P_b = 19$ bar, $P_i = 800$ bar, and $T_e = 0.5$ ms.....	71
Figure 4.48 Spray velocity at $P_b = 19$ bar, $P_i = 1200$ bar, and $T_e = 0.5$ ms.....	71
Figure 4.49 Spray velocity at $P_b = 19$ bar, $P_i = 800$ bar, and $T_e = 1.0$ ms.....	72
Figure 4.50 Spray velocity at $P_b = 19$ bar, $P_i = 1200$ bar, and $T_e = 1.0$ ms.....	72
Figure 4.51 Spray velocity at $P_b = 45$ bar, $P_i = 400$ bar, and $T_e = 0.5$ ms.....	73
Figure 4.52 Spray velocity at $P_b = 45$ bar, $P_i = 800$ bar, and $T_e = 0.5$ ms.....	73
Figure 4.53 Spray velocity at $P_b = 45$ bar, $P_i = 1200$ bar, and $T_e = 0.5$ ms.....	74
Figure 4.54 Spray velocity at $P_b = 45$ bar, $P_i = 400$ bar, and $T_e = 1.0$ ms.....	74
Figure 4.55 Spray velocity at $P_b = 45$ bar, $P_i = 800$ bar, and $T_e = 1.0$ ms.....	75
Figure 4.56 Spray velocity at $P_b = 45$ bar, $P_i = 1200$ bar, and $T_e = 1.0$ ms.....	75
Figure 4.57 Spray velocity at $P_b = 45$ bar, $P_i = 1600$ bar, and $T_e = 1.0$ ms.....	76
Figure 4.58 Spray volume at $P_b = 45$ bar, $P_i = 400$ bar, and $T_e = 1.0$ ms	77
Figure 4.59 Spray volume at $P_b = 45$ bar, $P_i = 800$ bar, and $T_e = 1.0$ ms	77
Figure 4.60 Spray volume at $P_b = 45$ bar, $P_i = 1200$ bar, and $T_e = 1.0$ ms	78
Figure 4.61 Spray volume at $P_b = 45$ bar, $P_i = 1600$ bar, and $T_e = 1.0$ ms	78
Figure A.1 Schematic of injector energizing and camera actuating mechanism.....	95
Figure A.2 Injector energizing and video capturing duration	96
Figure A.3 Injection pressure control mechanism.....	98

CHAPTER 1

INTRODUCTION

1.1. Background

Diesel engine is being used widely for power generation industrial and transport for a century. The unique combination of energy efficiency, power, reliability and durability, diesel technology plays a vital role in important sector of world economy. Due to these key factors, it is estimated that diesel engine will dominate for several coming decades in power generation and transportation sector. Conversely, it has been predicted that there will be no longer available of fossil fuel to meet market demand as the demand rate is going higher day by day. The Figure 1.1 shows the increasing demand of gasoline and diesel in the global market. However, it can be clearly seen that projected diesel fuel demand is almost 1.5 times of its counterpart gasoline fuel.

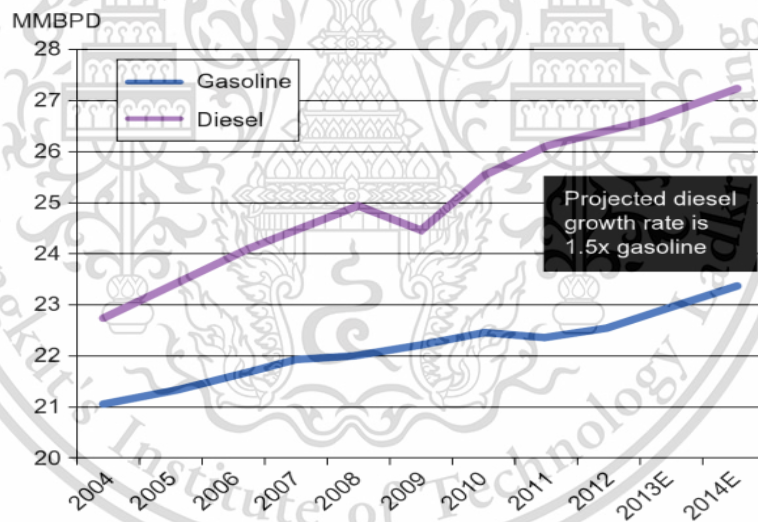


Figure 1.1 Global petroleum (diesel and gasoline) demand [1]

Since the availability of fossil oil and gas is finite, both the primary energy sources and the fuel types will have to be diversified over time. Therefore, advancement in the field of fuel technologies is necessary. In recent days many researchers focus on alternative fuels to fulfill the probable scarcity of fossil fuels. Throughout the time, three alternative fuel pathways have achieved some success in the market place, these include the renewable, ethanol and biodiesel, and GTL (gas to liquid). In some scenario ethanol and biodiesel can offer reasonable total energy

This material is reserved for educational use only, not allowed for commercial use.

Forbidden to modify the content, and cite the document when use.

balance and excellent greenhouse gas emission benefit. However, GTL is of interest because it offers a significant financial return for energy companies as a means to monetize their stranded natural gas reserves.

Table 1.1 EU emission standards for commercial vehicles (diesel engine) [2]

Category†	Stage	Date	CO	HC	HC+NOx	NOx	PM	PN
			g/km					
N ₁ , Class I ≤1305 kg	Euro 1	1994.1	2.72	-	0.97	-	0.14	-
	Euro 2 IDI	1998	1	-	0.7	-	0.08	-
	Euro 2 DI	1998.01 ^a	1	-	0.9	-	0.1	-
	Euro 3	2000	0.64	-	0.56	0.5	0.05	-
	Euro 4	2005	0.5	-	0.3	0.25	0.025	-
	Euro 5a	2009.09 ^b	0.5	-	0.23	0.18	0.005 ^f	-
	Euro 5b	2011.09 ^d	0.5	-	0.23	0.18	0.005 ^f	6.0×10 ¹¹
Euro 6	2014.1	0.5	-	0.17	0.08	0.005 ^f	6.0×10 ¹¹	
N ₁ , Class II 1305-1760 kg	Euro 1	1994.1	5.17	-	1.4	-	0.19	-
	Euro 2 IDI	1998	1.25	-	1	-	0.12	-
	Euro 2 DI	1998.01 ^a	1.25	-	1.3	-	0.14	-
	Euro 3	2001	0.8	-	0.72	0.65	0.07	-
	Euro 4	2006	0.63	-	0.39	0.33	0.04	-
	Euro 5a	2010.09 ^c	0.63	-	0.295	0.235	0.005 ^f	-
	Euro 5b	2011.09 ^d	0.63	-	0.295	0.235	0.005 ^f	6.0×10 ¹¹
Euro 6	2015.1	0.63	-	0.195	0.105	0.005 ^f	6.0×10 ¹¹	
N ₁ , Class III >1760 kg	Euro 1	1994.1	6.9	-	1.7	-	0.25	-
	Euro 2 IDI	1998	1.5	-	1.2	-	0.17	-
	Euro 2 DI	1998.01 ^a	1.5	-	1.6	-	0.2	-
	Euro 3	2001	0.95	-	0.86	0.78	0.1	-
	Euro 4	2006	0.74	-	0.46	0.39	0.06	-
	Euro 5a	2010.09 ^c	0.74	-	0.35	0.28	0.005 ^f	-
	Euro 5b	2011.09 ^d	0.74	-	0.35	0.28	0.005 ^f	6.0×10 ¹¹
Euro 6	2015.1	0.74	-	0.215	0.125	0.005 ^f	6.0×10 ¹¹	
N ₂	Euro 5a	2010.09 ^c	0.74	-	0.35	0.28	0.005 ^f	-
	Euro 5b	2011.09 ^d	0.74	-	0.35	0.28	0.005 ^f	6.0×10 ¹¹
	Euro 6	2015.1	0.74	-	0.215	0.125	0.005 ^f	6.0×10 ¹¹

† For Euro 1/2 the Category N₁ reference mass classes were Class I ≤ 1250 kg, Class II 1250-1700 kg, Class III > 1700 kg

a. until 1999.09.30 (after that date DI engines must meet the IDI limits)

b. 2011.01 for all models

c. 2012.01 for all models

d. 2013.01 for all models

e. applicable only to vehicles using DI engines

f. 0.0045 g/km using the PMP measurement procedure

On the contrary, internal combustion engines contribute significantly to air pollution, which has an acute impact on human health and environment. The

environmental benefit of diesels, such as reduction of low greenhouse gas emission, can be indicated above its counterpart, however the emission of nitrogen oxide and particulate matters grow more concerns about diesel emission. Concurrently, the emission regulation is being stricter worldwide. Table 1.1 summarizes the European Union emission standard for light commercial vehicle equipped with diesel engine.

Nowadays, many researches are mainly focusing on developing a fuel technology to minimize fuel consumption, get maximum performance and which could perform within the stringent combustion policy. The high thermal efficiency, low fuel consumption and no need to modify the physical structure of the diesel engine for using GTL as a fuel, it becomes attractive topic of interest for researcher to develop new fuel technology.

To reduce the exhaust emissions, it is necessary to understand fuel injection characteristics, which play a great role in diesel combustion. To improve further engine efficiency and reduce the environmental impacts of diesel combustion, the operation of the direct injection system is crucial [3].

Many involved processes, e.g. the fuel metering accuracy, the rate of fuel introduction into the combustion chamber, the consequence of spray evolution, fuel atomization and mixing with surrounding air, determines the combustion development and hence the engine performance with its limited pollutants [4].

In addition, the fuel spray plays a very important role in the diesel engine process since it is concerned with fuel atomization, air-fuel mixing, ignition process, combustion and consequent emissions [5]. The physical and chemical properties of fuel such as density, viscosity, surface tension, heating value, distillation temperature affect fuel injection process and spray characteristics in the diesel engine. Moreover, the injector geometry, injection pressure, injection duration and opening principle of injector are also the major components affecting fuel injection phenomena [6]. GTL fuel has different fuel properties as compared to conventional diesel fuel. Thus, it is important to study injection behavior and spray characteristics of the GTL fuel.

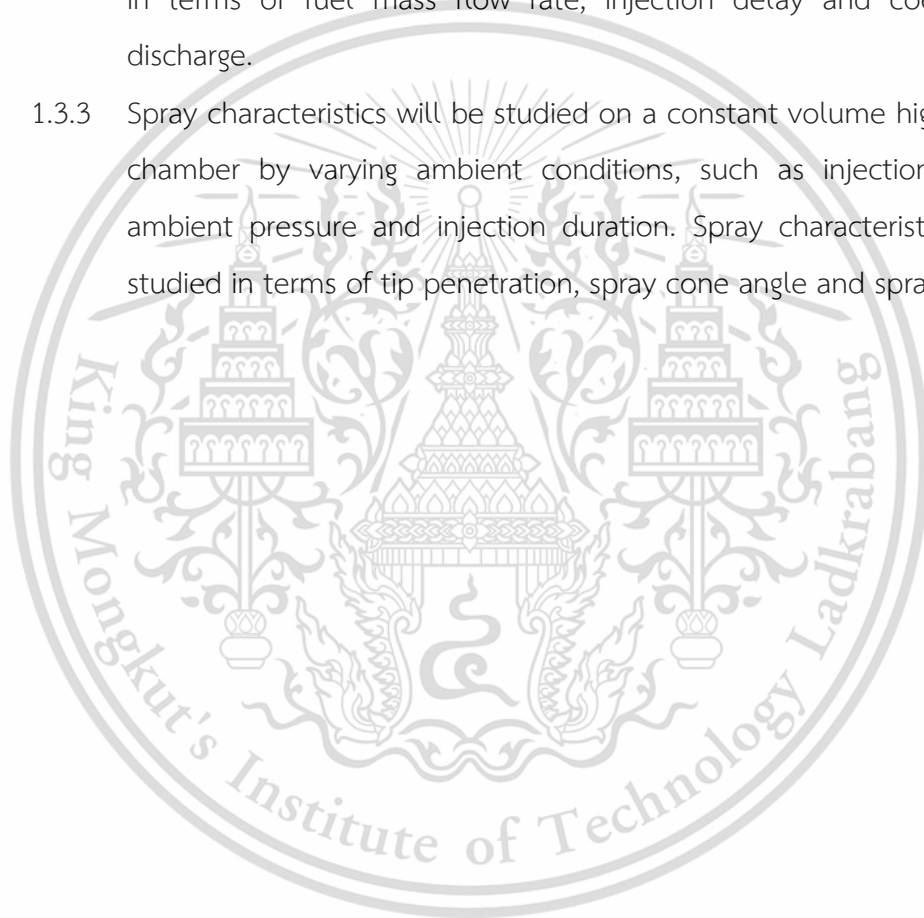
1.2. Objective

The objective of this thesis is to fundamentally understand how fuel properties effects on diesel fuel injection characteristics and comparative study on injection

characteristics and spray characteristics of different test fuels (GTL-diesel fuel blends) with various fuel properties.

1.3. Scope of work

- 1.3.1 Fuel matrix will be chosen by blending GTL with commercial diesel and physical/chemical fuel properties will be measured for individual mixed fuel.
- 1.3.2 Injection characteristics will be studied using Zeuch injection rate method in terms of fuel mass flow rate, injection delay and coefficient of discharge.
- 1.3.3 Spray characteristics will be studied on a constant volume high pressure chamber by varying ambient conditions, such as injection pressure, ambient pressure and injection duration. Spray characteristics will be studied in terms of tip penetration, spray cone angle and spray velocity.



CHAPTER 2

BACKGROUND THEORY AND LITERATURE REVIEW

2.1. Diesel engine

Diesel engine is a compression ignition engine of a two or four stroke type. Figure 2.1 represents p-V diagrams of two and four stroke diesel engine. From Figure 2.1, it can be seen that the duration of the whole diesel cycle is 360°CA for a two stroke engine and 720°CA for the four stroke engine. However, in automotive application, diesel engines are practically always of the four stroke type [7]. The whole cycle consists of, intake of air, compression of air, fuel injection, mixture formation, ignition, combustion, expansion and exhaust. The intake phase begins with the intake valve opening and lasts till the intake valve closing. After that the intake air is compressed to a level corresponding to compression ratios from 12:1 to 24:1 [4], depending on the type of diesel engine and whether the engine is naturally aspirated or turbocharged. The compression ratio is the geometrical quantity which represents the ratio of the volume of its combustion chamber from its largest capacity to its smallest capacity. Mathematically it can be defined as in Equation 2.1.

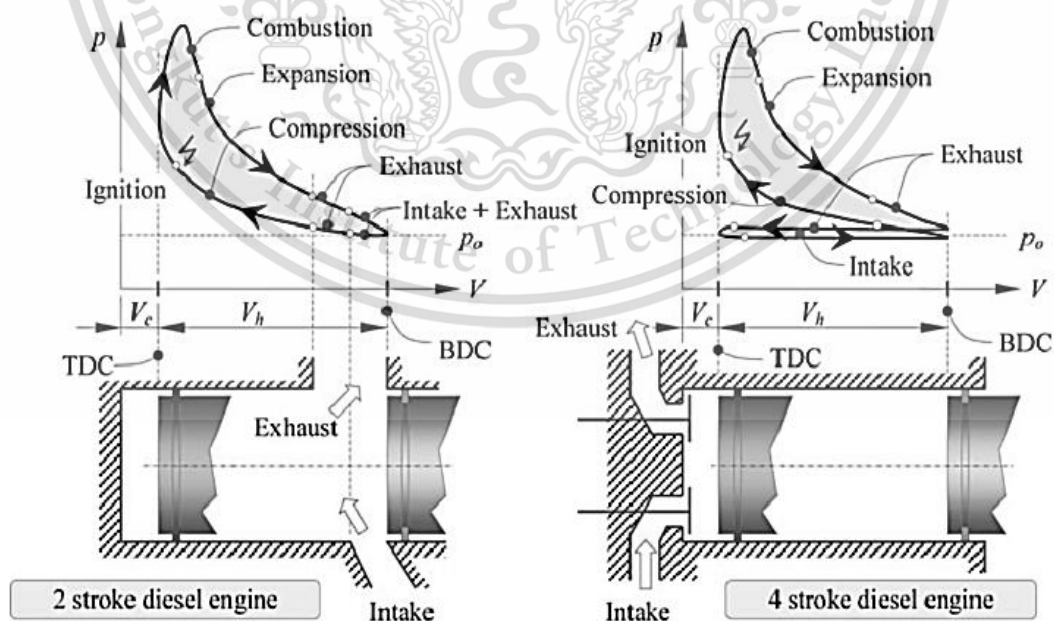


Figure 2.1 The p-V diagrams of two stroke and four stroke diesel engine [8]

This material is reserved for educational use only, not allowed for commercial use.

Forbidden to modify the content, and cite the document when use.

$$CR = \frac{V_{max}}{V_{min}} = \frac{V_s + V_c}{V_c} \dots\dots\dots 2.1$$

where V_{max} and V_{min} represent maximum and minimum volume above the piston, V_c is the clearance volume, and V_s is the swept volume.

During the compression stroke, at about 20° before top dead center fuel is injected in to the combustion chamber under high pressure as much as 4 MPa and temperature about 800 K [4]. The fuel in the spray mixes with the compressed hot air, evaporates, and then the mixture ignites by itself. It has to be pointed out that injection, atomization, spray development mixture formation, ignition, combustion, and emission formation processes occurs simultaneously and interact with each other. During the combustion process heat is released and both the in-cylinder pressure and the in-cylinder temperature increase further. At the end of expansion phase, the exhaust valve opens and the exhaust phase begins. Thus after exhaust phase, the whole cycle end as the exhaust valve closes.

2.2. Fuel injection system

Fuel injection into the cylinder is realized by the fuel injection system. The system is responsible for supplying the engine with fuel at the correct time and with the correct amount. Which is controlled either an electronically or mechanically. The main purpose of the system is to deliver fuel to the cylinders of a diesel engine, it is how that fuel is delivered that makes the difference in engine performance, emissions, and noise characteristics. The performance of diesel engines is heavily influenced by their injection system.

The diesel fuel injection system mainly consists of an injection pump, delivery pipes, fuel injector and nozzles. With a few exceptions, fuel system components can be divided in to two major component groups namely: low pressure side components and high pressure side components. Low pressure side components include the fuel tank, fuel supply pump and fuel filter while high pressure side components include the high pressure pump, fuel injector, fuel injection nozzle and delivery pipes from high pressure pump up to fuel injector.

The injection pump generates the pressure required for fuel injection, the pressurized fuel flows through the high pressure tube to the injector, injection nozzle

which then injects it into the combustion chamber. Different kinds of fuel systems are available today which can be grouped as follows: inline pumps, distribution pumps, unit injectors and common rail injection system.

In 1927 Bosch started to produce the first inline fuel injection pump, a large number of diesel engine kept in motion with those pumps [7]. We can find these classical diesel fuel injection technology still in use, but almost all of the present passenger cars with DI-diesel engines are exclusively equipped with the distributor pump, the unit injector and the common rail injection systems.

There are two different types of distributor pumps are available: axial piston and radial piston types. Both of them consists single plunger and barrel assembly for all the engine's cylinders. Distributor pumps are equipped with either mechanical governor or an electronic control with integrated timing device which allows a variable injection timing. A great advantage of these injection systems is their proven technology but, even though the latest models are equipped with electronic control that offer a higher flexibility, this technology doesn't permit the implementation of all the modern injection strategy.

In the unit injector system, the injection pump and injection nozzle form a single unit. One of these unit is installed in the engine's cylinder head for each engine cylinder and is driven directly by a tappet or indirectly from the engine's camshaft through a valve lifter. Compared to the inline and distributor injection pumps a considerably higher injection pressure is possible due to omission of the high pressure lines. Such high injection pressures coupled with the electronic map based control of the duration of injection including the shape of the injection rate profile permitted a considerable reduction of the diesel engine's toxic emission [9]. Electronic control concepts add a variety of additional functions, but due to the inherent design limitations unit injector systems will always be less flexible than common rail systems.

Common rail system is widely used most of recent DI engines. Common rail offers number of advantages, the fundamental differences compared to cam controlled injection system is its high flexibility in terms of injection timing, and the injection pressure is independent of the engine speed.

Today common rail has become the most commonly used fuel-injection system for modern, high-revolution passenger-car direct injection engines. The key

components of the common-rail system are the injectors. They are fitted with a rapid-action valve (solenoid valve or piezo-triggered actuator) which opens and closes the nozzle. This permits control of the injection process for each cylinder.

All the injectors are fed by a common fuel rail, this being the origin of the term “common rail”. The Figure 2.2 shows the basic operating concept of common rail injection system in which high pressure pump pressurizes the fuel in fuel rail and each injector are individually connected to the rail and controlled by electronic control unit independently. The electronic control unit gets signal from various sensor fitted in the engine and provides accurate signal to the injector to compile with engine running condition.

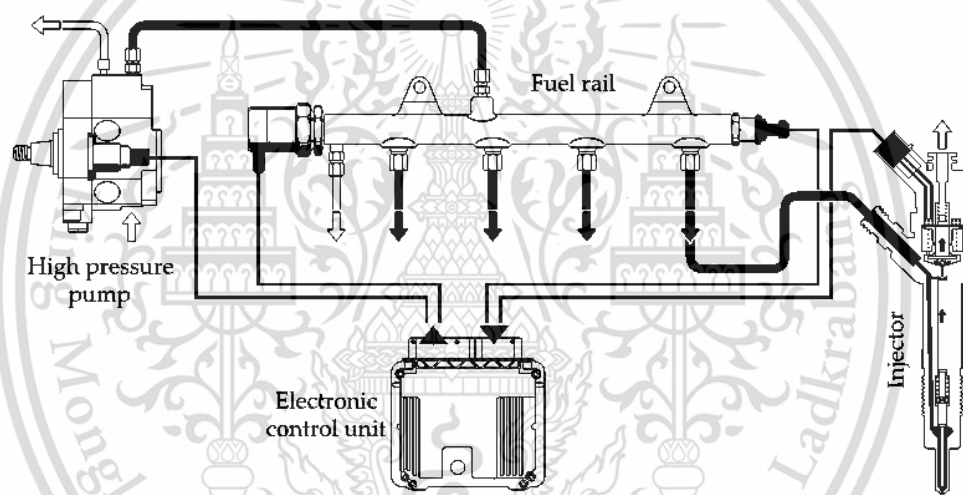


Figure 2.2 Operating concept of common rail injection system

2.3. Diesel engine combustion

Combustion in diesel engines is very complex and its detailed mechanisms are not well understood yet. However, the main objective of combustion is to release the chemical energy stored in the fuel. To perform this process, oxygen must be made available to the fuel in specific manner to facilitate combustion. Mixing of fuel and air which often termed as mixture preparation, is the most important aspect of diesel combustion. Hence the shape of the combustion chamber is one of the determining factor for combustion quality and therefore the performance and exhaust emission characteristics of diesel engine. The diesel engine combustion chamber is categorized in two types namely, direct injection and indirect injection. Direct injection system is

This material is reserved for educational use only, not allowed for commercial use.

further divided into two types based on its fuel injection methods, air distributed method and wall distributed method. Figure 2.3 shows the sectional view of two types of direct combustion chamber.

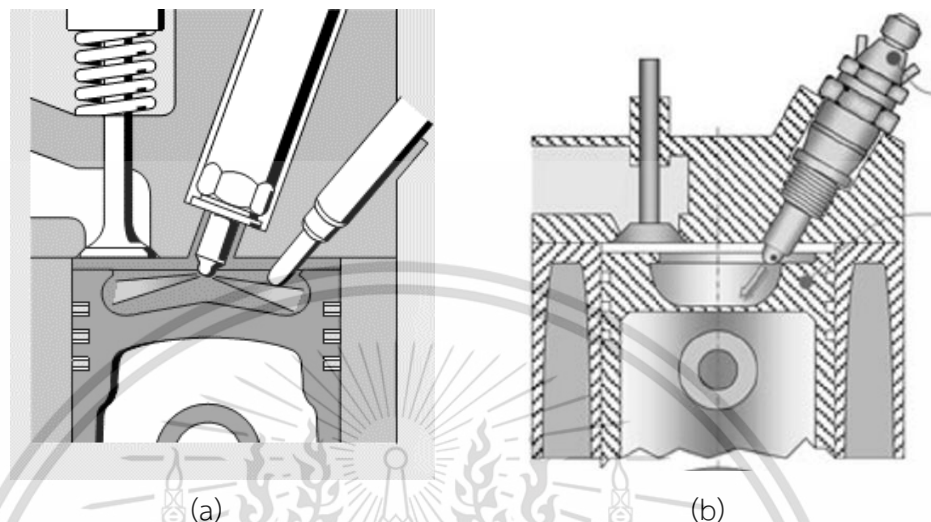


Figure 2.3 Direct injection combustion chamber, (a) air distributed (b) wall distributed

Similarly, indirect injection system is also divided into two types based on the construction and operation of its chambers, pre-chamber system and whirl chamber system. Figure 2.4 shows sectional view of two types of indirect injection combustion chamber.

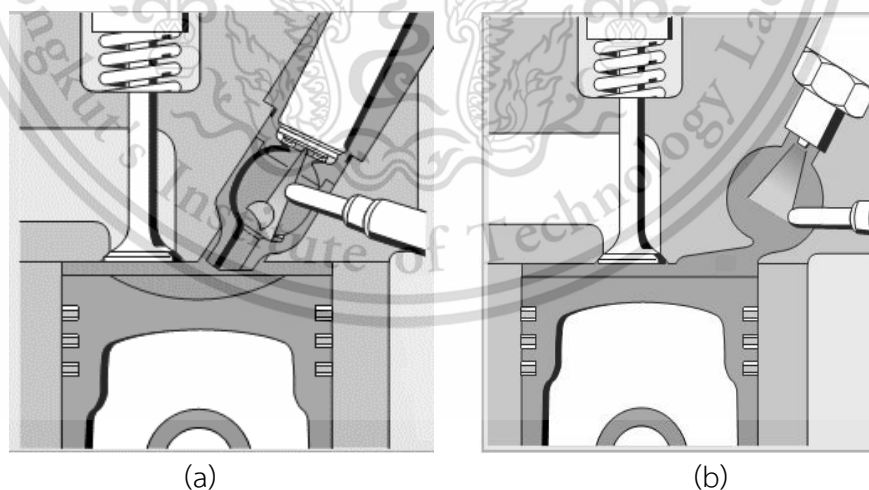


Figure 2.4 Indirect injection combustion chamber, a) pre chamber b) whirl chamber

In direct injection process, fuel is injected with high injection pressure directly into the combustion chamber. The atomization, heating, evaporation, and mixture formation of fuel occurs in very rapid succession. However, in case of indirect injection

This material is reserved for educational use only, not allowed for commercial use.

Forbidden to modify the content, and cite the document when use.

systems, the fuel is injected into the pre-chamber or whirl chamber relatively lower injection pressure as compared to direct injection system.

The overall process involved during the conversion of chemical energy of diesel fuel to get thermal energy using the phenomenon of diesel combustion can be summarized as the block diagram below, shown in Figure 2.5. However, this study focuses mainly on three parameters, namely; fuel characteristics, injection characteristics and spray characteristics.

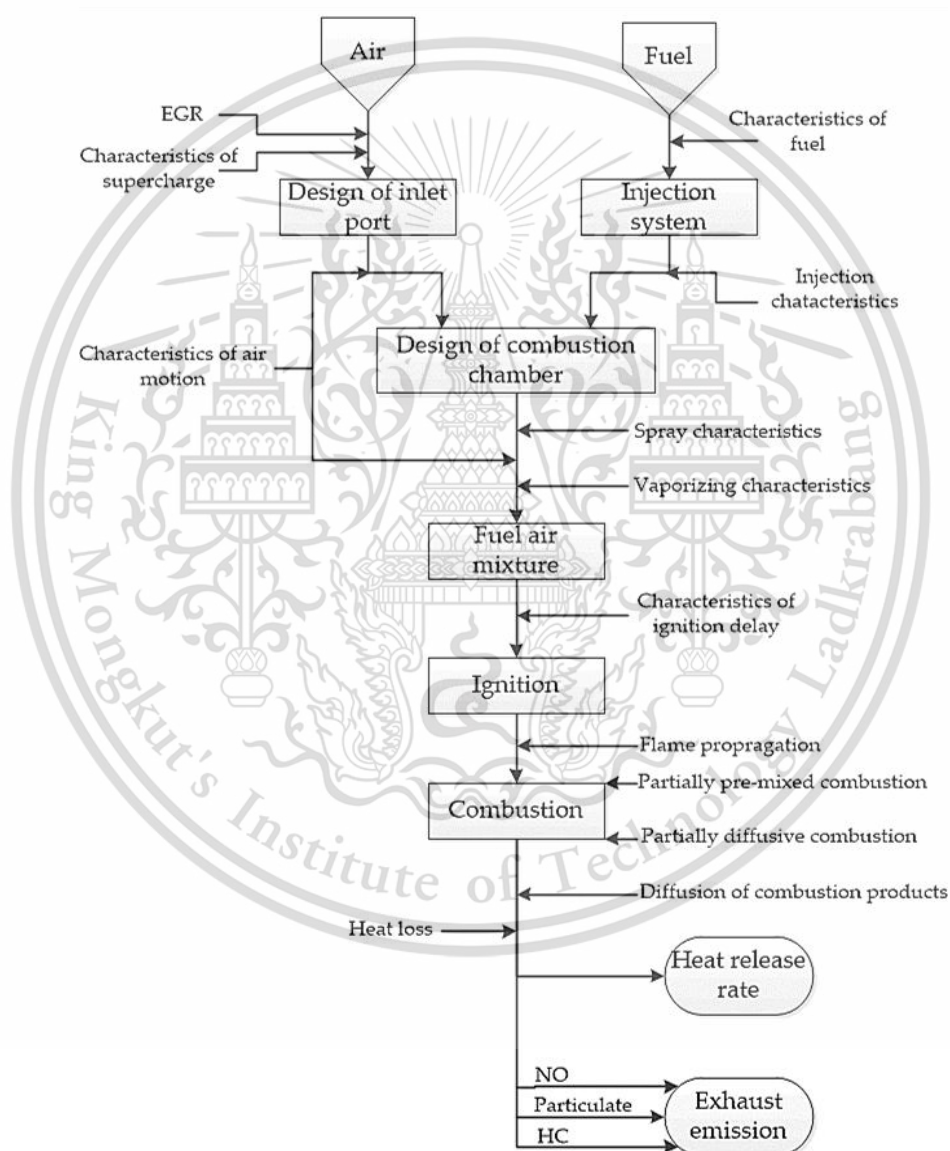


Figure 2.5 Block diagram of diesel combustion (adapted from [10]).

2.4. Diesel engine characteristics

Diesel engine, benefited having a higher thermal efficiency compared to gasoline engine, became more attractive in light duty applications in recent years. Moreover, there is no any substitutions for diesel engine in case of heavy duty applications. Another excellent feature of diesel engine is its operability with variety of different fuels. However, configuration of all diesel engines in practice are manufactured considering diesel fuel derived from crude oil. To develop the new fuel technology compatible for diesel engine it is essential to understand the features of common diesel engine. Those features are defined by its characteristics and are roughly classified into six groups as follows.

- Fuel injection characteristics
- Fuel spray characteristics
- Combustion characteristics
- Engine performance characteristics
- Ecology characteristics
- Economy characteristics

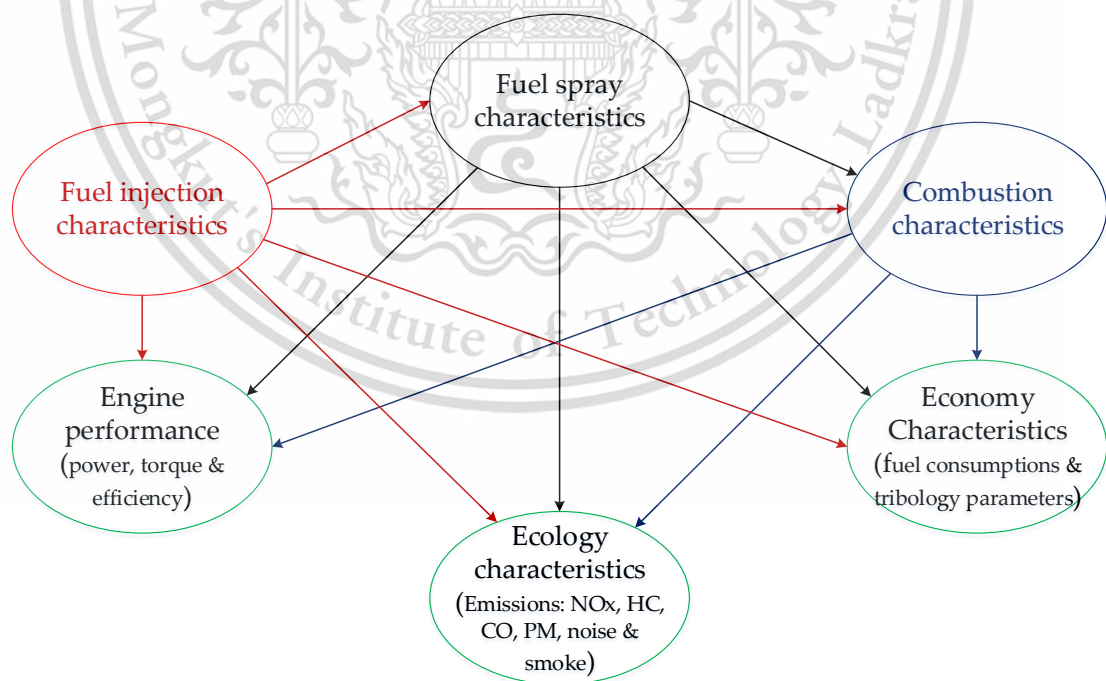


Figure 2.6 Diesel engine characteristics [11].

Figure 2.6 describes the relationship of diesel engine characteristics with each other. It is clearly shown that injection and fuel spray characteristics relates strongly to engine performance, ecology, economy, and tribology characteristics. All these characteristics depend on the most basic parameters such as fuel type or injection system type and on various process characteristics such as the injection process, fuel spray development, atomization, mixture fuel/air formation, ignition and combustion, and so on [12]. The diesel engine characteristics may be influenced by various geometrical and setup parameters either mechanically or electronically controlled fuel injection system.

All the most important injection characteristics like injection pressure, injection timing, injection duration, injection rate, and fueling history, as well as fuel spray characteristics like spray tip penetration, spray angle, and Sauter mean diameter, determine mixture formation, in-cylinder pressure and temperature, self-ignition, and heat release. The engine combustion process is further strongly related to the engine power, torque, emissions, specific fuel consumption, carbon deposits, wear of engine parts, and so on. Unfortunately, the possibilities to control the combustion process directly are quite limited. In a mechanically controlled fuel injection system, even the injection process cannot be controlled directly. However, we can control injection indirectly through the fuel delivery process. For this reason, it is very important to know as good as possible the relationships among all injection, spray, and engine characteristics.

In general, low injection pressure enlarges the fuel droplet diameters and increases the ignition delay period during the combustion. This situation leads to an increase of the in-cylinder pressure, NO_x, and CO emissions. An increase of injection pressure typically improves the atomization at the nozzle outlet, resulting in a more distributed vapor phase, hence resulting in better mixing [13]. When injection pressure is increased, fuel droplet diameters will become smaller and the mixing of the fuel with air during the ignition period improves, which leads to lower smoke level and CO emission. However, if the injection pressure is too high, the ignition delay becomes shorter. This worsens the mixing process and the combustion efficiency decreases. Consequently, smoke levels may rise [14]. It has to be pointed out that the objective should be to increase the mean injection pressure to some reasonable maximum level.

The maximum injection pressure is decisive for the mechanical loading of the fuel injection pump's components and drive. In a mechanically controlled fuel injection system, the injection pressure increases together with increasing engine speed and load. During the injection process, the maximum injection pressure can be more than double of the mean pressure. Therefore, the maximum fuel injection pressure is also limited by the strength of engine materials, wear of various elements of the injection system, and engine system cost.

At higher mean injection pressure the injection duration becomes shorter, if the fueling is kept constant. In order to keep specific fuel consumption, emissions of smoke, unburned HC, and NO_x at acceptable levels, and the injection duration must be adjusted properly to the operating regime and the start of injection. A long injection period, caused by low injection rate, makes poor spray tip penetration. Moreover, if the injection period is too long, it would inevitably produce excessive smoke and particulate emissions. In this case a pilot injection might be of some benefit [15].

The injection timing has a considerable influence on the start of combustion of the air–fuel mixture. In general, if the injection timing is advanced, the in-cylinder temperature increases, thus leading to an increase of NO_x emissions. The retarded injection timing leads to incomplete combustion and to higher unburned HC emissions [16]. Many studies confirm that the injection rate history affects ignition and combustion characteristics and the temporal history of smoke and NO_x formation in direct injection diesel engines [15, 17, 18]. Fuel injection quantity should be controlled by engine parameters such as engine speed, load, and air motion in the combustion chamber. In general, the fuel amount at the beginning of injection should be relatively small. After that it should be increased as the piston reaches the TDC and decreased after TDC to prevent too rapid increase of the combustion pressure. Therefore, injection rate modulation devices are being developed mainly to reduce this high initial heat release rate. A modulation device limits the fuel injected during the ignition delay period by a separated pilot injection, prior to the main injection, or by initial injection rate control. If the initial rate of injection is much lower during the main injection, less fuel is injected and mixed by the time the first element of fuel has evaporated to form a suitable mixture and auto-ignition occurs. Hence the initial heat release rate is low and consequently the combustion noise level is reduced. The main injection follows

with most of the fuel injected. Ideally, the degree of separation between the initial and main injections should be longer when the ignition delay is long, for example, when engine is running at low load and low-speed conditions or under transient loads in urban traffic.

In order to improve the efficiency of diesel/biodiesel engine development, the injection, fuel spray, and engine characteristics unavoidably have to be investigated experimentally and numerically. The more or less sophisticated mathematical models addressed briefly in this section have been tested at many operating regimes and with various fuels. On the basis on the comparison of the numerically and experimentally obtained results one can say that these mathematical models may perform quite well.

2.5. Diesel fuel and alternatives

2.5.1. Diesel fuel

Diesel fuels are the product of graduated distillation of crude oil. They obtain a whole range of individual hydrocarbons with boiling points ranging from roughly 180°C to 370°C. Diesel fuel ignites on average at approximately 350°C (lower limit 220°C), which is very early in comparison with gasoline (on average 500°C).

In order to cover the growing demand for diesel fuels, refineries are increasingly adding conversion products, i.e. thermal and catalytic-cracking products. They are obtained by cracking large heavy-oil molecules.

In Europe, the standard for diesel fuels is EN 590 while the U.S. standard for diesel fuels, ASTM D975, for example, specifies fewer criteria and applies less stringent limits to these quality criteria. The requirements for marine and fixed-installation engines are also much less demanding.

High-quality diesel fuels are characterized by the following features:

- High cetane number
- Relatively low final boiling point
- Narrow density and viscosity spread
- Low aromatic compounds (particularly polyaromatic compounds) content
- Low sulfur content

In addition, the following characteristics are particularly important for the service life and constant function of fuel-injection systems:

This material is reserved for educational use only, not allowed for commercial use.

Forbidden to modify the content, and cite the document when use.

- Good lubricity
- Absence of free water
- Limited pollution with particulate

2.5.2. Biodiesel

The term biodiesel covers fatty acid esters which are created through cracking of oils or greases and then converting with methanol or ethanol. This creates fatty acid methyl ester (FAME) or fatty acid ethyl ester (FAEE). The molecules of biodiesel are in terms of size and properties much more similar to diesel fuel than to vegetable oil. Therefore, biodiesel cannot under any circumstances be equated with vegetable oil.

Vegetable oils or animal fats can be used to produce biodiesel. The choice of starting materials is essentially determined by their respective availability. In Europe primarily rape oil is used, in North and South America soybean oil, in the ASEAN countries palm oil, and on the Indian subcontinent the oil from the jatropha. Because esterification can be technically carried out much more easily with methanol than it can with ethanol, the methyl esters of these oils are produced by way of preference. Used frying oil methyl ester is produced worldwide. Because methanol is generally produced from coal, fatty acid methyl ester cannot strictly speaking be seen as fully biogenous. Fatty acid ethyl ester on the other hand is made up of 100 % biomass when bioethanol is used for production.

The properties of biodiesel are determined by various factors. Oils of different vegetable oil differ in the composition of the fatty acid blocks and demonstrate typical fatty acid patterns. The type and quantity of unsaturated fatty acids have, for example, a decisive influence on the stability of the biodiesel. The properties are also affected by the pretreatment of the vegetable oil and the production process of the biodiesel.

2.5.3. Synthetic fuel

Synfuels can be produced from coal, natural gas, or biomass feedstock through chemical conversion into syncrude and synthetic liquid products. Huge industrial facilities gasify the feedstock to produce synthesis gas (carbon monoxide and hydrogen) as an initial step. Synfuel plants commonly employ the Fischer-Tropsch process, with front-end processing facilities that vary, depending on the feedstock. The

manufacturing process for the synthetic fuels typically bypasses the traditional oil refining system, creating fuels that can go directly to final markets.

In the basic Fischer-Tropsch reaction, syngas is fed to a reactor where it is converted to a paraffin wax, which in turn is hydrocracked to produce hydrocarbons of various chain lengths. End products are determined by catalyst selectivity and reaction conditions, and product yields are adjustable within ranges, depending on reaction severity and catalyst selection. Potential products include naphtha, kerosene, diesel, methanol, dimethyl ether, alcohols, wax, and lube oil stock. A product workup section separates the liquids and completes the transformation into final products. The diesel fuel produced is limited by a lack of natural lubricity, which can be remedied by additives. Water and CO₂ are typically produced as byproducts of the process.

2.6. Diesel fuel properties

Diesel fuel is characterized by several of its distinguished fuel properties. Some of the main fuel properties regarding diesel fuel are discussed below.

2.6.1. Cetane number or cetane index

The Cetane Number (CN) expresses the ignition quality of the diesel fuel. The higher the cetane number, the greater the fuel's tendency to ignite. As the diesel engine dispenses with an externally supplied ignition spark, the fuel must ignite spontaneously (auto-ignition) and with minimum delay (ignition lag) when injected into the hot, compressed air in the combustion chamber. Cetane number 100 is assigned to n-hexa -decane (cetane), which ignites very easily, while slow-igniting methyl naphthalene is allocated cetane number 0. The cetane number of a diesel fuel is defined in a standard CFR single-cylinder test engine with variable compression pistons. The compression ratio is measured at constant ignition lag. The engine is run on reference fuels comprising cetane and α -methyl naphthalene at the measured compression ratio. The proportion of cetane in the mixture is altered until the same ignition lag is obtained. According to the definition, the cetane proportion specifies the cetane number. A cetane number in excess of 50 is desirable for optimized operation in modern engines (smooth running, low exhaust-gas emissions). High-quality diesel fuels contain a high proportion of paraffin with high CN ratings. Conversely, aromatic

This material is reserved for educational use only, not allowed for commercial use.

compounds reduce ignition quality. Yet another parameter of ignition quality is provided by the cetane index, which is calculated on the basis of fuel density and various points on the boiling curve. This purely mathematical parameter does not take into account the influence of cetane improvers on ignition quality. In order to limit the adjustment of the cetane number by means of cetane improvers, both the cetane number and the cetane index have been included in the list of requirements in EN 590. Fuels whose cetane number has been enhanced by cetane improvers respond differently during engine combustion than fuels with the same natural cetane number.

2.6.2. Boiling range

The boiling range of a fuel, i.e. the temperature ranges at which the fuel vaporizes, depends on its composition. A low initial boiling point makes a fuel suitable for use in cold weather, but also means a lower cetane number and poor lubricant properties. This raises the wear risk for central injection units. On the other hand, if the final boiling point is situated at high temperatures, this can result in increased soot production and nozzle coking (deposit caused by chemical decomposition of not easily volatilized fuel constituents on the nozzle cone, and deposits of combustion residues). For this reason, the final boiling point should not be too high.

2.6.3. Cold flow properties

Precipitation of paraffin crystals at low temperatures can result in fuel-filter blockage, ultimately leading to interruption of fuel flow. In the worst-case, paraffin particles can start to form at temperatures of 0°C or even higher. The cold-flow properties of a fuel are assessed by means of the “filtration limit” (Cold Filter Plugging Point (CFPP)). European Standard EN 590 defines the CFPP for various classes, and can be defined by individual member states depending on the prevailing geographical and climatic conditions. Formerly, owners sometimes added regular gasoline to their vehicle fuel tanks to improve the cold response of diesel fuel. This practice is no longer necessary now that fuels conform to standards, and, in any case, this would invalidate any warranty claims if damage occurs.

2.6.4. Flash point

The flash point is the temperature at which the quantities of vapor which a combustible fluid emits to the atmosphere are sufficient to allow a spark to ignite the

This material is reserved for educational use only, not allowed for commercial use.

Forbidden to modify the content, and cite the document when use.

air/vapor mixture above the fluid. For safety reasons, (e.g. for transportation and storage), diesel fuel is placed in Hazard Class A III, i.e. its flash point is over 55°C. Less than 3% gasoline in the diesel fuel is sufficient to lower the flash point to such an extent that ignition becomes possible at room temperature.

2.6.5. Viscosity

Viscosity is a measure of a fuel's resistance to flow due to internal friction. Leakage losses in the fuel-injection pump result if diesel-fuel viscosity is too low, and this in turn results in performance loss. Much higher viscosity – e.g. Fatty Acid Methyl Ester (biodiesel) – causes a higher peak injection pressure at high temperatures in non-pressure-regulated systems (e.g. unit injector systems). For this reason, mineral-oil diesel may not be applied at the maximum permitted primary pressure. High viscosity also changes the spray pattern due to the formation of larger droplets.

2.6.6. Density

The energy content of diesel fuel per unit of volume increases with density. Assuming constant fuel-injection-pump settings (i.e. constant injected fuel quantity), the use of fuels with widely different densities cause variations in mixture ratios due to fluctuations in calorific value. When an engine runs on fuel that has a high type-dependent density, engine performance and soot emissions increase; as fuel density decreases, these parameters drop. As a result, the requirements call for a diesel fuel that has a low type-dependent density spread.

2.6.7. Heating value

Heating value of fuel is the amount of heat released during the combustion of a specified amount of it. The energy value is a characteristic for each fuel oil. It is measured in units of energy per unit of the substance, usually mass, such as: kJ/kg, however, energy per unit volume is common in practice in the case of liquid fuel. Heating value is commonly determined by use of a bomb calorimeter.

2.6.8. Lubricity

In order to reduce the sulfur content of diesel fuel, it is hydrogenated. In addition to removing sulfur, the hydrogenation process also removes the ionic fuel components that aid lubrication. After the introduction of desulfurized diesel fuels, wear-related problems started to occur on distributor fuel-injection pumps due to the

This material is reserved for educational use only, not allowed for commercial use.

lack of lubricity. As a result, they were replaced by diesel fuels containing lubricity enhancers.

2.6.9. Sulfur content

Diesel fuels contain chemically bonded sulfur, and the actual quantities depend on the quality of the crude petroleum and the components added at the refinery. In particular, crack components mostly have high sulfur contents.

2.7. Literature review

In recent years, so many researchers are putting their effort to improve emission from diesel engine and a lot of research articles are published as their outcome to enhance fuel technology for modern diesel engine. Most of the researches have been working for alternative diesel fuel so as to cope with increasing energy demand every year. As one of these types, GTL has been taken as one of the prominent alternative diesel fuel to enhance exhaust emission. So, many researches have been performed regarding spray behavior of GTL fuel to utilize it as diesel fuel alternative. However, the spray mechanism and the effect of fuel on injection behavior is not fully understood yet. There are still so many contradictions between the researcher's finding about the spray and injection behavior of GTL. In this heading, few numbers of previous study related to GTL fuel properties, effect on engine performance and emission, injection characteristics and spray behavior are being summarized briefly.

GTL fuel has different physical and chemical properties from those of standard diesel and their effect on combustion and its associated pollutant emissions are not yet well understood. To foresee the evolution of the fuel properties, it is necessary to characterize their impact and potential on every phase affecting the combustion process. Among the important characteristics driving diesel combustion feature the breakup of the fuel spray, its development, and mixing with the ambient gas. These stages are controlled by many factors, such as the nozzle geometry, the operating conditions and the physical properties of the fuels. The properties that have been demonstrated to influence the flow characteristics and the spray characteristics in non-evaporating conditions are mainly fuel density, kinematic viscosity, and surface tension [19-21]. Qualitative spray characteristics such as its angle, tip penetration, and droplet size play a dominant role in the processes occurring during combustion. These

This material is reserved for educational use only, not allowed for commercial use.

Forbidden to modify the content, and cite the document when use.

characteristics provide useful information with regard to air entrainment, air-fuel mixing, and temporal evolution of the mixture [22].

Dernotte et al. [23] investigated on influence of physical fuel properties on the injection rate in diesel injector. In this study mainly the fuel density and fuel viscosity were taken in to account and flow characteristics has been generated by using high pressure diesel injector equipped with conical orifice. In this experiment, mass flow rate measurement was performed with nine different fuels over operating conditions from 300 to 1800 bar, from 1 to 9 MPa of back pressure, fuel viscosity was varied from 0.6 to 7 and fuel density from 683 to 876 kg/m³ at the operating temperature. The result showed fuel viscosity induces a decrease of up to 10% in the discharge coefficient at low pressure difference but for higher pressure difference, no significant impact of fuel viscosity was observed. The result also suggests, fuel density does not have a significant influence on discharge coefficient and it remains only the fuel property driving mass flow rate for pressure difference higher than 55 MPa. A correlation has been suggested to estimate the discharge coefficient taking into account the fuel properties and the operating conditions.

Han et al [24] has studied experimentally on injection characteristics of fatty acid esters on diesel engine common rail system. Three fatty acid esters namely, Methyl laurate, methyl oleate and ethyl oleate were investigated on a high pressure common rail injection system and compared to that of diesel fuel. The cycle injection rate, cycle injection quantity and pressure fluctuation at the injector inlet during and after the injection event are studied across a range of injection pressure and injector energizing time. High dense fatty acid esters show smoother rising slopes at the start of injection and lower injection rate at the stable injection period in the volumetric injection rate curve, but the mass injection rates among all test fuels are quite close. Fatty acid esters have longer injection delay than diesel fuel: while increased injection pressure causes reduced injection delay but prolonged injection duration. Injector emerging time significantly influences the shape of injection rate curve and the pressure fluctuation at the injector inlet. After the needle valve closure, pressure oscillation damps more rapidly for methyl oleate and ethyl oleate, due to their high density, viscosity and bulk modulus of compressibility.

The spray tip penetration of GTL fuel has been presented in previous studies, although a clear trend was not observed. Kim et al. [25] showed that GTL had a longer penetration than diesel fuel at ambient gas temperature and pressure of 300 K and 4 MPa, respectively. They found that GTL fuel had a 12% larger mean drop size than diesel fuel. Therefore, they concluded that the larger drop size of GTL fuel caused the longer spray penetration, due to greater momentum. On the other hand, Payri et al. [26] found that there were no significant differences in spray penetration and cone angle between standard diesel and Sasol-GTL fuel. However, their results showed large temporal fluctuations in the spray penetrations of the tested fuels. Kitano et al. [27] (2005) showed slightly shorter spray penetrations for different types of GTL fuel compared to diesel fuel. Upon evaluation of the influence of physical properties on spray penetration, we would conclude that a decrease in fuel density results in a decrease in the mass injection rate and an increase in the jet velocity. The microscopic behavior of the jet depends on the momentum flux [28, 29], and the momentum is not affected by the two effects described above. On the other hand, viscosity and surface tension have significant effects on spray dynamics [30]. The spray angle and the SMD are related to fuel viscosity. The spray angle is widened, and the SMD is reduced as fuel viscosity decreases. Kitano et al. [27] showed that as the fuel viscosity decreases, the SMD also decreases and the spray angle increases.

Hiroyasu and Arai [10] studied the behavior of high speed injection through diesel nozzle in to a high pressure chamber using various techniques, including an electric resistance method, photographic observation, photo transistors array system and laser diffraction method to measure various aspects of diesel spray. The experimental result summarized and reported empirical equations for break up length, spray angle, spray tip penetration and drop size distribution of the diesel sprays are introduced to discuss the internal structure of the spray. The spray structure has been divided in to two categories according to the effect of injection pressure and ambient pressure on break up length. Since an injection period of the diesel spray was usually far longer than a period that need to break up a small lump of the injected liquid, it was considered that transient behavior of a diesel spray appeared only in the tip motion of the spray and main body of the diesel spray was subjected to the

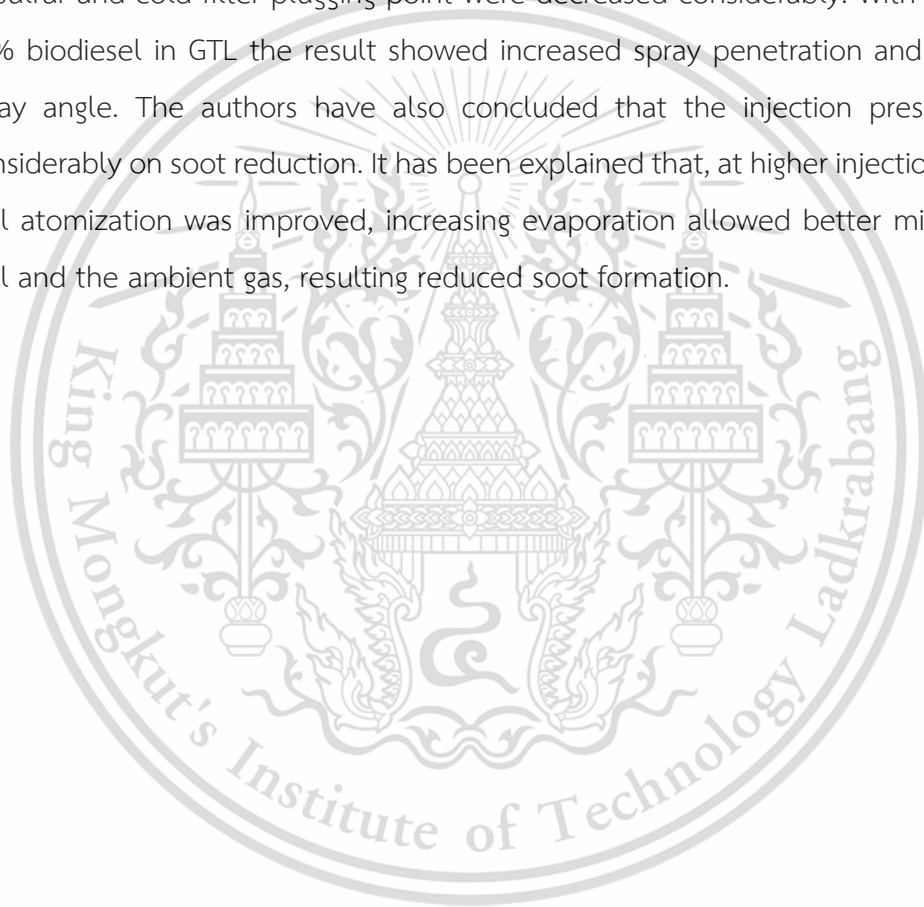
continuous spray. Most of the recent studies follows the equations suggested from this study.

Arregle et al [31] studied on influence of injection parameters on diesel spray characteristics. Macro and microscopic behavior of diesel spray generated from common rail system were characterized and the influence of injection parameters and boundary conditions through a board were quantified. In this research they have validate different correlations of spray generated by common rail system. The sprays were characterized in an environment which simulates the in-cylinder air density existing in the real engine when the injection starts. A wide parametric study has generated evidence needed to quantify the influence of the common rail pressure, nozzle hole diameter and environment gas density on the spray tip penetration, spray cone angle and geometric volume of the spray, as well as the spatial and temporal evolution of drop size distribution. A theoretical analysis is made and the results obtained were compared with the experiments of this study and with some previous studies. Regarding macroscopic spray characteristics, despite the small variations present in the shape of the injection rate curves considered, the influence of each test parameters such as, injection pressure, nozzle diameter, and gas density has been clearly evidenced in this work. For a given nozzle geometry, the spray cone angle seems to be independent of the injection pressure but changes significantly with the gas density. Strong dependence of the cone angle upon the nozzle hole geometry makes difficulty in generalization of global behavior of diesel sprays.

Delacourt et al [32] have investigated the effect of injection pressure on the macroscopic spray characteristics for a wide pressure range up to 250 MPa and injection environment air density 15 to 45 kg/m³. In this research, the researchers developed a measurement technique able to extract these characteristics both quickly and reliably. The result obtained widen the application field of the temporal evolution law to establish new laws for other spray characteristics including spray angle, spray area, spray volume as well. They observed that the instantaneous spray tip velocity is twice as slow as the mean velocity of the jet obtained at the beginning of the injection. The spray velocity evolution according to the pressure decreases very quickly over time regardless of the injection pressure value, for a given penetration, increased pressure

slowdowns spray tip velocity changes. The spray angle does not vary so much with injection pressure.

Azimov et al. [33] has performed an experimental study on spray combustion of diesel, GTL and GTL-biodiesel fuel under high pressure, high temperature quiescent conditions. Instantaneous images of spray were captured using high speed camera. The authors confirmed that, fuel properties like density, viscosity, surface tension, volatility and lower heating value of GTL fuel could be make more likely to conventional diesel by adding twenty percent of rapeseed biodiesel. However, the properties like amount of sulfur and cold filter plugging point were decreased considerably. With addition of 20% biodiesel in GTL the result showed increased spray penetration and decreased spray angle. The authors have also concluded that the injection pressure affect considerably on soot reduction. It has been explained that, at higher injection pressure, fuel atomization was improved, increasing evaporation allowed better mixing of the fuel and the ambient gas, resulting reduced soot formation.



CHAPTER 3

EXPERIMENTAL EQUIPMENTS AND METHODS

In this chapter, the methods and materials used in this research are described. In present work, it is divided in to three parts namely, 1. Fuel properties test 2. Injection behavior test and 3. Spray characteristics test. Therefore, the materials, methods and methodologies involved in each part are described briefly in this session.

3.1. Fuel properties test

The physical and chemical features of fuel play key role in injection, fuel atomization, air fuel mixing and hence in overall combustion efficiency. Hence it is vitally important to know properties of diesel fuel. In this section, the equipment and method used to measure different fuel properties are discussed below.

3.1.1. Density meter

The DMA 4500 density meter as shown in Figure 3.1 has been used to measure the fuels density. The measurement is based on the proven oscillating U-tube principle ensuring highly accurate density values of any liquid. It provides unparalleled ease of use and complete transparency and traceability of the sample filling and measurement process. ASTM D4052 standard has been followed to measure densities of all test fuels. Figure 3.1 shows the picture of density meter used in this research.



Figure 3.1 Density Meter DMA 4500

This material is reserved for educational use only, not allowed for commercial use.

Forbidden to modify the content, and cite the document when use.

3.1.2. Kinematic viscosity measurement

Viscosity is a measure of a fluid's resistance to flow. It is one of the most important properties of a diesel fuel and plays a very prominent role in the fuel injection system. The miniAV® from CANNON Instrument Company as shown in Figure 3.2 has been used to measure kinematic viscosity of all test fuels. This device determines viscosity by measuring the time it takes for a volume of fluid to flow under gravity through a calibrated glass capillary viscometer. Temperature is the most important parameter for obtaining accurate and precise kinematic viscosity measurements.



Figure 3.2 Viscometer

The user fills the sample vial, places it in the vial holder beneath the viscometer, and raises it into the position. Sample ID information is entered via the computer. The user initiates the test with a single mouse click. Without further operator intervention, the sample is drawn up into the viscometer tube, held for temperature equilibration, and then measured. Data is automatically transferred to the computer database via serial port connection. The sample is then ejected as waste, and the sample vial becomes a wash station as solvent is automatically metered into the viscometer tube and then evacuated to complete the cleaning cycle. Following tube

This material is reserved for educational use only, not allowed for commercial use.

Forbidden to modify the content, and cite the document when use.

drying, the vial holder is lowered to its original position, ready to receive the next sample. Total cycle time for a test is about five to eight minutes depending on the viscosity. ASTM D445 has been utilized for measurement of fuel viscosity. Figure 3.2 shows the real picture of viscoumeter used in this research.

3.1.3. Bomb calorimeter

The LECO AC-350 Automatic Calorimeter shown in Figure 3.3 has been used to measure heating value of all test fuels. It is a Digital Signal Processing (DSP) microprocessor based instrument, developed to measure the calorific content of various organic materials such as coal, coke, and fuel oil. The calorific value of a sample is determined by burning the sample in a controlled environment. The heat released by combustion is proportional to the calorific value of the substance. In this apparatus, the sample being analyzed was placed in a high-pressure atmospheric environment called a Combustion Vessel. The Combustion Vessel was surrounded by water. The temperature of the water is then measured by an electronic thermometer with a resolution of 1/10,000 of a degree. During analysis, the fan speed was modulated to control the jacket temperature. ASTM D240 has been utilized to measure heating value of all test fuels.



Figure 3.3 Bomb Calorimeter

3.1.4. CHNS analyzer

The LECO 628 series with 628S module as shown in Figure 3.4 has been used to determine carbon, hydrogen nitrogen and sulfur content in fuel. This equipment This material is reserved for educational use only, not allowed for commercial use.

Forbidden to modify the content, and cite the document when use.

utilizes a combustion technique to determine CHN elements in fuel. A sample is weighed into a foil or capsule and loaded into autoloader. Simple, gravity-fed autoloader allows for analysis and provides a result within 4.5 minutes for all the elements being determined. 628 S module is specifically designed to determine the sulfur content in a wide variety of organic materials such as coal, coke, and fuel oils, as well as some inorganic materials such as soil, cement, and limestone.



Figure 3.4 CHN analyzer

3.1.5. Flash point measurement

The TANAKA APM-7 as shown in Figure 3.5 has been used to measure flash point of all test fuel in this research. ASTM D93 method has been selected a test mode. Before the instrument execute testing, it is necessary to put expected flash point for test fuel. The instrument follows the exact procedures prescribed in the test method, and the completion of the test cycle is signaled by beep tones. The test result is brightly shown on the vacuum fluorescent display module.



Figure 3.5 Flash point measuring device

This material is reserved for educational use only, not allowed for commercial use.

Forbidden to modify the content, and cite the document when use.

3.1.6. Cloud point and pour point measurement

The ISL 5Gs as shown in figure 3.6 has been used to measure cloud and pour point of the test fuels. The cloud point test permits determining the temperature at which the paraffin-base constituents of the products may precipitate, a reaction which may cause pipework or filter clogging or the downgrading of performance of fuel oils. As to the pour point test, it yields the lowest temperature at which the product continues to flow. The CPP 5Gs is flexible enough to accommodate all unique testing requirements, yet also provides strict compliance to international standard test methods. Pour point is detected by tilting the sample no turning, pressing or twisting as an optical surface, whereas detection system precisely monitors movement of the specimen surface. Optics detect cloud point in the specimen when wax crystals first appear. In present work ASTM D5771 is used for cloud point and ASTM D5950 is used for pour point.

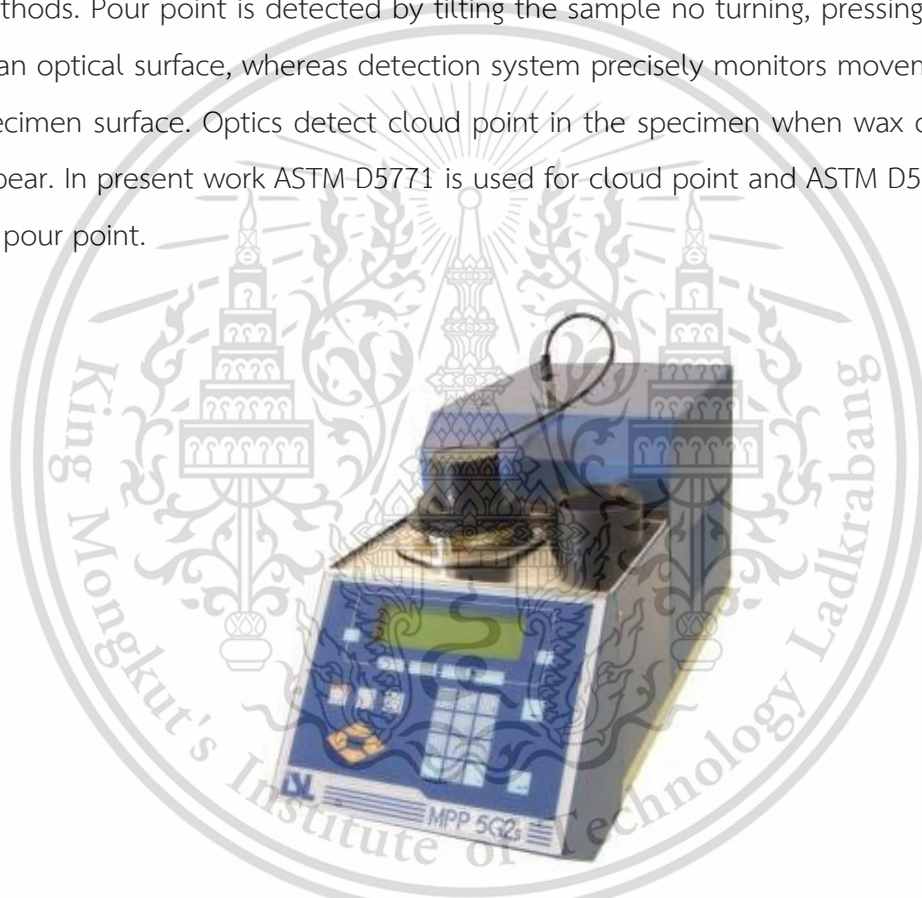


Figure 3.6 Cloud and pour point measuring device

3.2. Injection behavior analysis

The materials and methods used to study injection behavior of test fuel is being summarized in this section.

3.2.1. Test fuels

Six types of fuel including four GTL-diesel blends, pure GTL and commercial diesel have been experimentally tested to study their injection behavior in modern This material is reserved for educational use only, not allowed for commercial use.

Forbidden to modify the content, and cite the document when use.

common rail diesel injection system. GTL and commercially available diesel has been blended together to get GTL 20, GTL 40, GTL 60 and GTL 80, where numeric digits attached behind GTL represents percentage of GTL in those fuel blends by weight. Here, pure GTL is termed as GTL 100 and simply 'Diesel' for commercial diesel. Figure 3.7 shows the picture of test fuel used in this study. The detail of fuel properties will be discussed in later chapter.



Figure 3.7 Test fuels

3.2.2. Experimental conditions

Table 3.1 shows the experimental conditions for injection characteristics for all test fuels. Effect of ambient temperature is not considered in this experiment. The test fuels were injected into the Zeuch chamber with different pressure between 400 – 1600 bar via single hole nozzle with diameter of 0.14 mm using common rail injection system.

Table 3.1 Experimental test condition

Variables	Test conditions
Test fuel	Diesel, GTL 20, GTL 40, GTL 60, GTL 80, GTL 100
Back pressure (P_b)	45 bar
Injector energizing duration (T_e)	0.5, 1.0 and 2.5 ms
Injection pressure (P_i)	400, 800, 1200 and 1600 bar

3.2.3. Experimental setup

The schematic diagram of experimental apparatus is shown in Figure 3.8. Zeuch injection rate measurement technique has been used to measure injection rate. Above the cubic Zeuch chamber of 40 cm³ in chamber volume, the second generation solenoid diesel injector manufactured from DENSO Company with single-hole of 0.14 mm injection diameter was installed above could be on the top of the chamber to inject the test fuel. In order to provide back pressure, the chamber was filled with the test fuel by a hand pump. A static pressure sensor, modeled MURPHY PXT2000 and a dynamic pressure sensor modeled KISTLER 6052C were installed to measure downstream pressure and dynamic chamber pressure respectively. The signal from dynamic pressure sensor is amplified with charge amplifier KISTLER Type 5011. Those data were then recorded by a data acquisition system Tektronix TDS2024C oscilloscope. For fuel system, the high pressure pump was driven by three-phase electric motor controlled by an inverter. The pressure was kept constant by controlling the electric motor revolution. The injector energizing duration and trigger time was controlled by a programmable microcontroller ET-Easy328, which then actuated the Electronic Driver Unit (EDU) to inject fuel into the test chamber. For measurement of bulk modulus, nitrogen from pressurized container was used to push pneumatic cylinder aligned with a dial gauge to measure displacement and hence the displace volume. The detail of devices used in this experiment are shown in appendix.

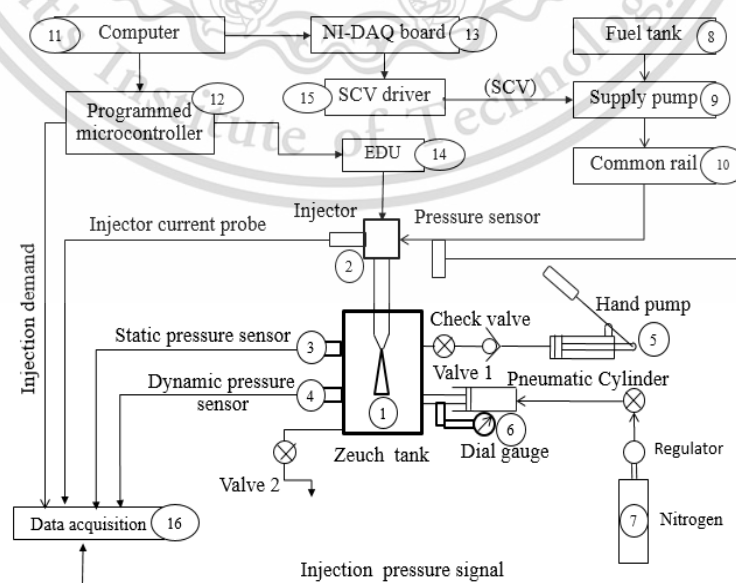


Figure 3.8 Schematic diagram of experimental setup for injection analysis

This material is reserved for educational use only, not allowed for commercial use.

Forbidden to modify the content, and cite the document when use.

3.2.4. Data acquisition

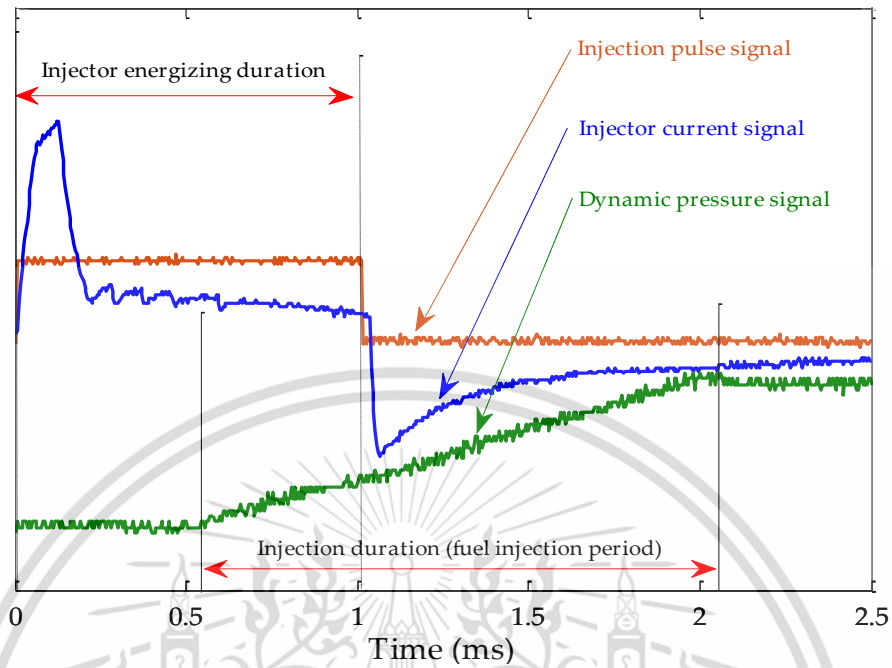


Figure 3.9 Data acquisition (oscilloscope traces)

Figure 3.9 shows the oscilloscope traces of data acquisition for injection rate measurement. In this experiment, injector energizing duration was controlled by programmable micro controller and the signal is recorded by the oscilloscope along with injector current signal. The dynamic pressure increased Zeuch chamber which is varied due to fuel injection was recorded by the oscilloscope. Resolution of the recorded data is 0.004 ms. Furthermore, the recorded pressure data was filtered in LabVIEW program using low pass Bessel filter with frequency of 1.2 kHz. Then the filtered data has been used for further calculation of injection rate measurement.

3.2.5. Bulk modulus and Zeuch method

In Zeuch's method, the fuel is injected into a chamber filled with tested fuel at a certain pressure. As the mass of fuel in the chamber increases due to the injected fuel, the chamber pressure increases in proportion to the injected mass. According to the bulk modulus of elasticity, the derivative of the chamber pressure with respect to volume provides the injection rate signal. The fuel bulk modulus of elasticity is

$$K = V \frac{dp}{dv} \dots\dots\dots 3.1$$

Where, K is the fuel bulk modulus of elasticity, V the chamber volume, p the pressure inside chamber. From the definition, bulk modulus of elasticity is the in pressure variation due to a finite volume of injected fuel multiplied by the initial chamber volume. Figure 3.10 shows the schematic diagram to measure bulk modulus of test fuels.

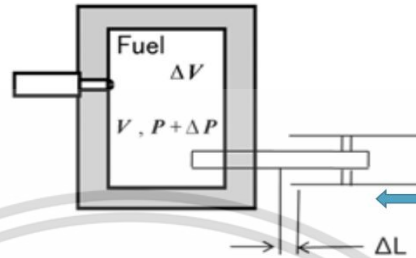


Figure 3.10 Schematic diagram for bulk modulus measurement

Bulk modulus of elasticity of all test fuel has been measured using the constant volume chamber filled with the test fuel. A small plunger actuated with pneumatic pump was fitted within the chamber, which is inserted into the pre compressed fuel so as to change the volume and hence the pressure inside. The dynamic pressure sensor installed above the chamber detects pressure raise due insertion of small cylindrical end of plunger. The increased pressure value is then substituted in Equation 3.1 to get the bulk modulus value for each test fuel. Moreover, bulk modulus is highly dependent on temperature and pressure. However, the pressure inside the fuel chamber is maintained by supplying fuel through hydraulic hand pump and made equivalent to test condition pressure. In addition, temperature is not considered as all the experiments has been done in normal room temperature.

The Zeuch injection rate measuring method is derived based on the conservation of mass. By inserting the fuel bulk modulus in time derivative of mass, the equation becomes

$$\frac{dm}{dt} = \rho \frac{V}{K} \frac{dp}{dt} \dots\dots\dots 3.2$$

Here, m is the mass of fuel and ρ is the fuel density.

3.2.6. Injection characteristics analysis

The injection rate measured from Equation 3.2 is plotted in y-axis with time after injector energizing in x-axis to obtain injection rate graph. The area under the

injection rate curve gives measured value of fuel injected into the chamber, which is represented as $m_{measured}$. The injection delay time is the time lag between start of injector energizing point (supply of voltage to the injector) to the start of injection (where the actual injection of fuel starts). After supplying the signal to the injector it is noted that, there is some lag of the injector needle open (or close) which are termed as the transitional period. The graphical representation of injection quantity, injection delay time, needle opening and needle closing time is clearly shown in Figure 3.11.

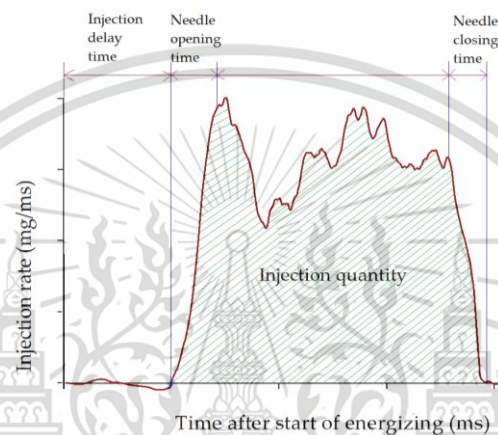


Figure 3.11 Definition of injection quantity and injection delay time

The discharge coefficient C_d is a ratio between measured mass of injected fuel and the theoretical injected mass, m_{th} .

$$C_d = \frac{m_{measured}}{m_{th}} \quad \dots\dots\dots 3.3$$

The theoretical mass of injected fuel, m_{th} , is calculated from a combination of continuity equation.

$$m_{th} = n_{orifice} \cdot A \cdot \sqrt{2 \cdot \Delta P \cdot \rho} \quad \dots\dots\dots 3.4$$

Where $n_{orifice}$ is the number of orifices, A is the cross-sectional area, ΔP the pressure difference (injection pressure - back pressure), and ρ the fuel density at operating temperature.

3.3.Spray analysis

The material and methods used in spray analysis is briefly discussed in this section. Test fuels used in this study are identical to the fuels discussed in section 3.2.1. However, important fuel properties of pure GTL and diesel fuels used in this

experiment are listed in Table 3.2 below and the experimental conditions used during study of spray analysis is shown in Table 3.3.

Table 3.2 Fuel properties for spray analysis

Properties	Method	GTL	Diesel
Heating value (MJ/kg)	ASTM D240	47.3	45.1
Density@15 ⁰ C (kg/m ³)	ASTM D4052	785.1	837.2
Kinematic viscosity (mm ² /s)	ASTM D445	3.433	3.205
Surface tension (mN/m)	ASTM D1590	23.3	28.7

Table 3.3 Experimental condition for spray analysis.

Experimental variable	Test conditions
Test fuels	Diesel, GTL20, GTL40, GTL60, GTL80, GTL100
Back pressure (P_b)	19 and 45 bar
Injector emerging time (T_e)	0.5 and 1.0 ms
Injection pressure (P_i)	400, 800, 1200, and 1600 bar

3.3.1. Experimental setup

In this experiment, the constant volume chamber with cylindrical shape of 80 mm diameter with observation window is used. To visualize spray characteristics, quartz discs, being transparent and high strength were used as optical accessible windows to both side of the chamber. The spray images were captured using the Schlieren photography technique. The single hole solenoid type injector with injector diameter 0.14 mm was installed to supply fuel to the high pressure chamber. Series of image were captured using high speed video camera at a rate of 10,000 frames per second with resolution of 640x480 pixel and 1/64000 sec shutter speed.

The schematic diagram of experimental setup is shown in Figure 3.12, consists of four major systems. First, the high pressure chamber in which nitrogen is supplied through a nitrogen cylinder fitted with pressure gauge and regulator to maintain required ambient pressure. Second, the fuel system, a feed pump is used to deliver test fuel to the high pressure pump. The high pressure pump which is coupled with 5hp motor and 3 phase inverter was used to control rotational speed of motor. Third is the DAQ National Instrument model NI-6221 with LabVIEW, personal computer, This material is reserved for educational use only, not allowed for commercial use.

which were used to control constant rail pressure by PID control, closed loop from rail pressure sensor with a limit of rail pressure by suction control valve (SCV). The injection duration and trigger timing were controlled by a programmable microcontroller which then actuates injector driver to inject fuel to the high pressure chamber and turns on high speed video (HSV) camera. Fourth is the high speed video camera, Photorn FASTCAM Mini UX100, which was used to capture the spray characteristics with shadowgraph imaging method.

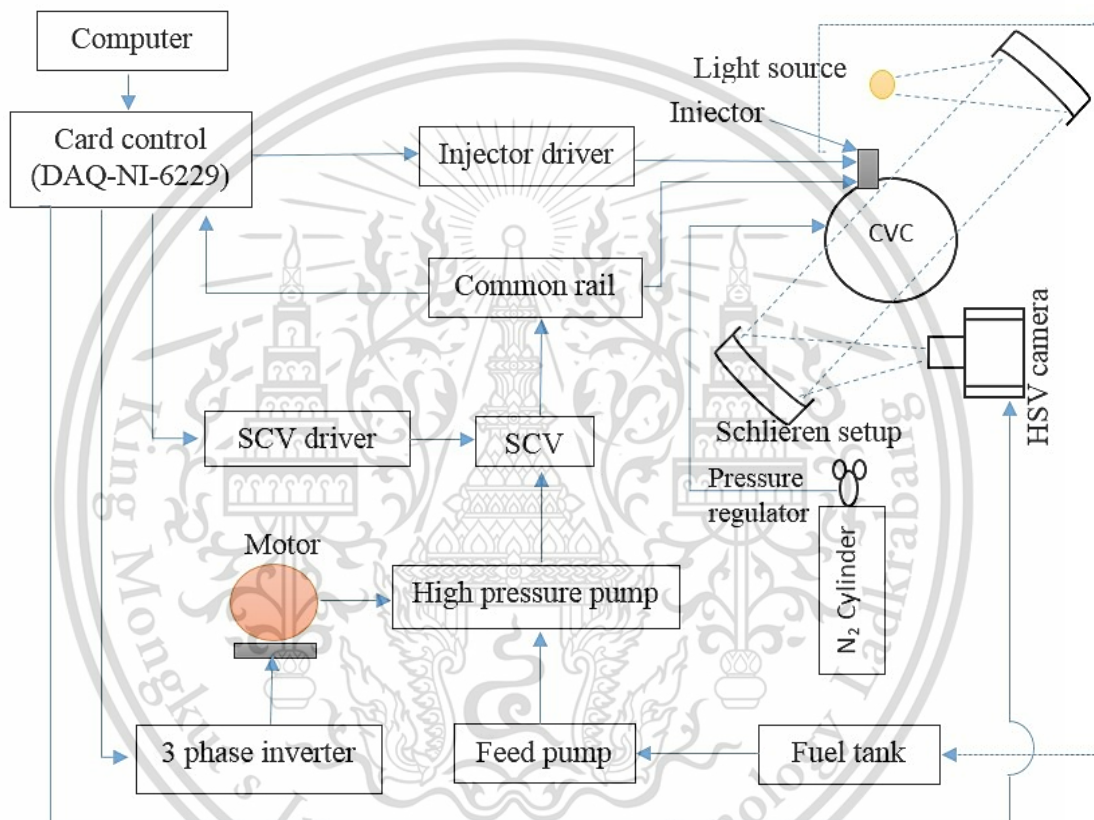


Figure 3.12 Schematic of experimental setup

3.3.2. Schlieren photography setup

Two parabolic and off-axis concave mirrors are used in Schlieren equipment. The combination of diverging illuminator beam, an opposite converging analyser beam and a parallel beam between the two mirrors suggest the letter Z, hence this kind of setup is generally known as “Z type 2-Mirror Schlieren System” [34]. Figure 3.13 represents the Schlieren setup used to capture spray images in this experiment. The high pressure chamber is placed parallel beam in between two parabolic mirrors of focal length 1.8m. The fuel injector is fitted on the high pressure chamber. To visualize the spray from

the injection, high intensity halogen lamp is used, which then a convex lens is used to converge the light and passed through a pin hole. At the other end, Photron UX-100 modeled high speed video camera is focused on the reflected mirror to capture the images.

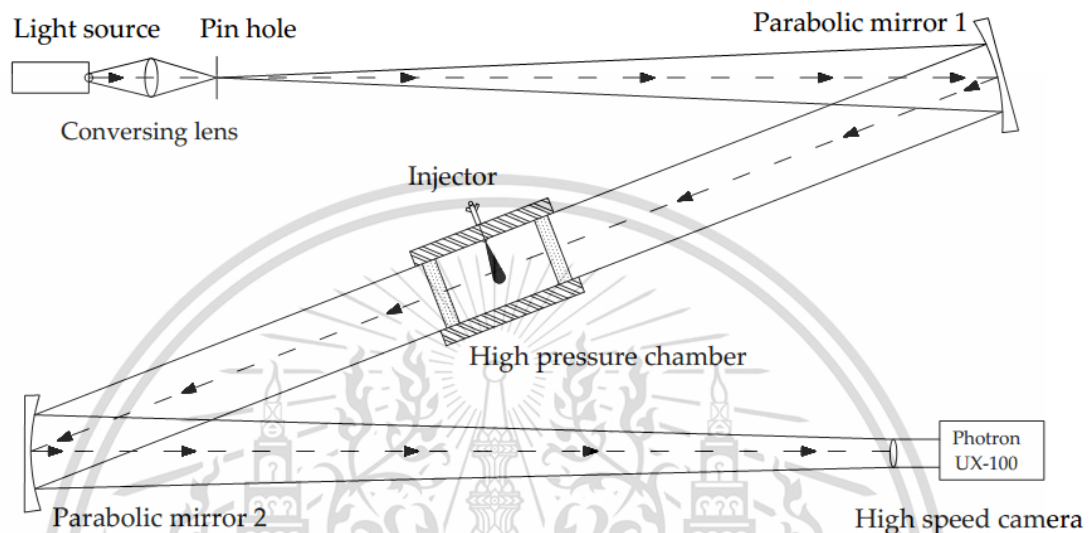


Figure 3.13 Schematic of spray image capturing technique

3.3.3. Spray image analysis

The evaluation of recorded spray video was performed manually by image processing routine. The image analysis is mainly focused on measurement of spray tip penetration and spray cone angle. The flow diagram of procedure involved is shown in Figure 3.14. The PFV software has been used to subtract the background by choosing the appropriate threshold level. Then the images of spray were saved in TIFF format. This sequence of images is then transferred to MATLAB script in which image is binarized according to the Otsu method [35], to separate the spray from the background. The digitized images were used to measure spray tip penetration and spray cone angle by calculating the axial profile. Considering the sensitivity and high gradient at the spray tip, 80% of the maximum value is taken as spray tip penetration length [6]. The raw and digitized images are shown in appendix. Spray velocity is calculated from the difference in spray penetration length divided by the time gradient in each successive frame.

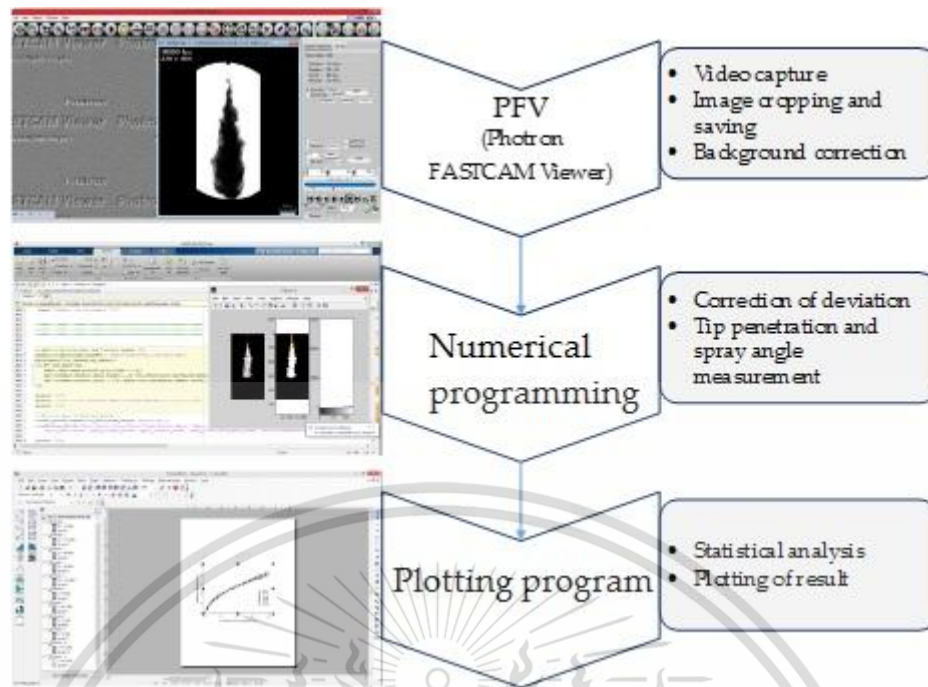


Figure 3.14 Procedure involved in spray measurement

The definition of spray penetration and spray angle presented in this report is shown in Figure 3.15. Where, the spray penetration (S) is defined as a distance of spray tip from the injector tip in axial direction and spray angle is defined as maximum angle in each side of spray at $S/2$ [10]. Furthermore, spray velocity is calculated by dividing the difference in penetration length each successive frame with the time difference between the frames. Mathematically, the calculation of spray velocity is illustrated in Equation 3.5.

$$\text{spray velocity} = \frac{S_n - S_{n-1}}{t_n - t_{n-1}} \dots\dots\dots 3.5$$

Where, S_n = Spray penetration length measured for nth frame

t_n = Time taken to reach nth frame after start of injection

Spray volume is presented for selective test condition and in this work is calculated by using the Equation 3.6 developed by [36] as shown below.

$$V_T = (\pi/3) S^3 [\tan^2(\theta/2)] \frac{1 + 2 \tan(\theta/2)}{[1 + 2 \tan(\theta/2)]^3} \dots\dots\dots 3.6$$

Where, V_T = Spray volume

S = Spray penetration.

θ = Spray angle

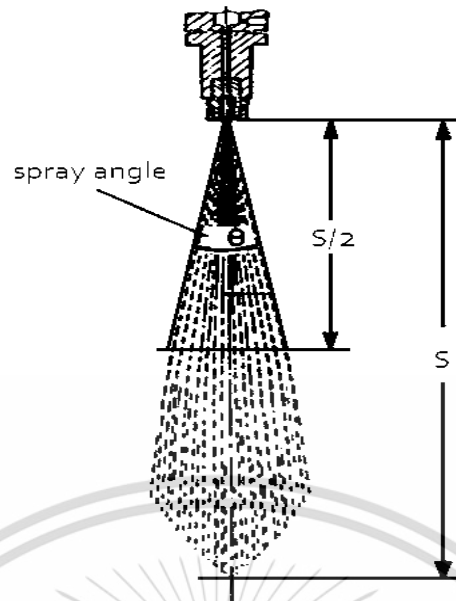
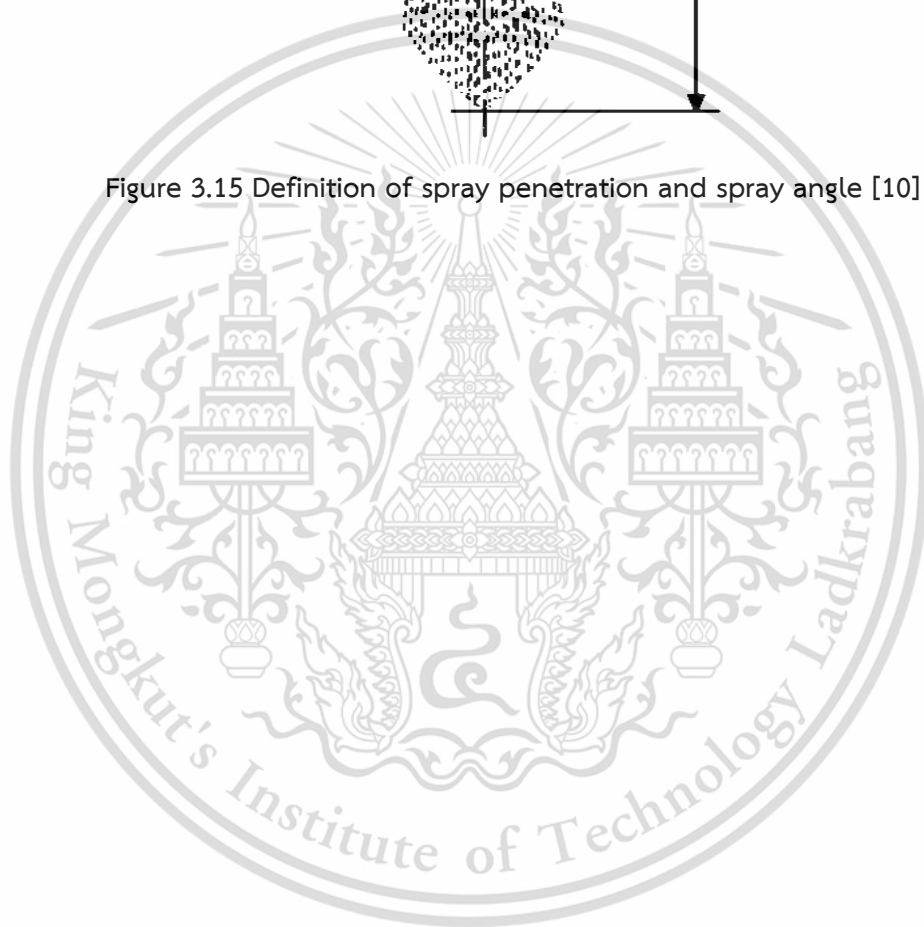


Figure 3.15 Definition of spray penetration and spray angle [10]



CHAPTER 4

RESULTS AND DISCUSSION

4.1. Fuel properties results

Different physical and chemical properties of GTL and commercial diesel has been measured and discussed in this chapter. Table 4.1 summarizes the overall fuel properties of neat GTL and commercial diesel measured in lab. However, the fuel properties which are prone to injection are explained for individual fuel blends.

Table 4.1 Fuel properties results measured for neat fuels

Property	GTL 100	Diesel	Units	Test standard	
Cetane index	80.22	-		ASTM D4737	
T90	336.8	-	⁰ C	ASTM D86-09e1	
Copper corrosion	1a	1a		ASTM D130	
Heating value	47.3	45.83	MJ/kg	ASTM D240	
Density @15 ⁰ C	0.7851	0.8301	gm/cc	ASTM D4052	
Flash point	102.5	65	⁰ C	ASTM D93	
Pour point	-1.6	-11.2	⁰ C	ASTM D5951	
Cloud point	4.1	7.8	⁰ C	ASTM D5773-10	
Kinematic Viscosity	3.433	3.205	mm ² /s	ASTM D445	
CHN analysis	C	84.9015	85.0460	%	-
	H	15.4730	14.0030		
	N	0.0240	0.2812		

4.1.1. Effects on density

Density plays a significant role in diesel fuel injection system. Higher density indicates higher volumetric energy concentration in the fuel but it effects on spray atomization efficiency resulting in poor combustion and more emission [37]. Figure 4.1 shows the density for all test fuels. It can be clearly seen that pure diesel fuel has the highest density value where pure GTL has lowest. The densities value for fuel blends

This material is reserved for educational use only, not allowed for commercial use.

show, with increasing in GTL fraction, density of the mixtures decreases proportionally. The density value of GTL is 6.86% lower than that of commercial diesel and it varies linearly for all fuel blends. The difference in density between GTL and diesel fuel presented by [38, 39] agree with the obtained results in this experiment.

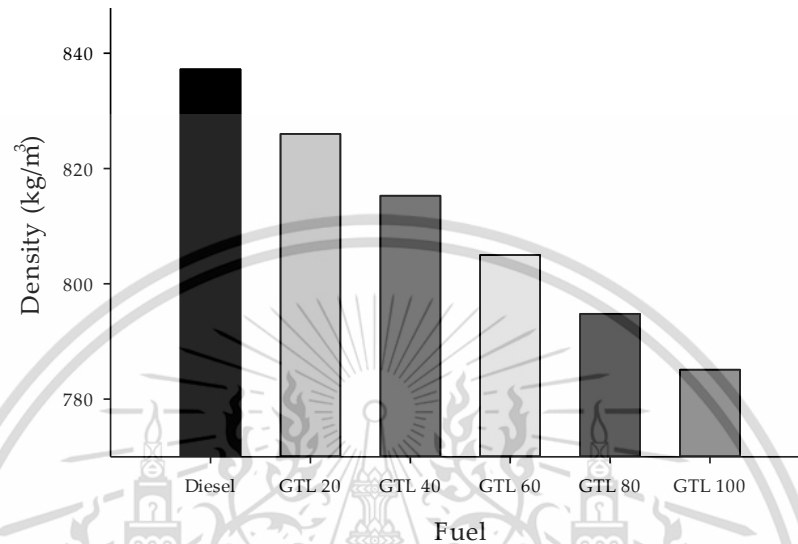


Figure 4.1 Fuel type vs density

4.1.2. Effect on heating value

Higher heating value of fuel is favorable for the combustion engine. Figure 4.2 shows the heating value by weight and by volume for all test fuels. In spite of having low density, the result of heating value shows, GTL has high heating value by weight compared to commercial diesel but slightly low by volume. The lower heating value by volume leads to less power for fixed injection volume [40]. It has been found that, GTL has 4.58% higher of heating value by weight and 1.8% lower heating value by volume than that of diesel fuel.

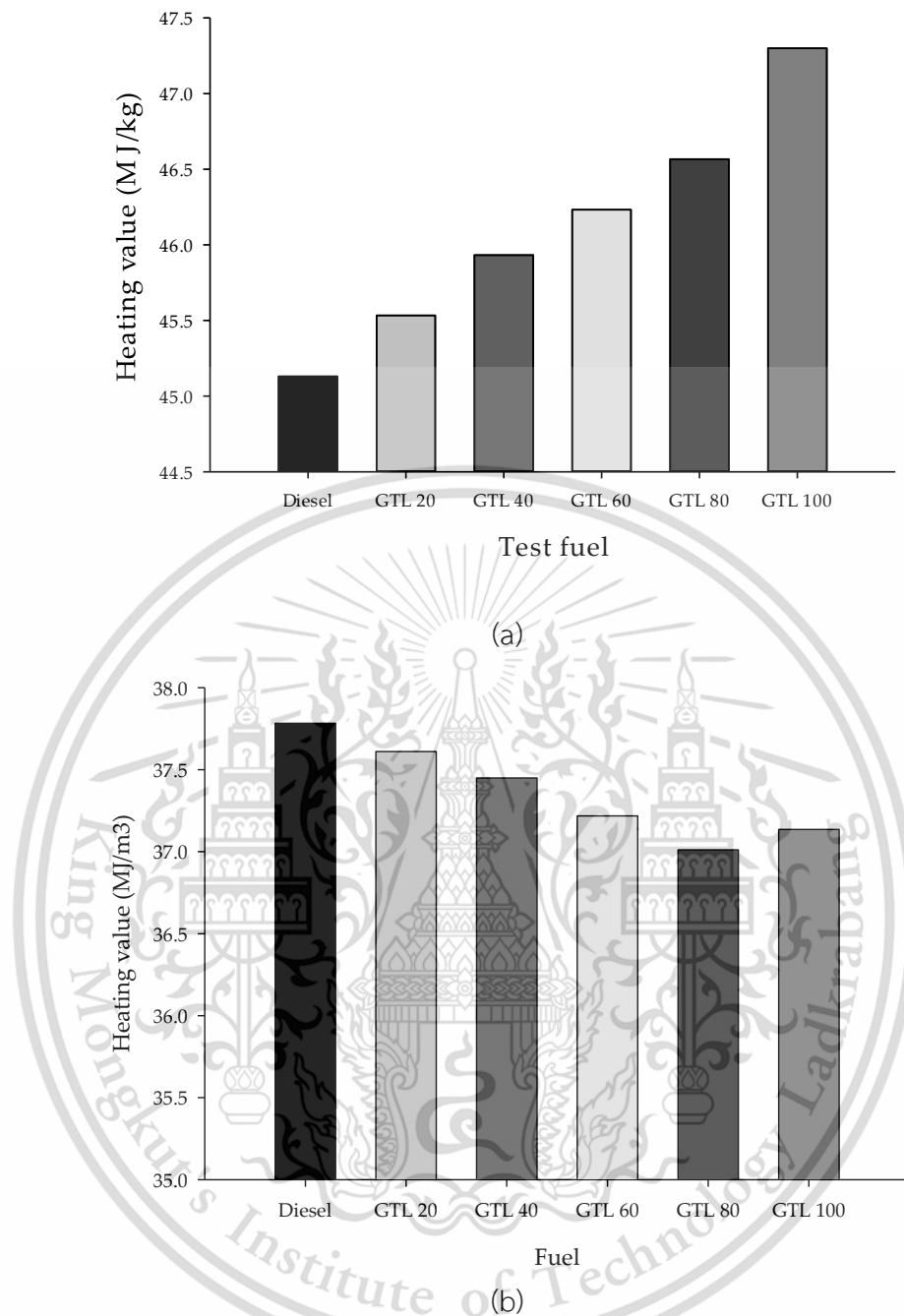
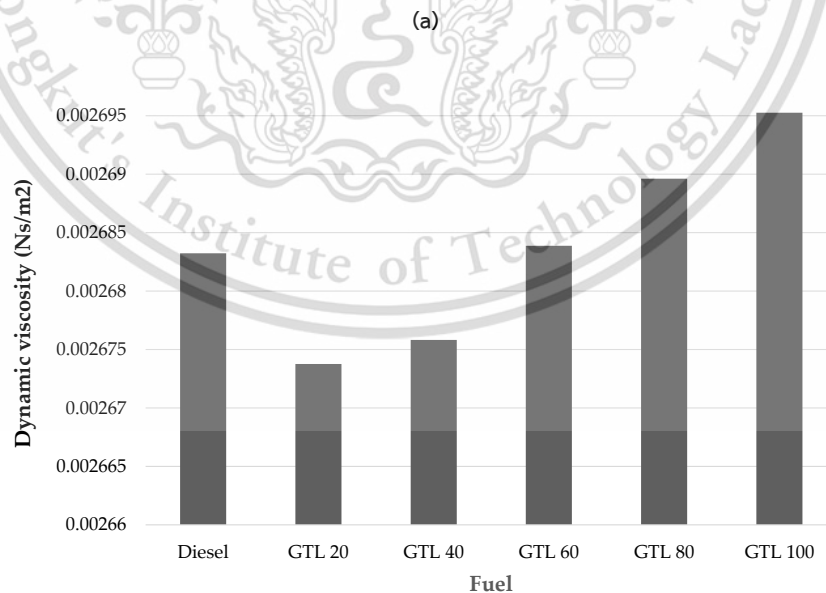
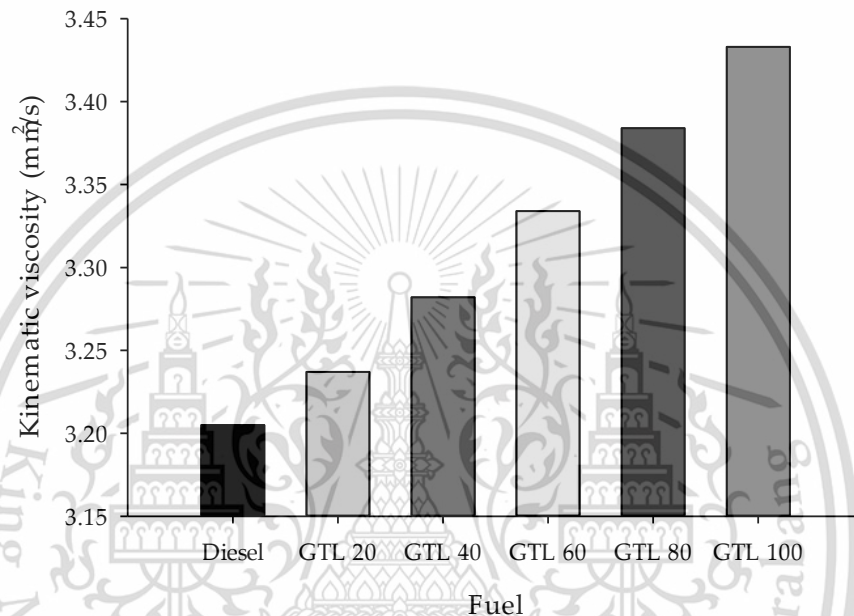


Figure 4.2 Fuel type vs heating value (a) by weight (b) by volume

4.1.3. Effect on viscosity

Viscosity affects the fuel injection and spray atomization. Figure 4.3 shows the kinematic and dynamic viscosity of all test fuels. The result shows; GTL has higher kinematic viscosity value compared to commercial diesel. Therefore, kinematic viscosity of fuel blends increases with increasing of GTL fraction. However, dynamic viscosity fluctuates in fuel blends. Although GTL100 shows higher dynamic viscosity

among tested fuel blends. It has been found that, GTL has 6.64% higher kinematic viscosity than that of diesel fuel. The result observed by Wu et al. [38] is quite different to this experiment, where the team reported unchanged kinematic viscosity till 50% volume ratio but rapid increment in further GTL addition to the blend fuel. However, the viscosity of the synthetic fuel greatly depends on feedstock and can easily vary by using additives.



(b)

Figure 4.3 Fuel type vs viscosity (a) kinematic (b) Dynamic

This material is reserved for educational use only, not allowed for commercial use.

Forbidden to modify the content, and cite the document when use.

4.1.4. Effect on H-C ratio

The CHN analysis has been performed for all blended fuels in this research. The summary of CHN analysis has been summarized in terms of H/C ratio in Figure 4.5 below. It can be clearly seen that GTL has higher H/C value compared to diesel and the value is decreased with reduction of GTL fraction in the fuel blends. Thus, as reported by Ryan et al [41], GTL shows advantage over commercial diesel for emission reduction with its higher H/C ratio.

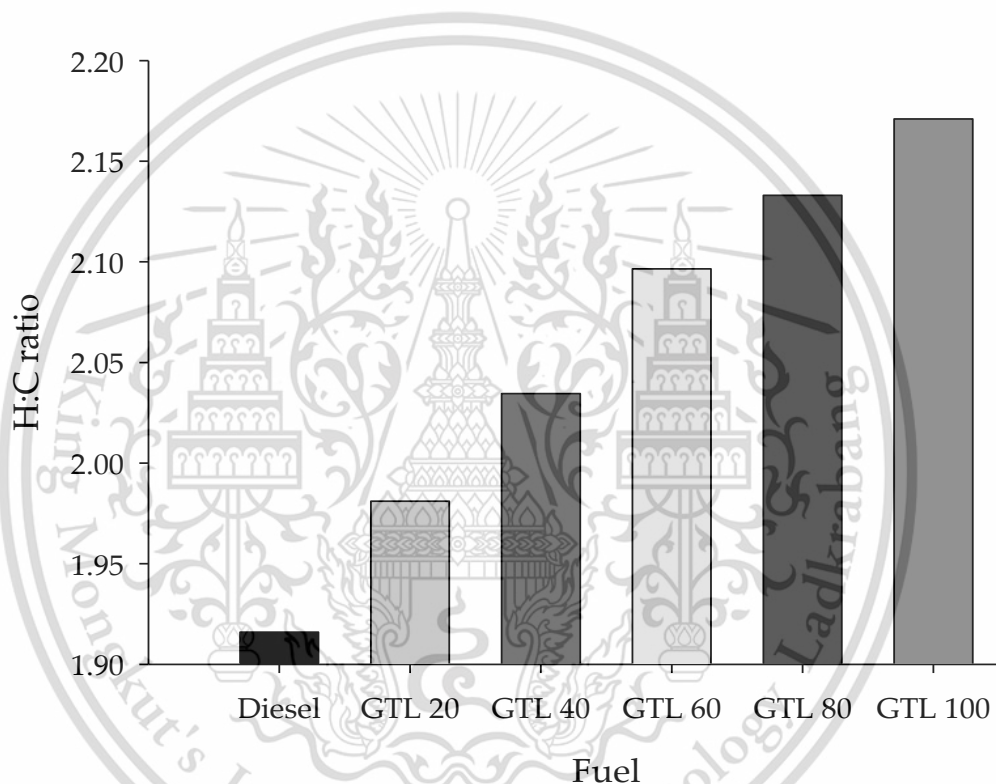


Figure 4.5 Fuel type vs H/C ratio

4.1.5. Effect on bulk modulus

Bulk modulus of all the blended fuels has been measured at pressure of 45 bar and normal room temperature. The obtained result is plotted in Figure 4.6 below. The result shows pure diesel fuel has highest bulk modulus value amongst the blended fuels and GTL has the lowest. It varies quite linearly for other fuel blends too. Bulk modulus of GTL is 16.66% lower than that of diesel fuel at same test condition.

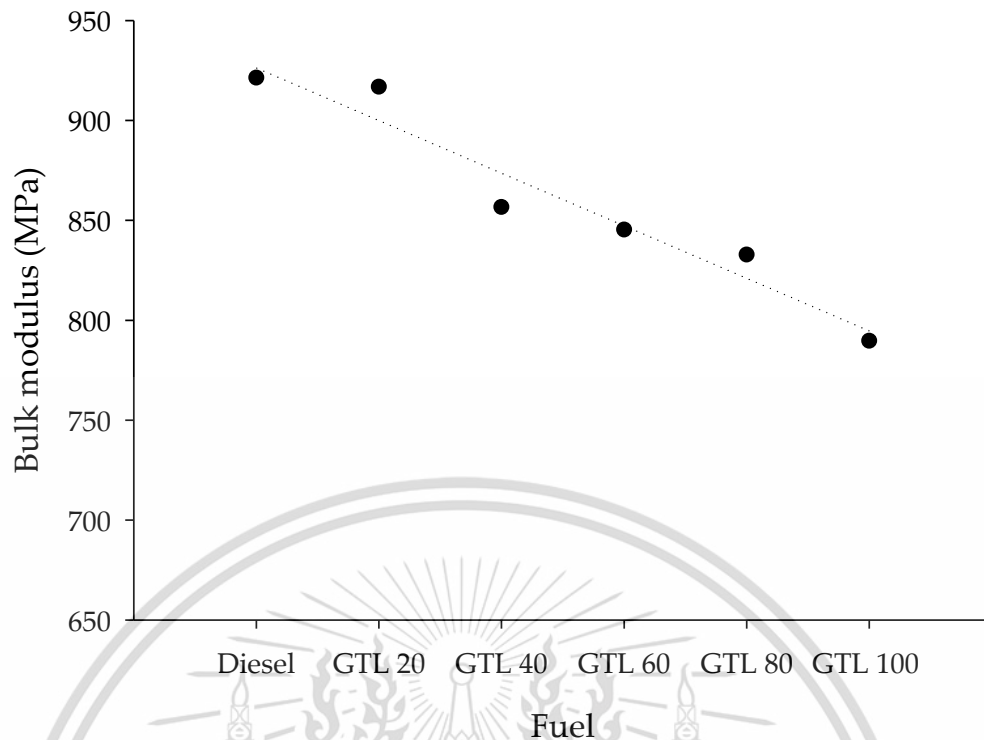


Figure 4.6 Bulk modulus of test fuels at 45 bar

4.2. Injection characteristics

4.2.1. Injection rate profiles

In order to understand the effect of fuel properties on the injection process, injection rate profiles of various blended fuels were compared under the same measurement conditions.

4.2.1.1 Injection rate profiles at $T_e = 0.5$ ms

The injection rate profile for all the studied fuels, performed with an injector energizing duration of 0.5 ms, injection pressure of 400 to 1600 bar and ambient pressure of 45 bar are illustrated from Figure 4.7 to Figure 4.10. Nonetheless of the fuel types, the observed result of injection rate profile is nearly of rectangular form. For all studied fuels, it can be seen that the injection of fuel initiates faster and ends slower when the GTL fraction is higher in fuel blends. It can be clearly seen in the case of lower injection pressure i.e. 400 bar. However, there is not such a big difference for higher injection pressure over 800 bar.

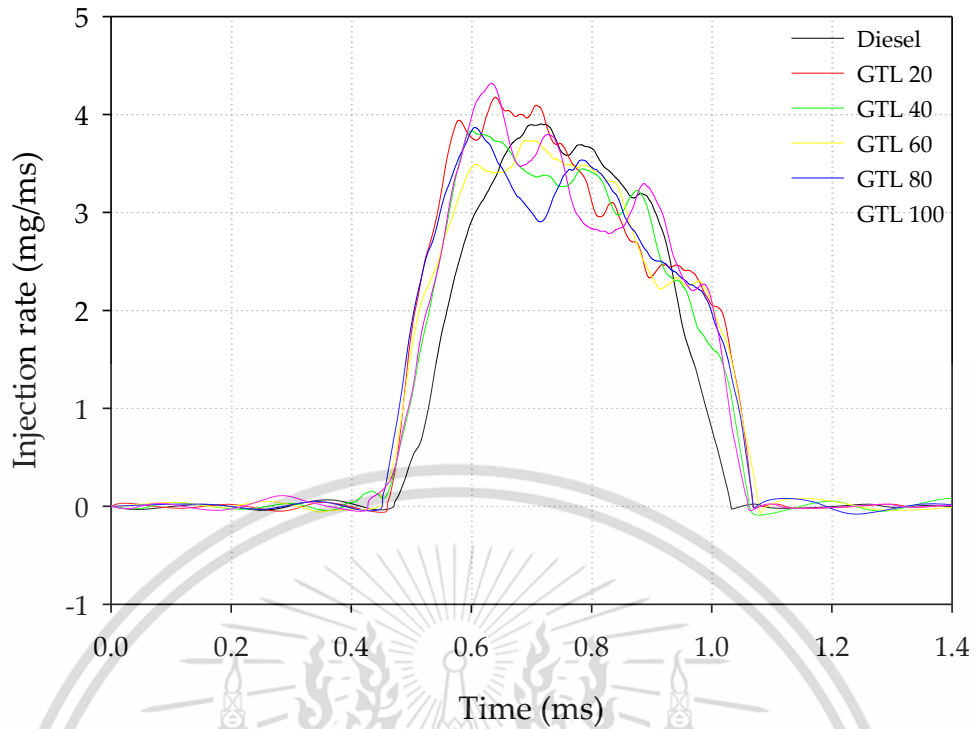


Figure 4.7 Injection rate profile at $P_i = 400$ bar, $T_e = 0.5$ ms, and $P_b = 45$ bar

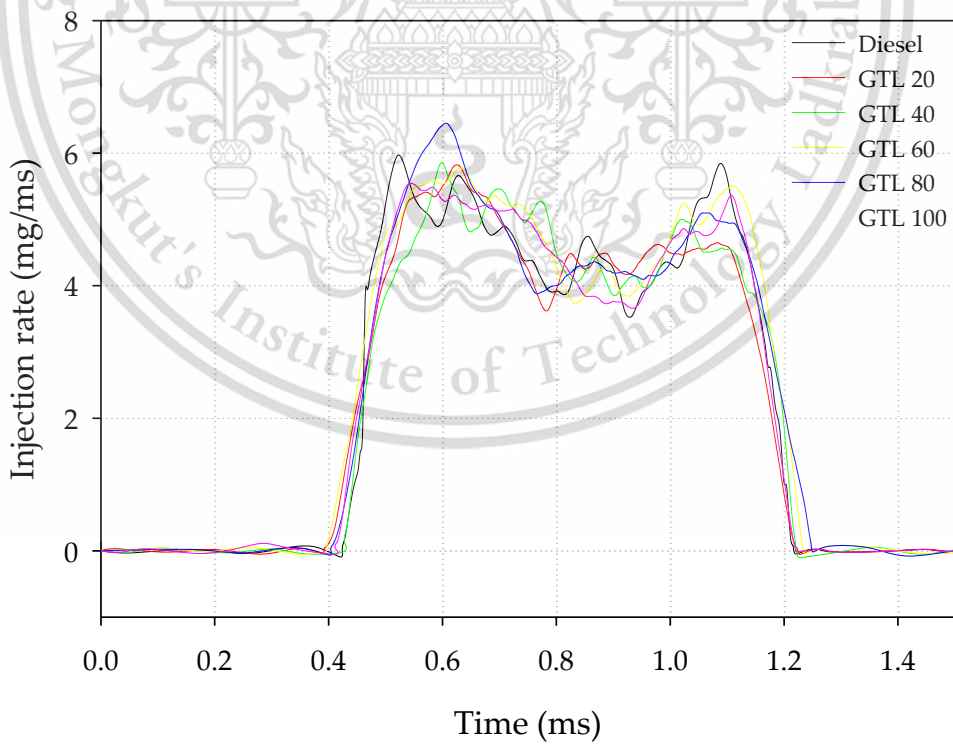


Figure 4.8 Injection rate profile at $P_i = 800$ bar, $T_e = 0.5$ ms, and $P_b = 45$ bar

This material is reserved for educational use only, not allowed for commercial use.

Forbidden to modify the content, and cite the document when use.

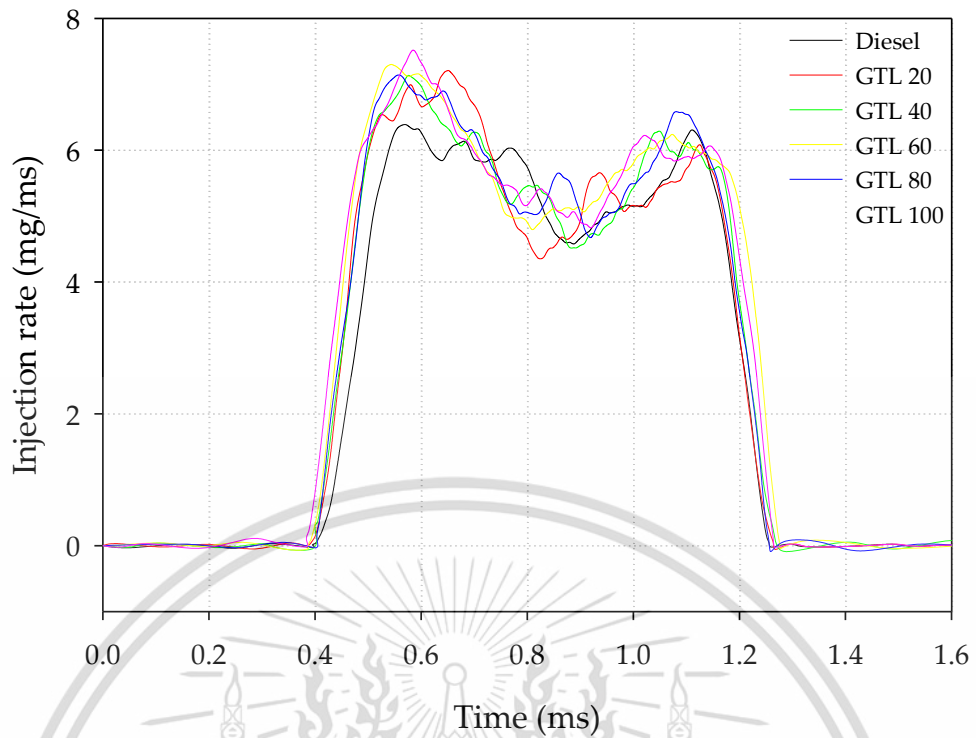


Figure 4.9 Injection rate profile at $P_i = 1200$ bar, $T_e = 0.5$ ms, and $P_b = 45$ bar

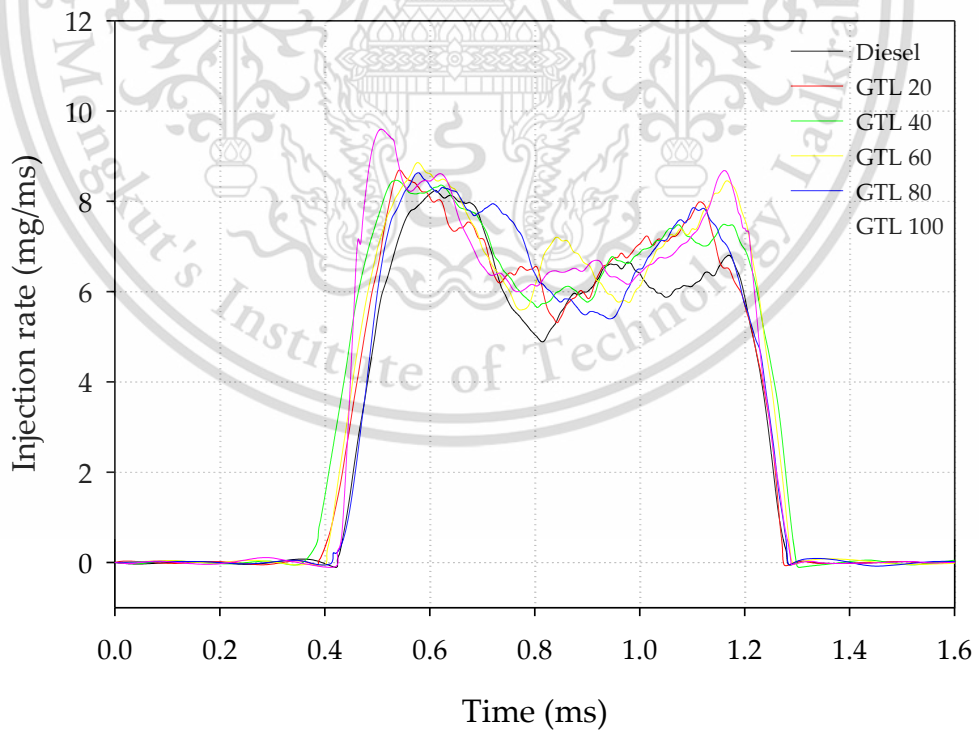


Figure 4.10 Injection rate profile at $P_i = 1600$ bar, $T_e = 0.5$ ms, and $P_b = 45$ bar

4.2.1.2 Injection rate profiles at $T_e = 1.0$ ms

The injection rate profile for all the studied fuels, performed with an injector energizing duration of 1.0 ms, injection pressure of 400 to 1600 bar and ambient pressure of 45 bar are illustrated from Figure 4.11 to Figure 4.14. For all fuel types, the observed injection rate profiles are in rectangular shape. For all studied fuels, it can be seen that the injection of fuel initiates faster and ends slower when the GTL fraction is higher in fuel blends at lower injection pressure. However, there is no such a great effect for higher injection pressure over 800 bar.

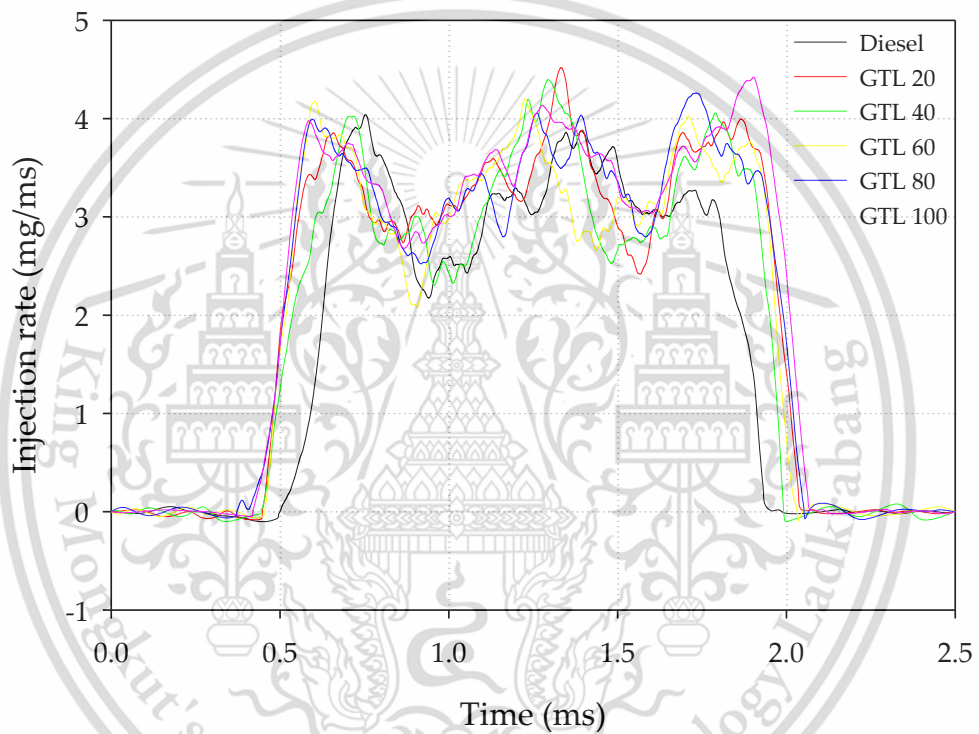


Figure 4.11 Injection rate profile at $P_i = 400$ bar, $T_e = 1.0$ ms, and $P_b = 45$ bar

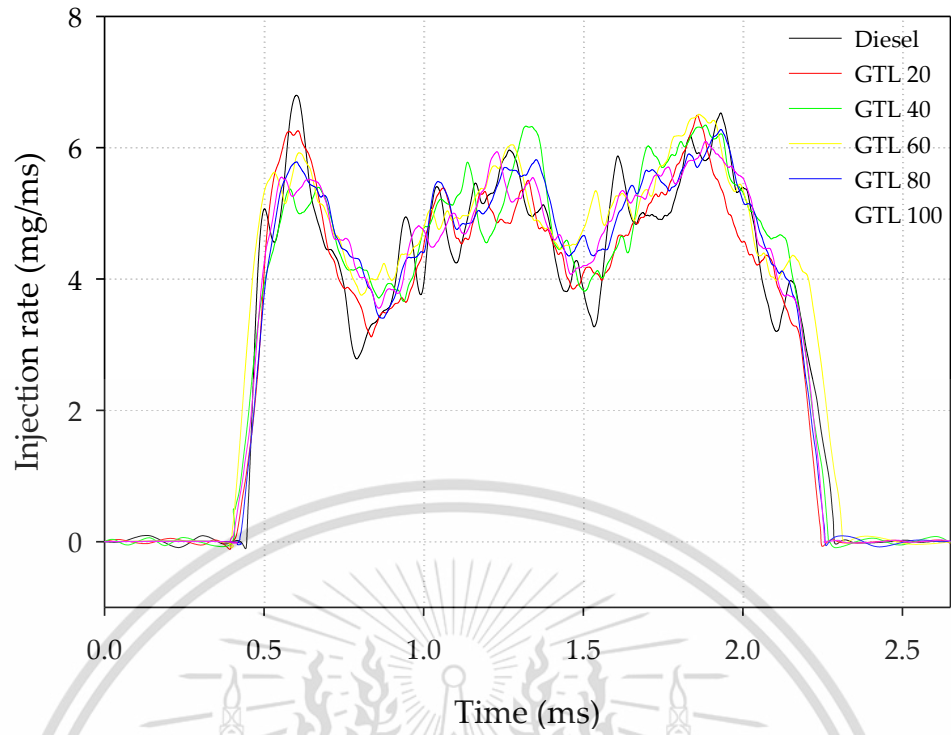


Figure 4.12 Injection rate profile at $P_i = 800$ bar, $T_e = 1.0$ ms, and $P_b = 45$ bar

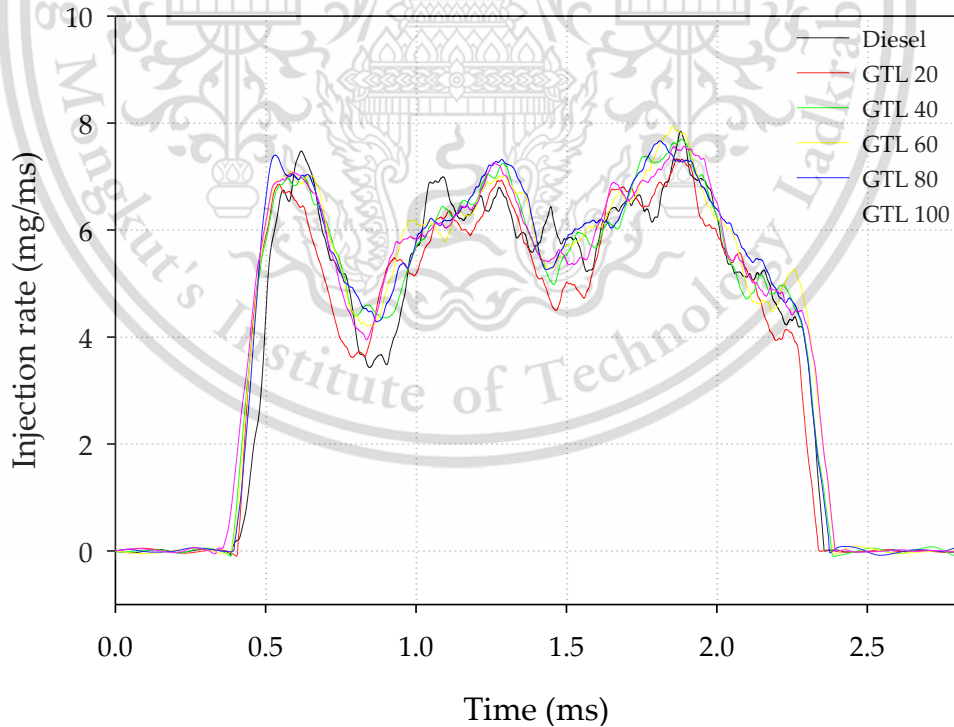


Figure 4.13 Injection rate profile at $P_i = 1200$ bar, $T_e = 1.0$ ms, and $P_b = 45$ bar

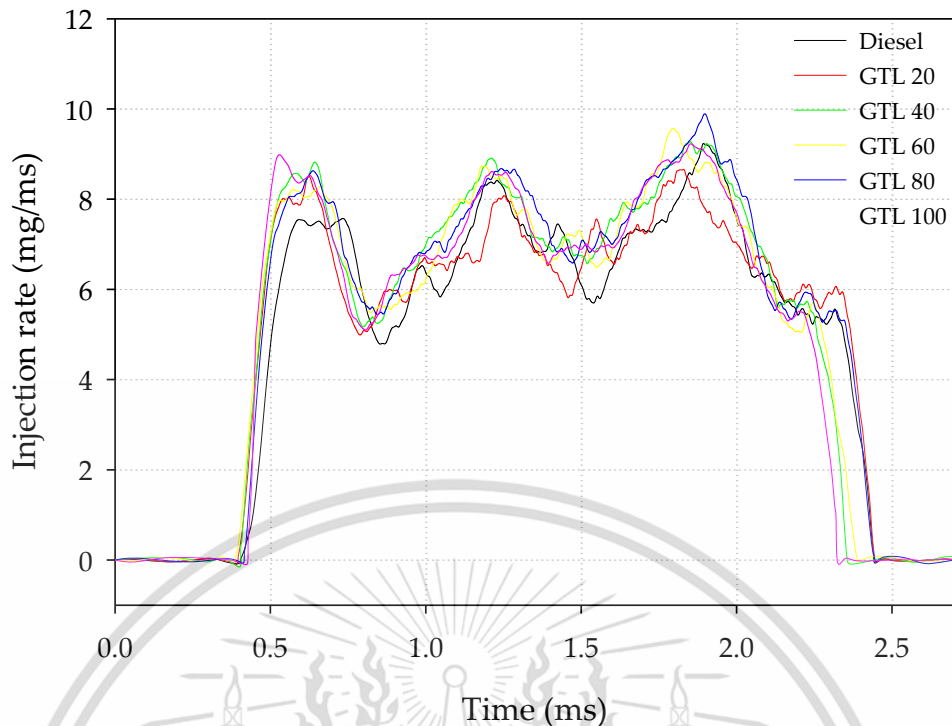


Figure 4.14 Injection rate profile at $P_i = 1600$ bar, $T_e = 1.0$ ms, and $P_b = 45$ bar

4.2.1.3 Injection rate profiles at $T_e = 2.5$ ms

The injection rate profile for all the studied fuels, performed with an injector energizing duration of 2.5 ms, injection pressure of 400 to 1600 bar and ambient pressure of 45 bar are illustrated from Figure 4.15 to Figure 4.18. For all fuel types, the observed injection rate profiles are of rectangular form. In case of long injector energizing duration 2.5 ms, the injection behavior is quite different than short energizing duration 0.5, 1.0 ms. It can be seen that the injection of fuel initiates faster and also ends faster when the GTL fraction is higher in fuel blends. For lower injection pressure i.e. 400 bar, the initiation of fuel injection is earlier for neat GTL and injection stops quite earlier as well. However, for higher injection pressure over 800 bar, there is not much difference in initiation of fuel injection, but the end period of fuel injection is same as low injection pressure condition.

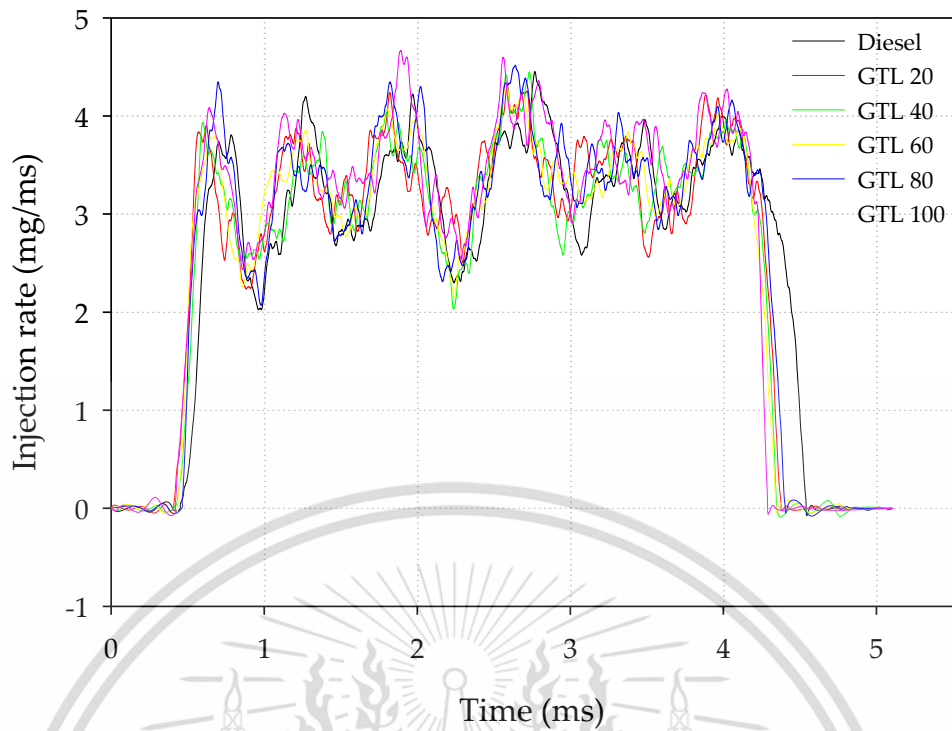


Figure 4.15 Injection rate profile at $P_i = 400$ bar, $T_e = 2.5$ ms, and $P_b = 45$ bar

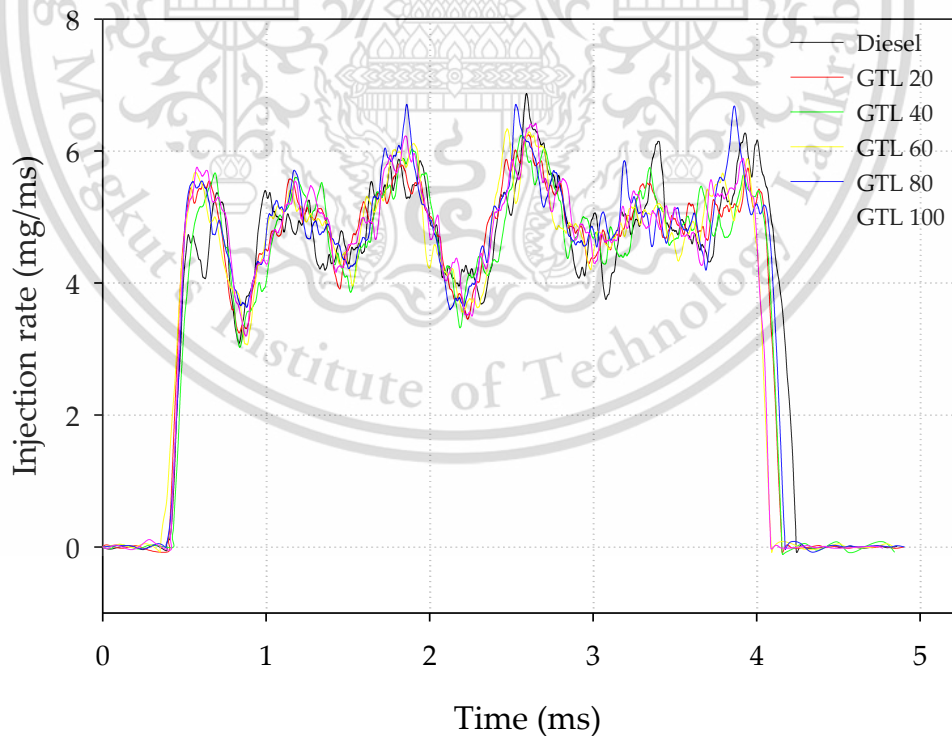


Figure 4.16 Injection rate profile at $P_i = 800$ bar, $T_e = 2.5$ ms, and $P_b = 45$ bar

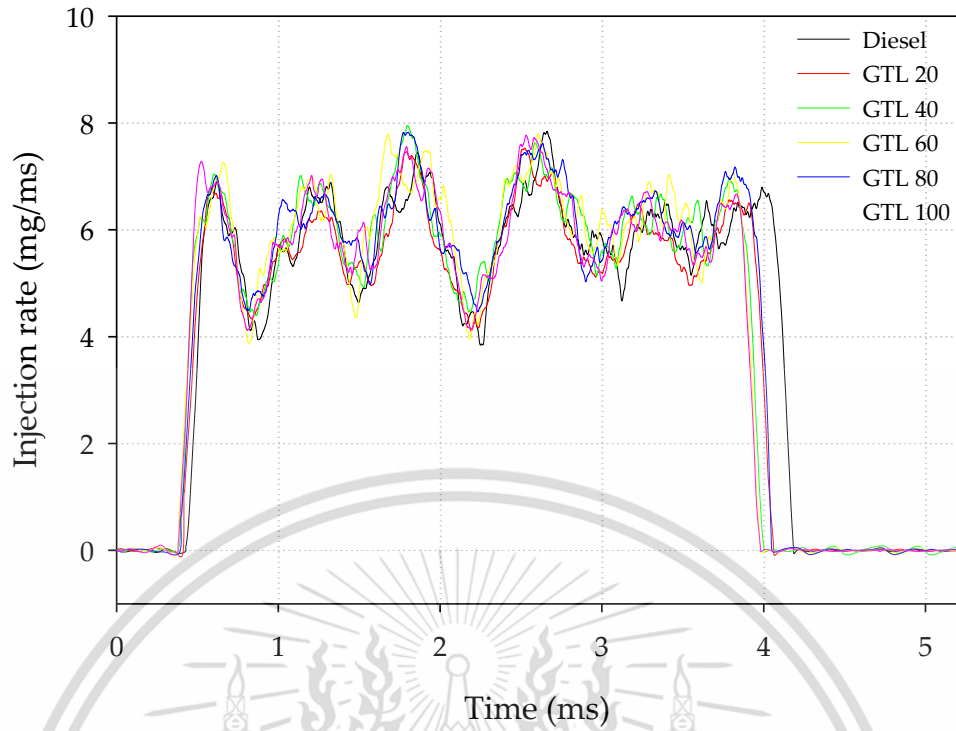


Figure 4.17 Injection rate profile at $P_i = 1200$ bar, $T_e = 2.5$ ms, and $P_b = 45$ bar

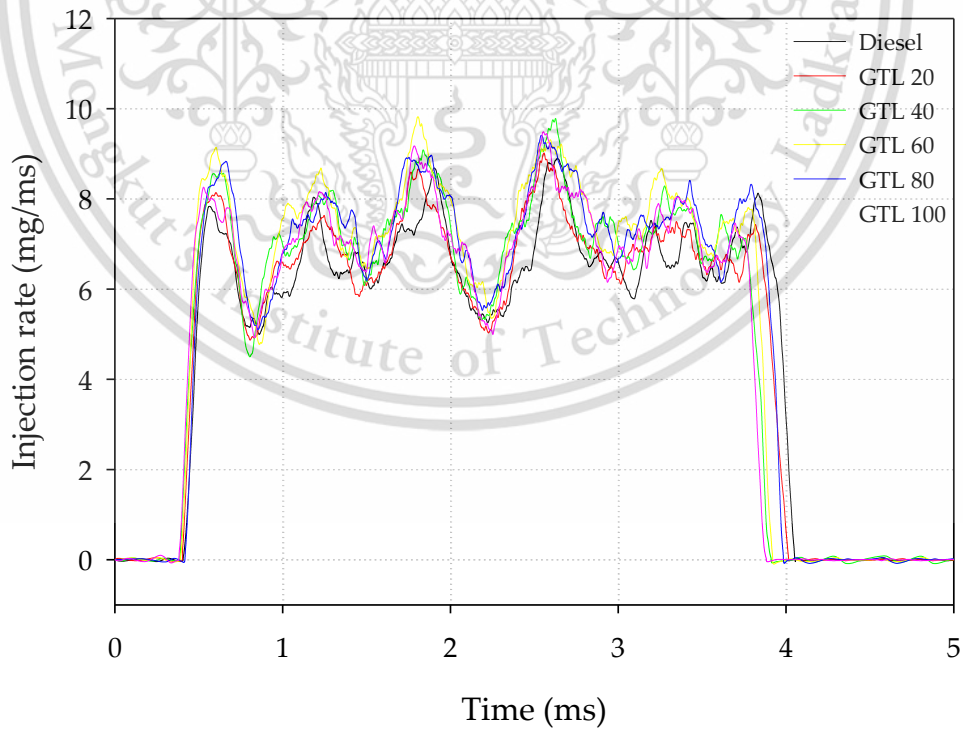


Figure 4.18 Injection rate profile at $P_i = 1200$ bar, $T_e = 2.5$ ms, and $P_b = 45$ bar

4.2.2. Injection delay time

The injection delay time for all test fuels have been measured and compared for all injection pressure and compared. The Figure 4.19 illustrates the detail of injection delay time for all test fuels at injection pressure of 400, 800, 1200 and 1600 bar. The experiment was performed in room temperature and back pressure was identical at 45 bar. From the result, it can be seen that commercial diesel fuel shows quite longer and GTL 100 shows relatively shorter injection delay timing in comparison with rest of the test fuels in all injection pressure condition. The higher viscosity of GTL may lead to reduced fuel losses during injection process leading faster evolution of pressure and thus advance in fuel injection timing [42]. However, in the case of GTL-diesel blends, it is quite different for each injection pressure conditions.

All injection delay data lie in a range of 0.37 to 0.47 ms. It is observed that the value is decreased with increased injection pressure which may be because of higher injection pressure. This injection pressure provides higher force to lift the needle more quickly so as to lowering the delay time [24]. When the pressure increased from 400 to 800 bar, a trivial decrease in injection delay time is noticed. Furthermore, when injection pressure goes higher from 800 to 1200 and 1200 to 1600 bar, delay time is not significantly decreased. The decreasing trend shows a good agreement with work presented by Han et al [24].

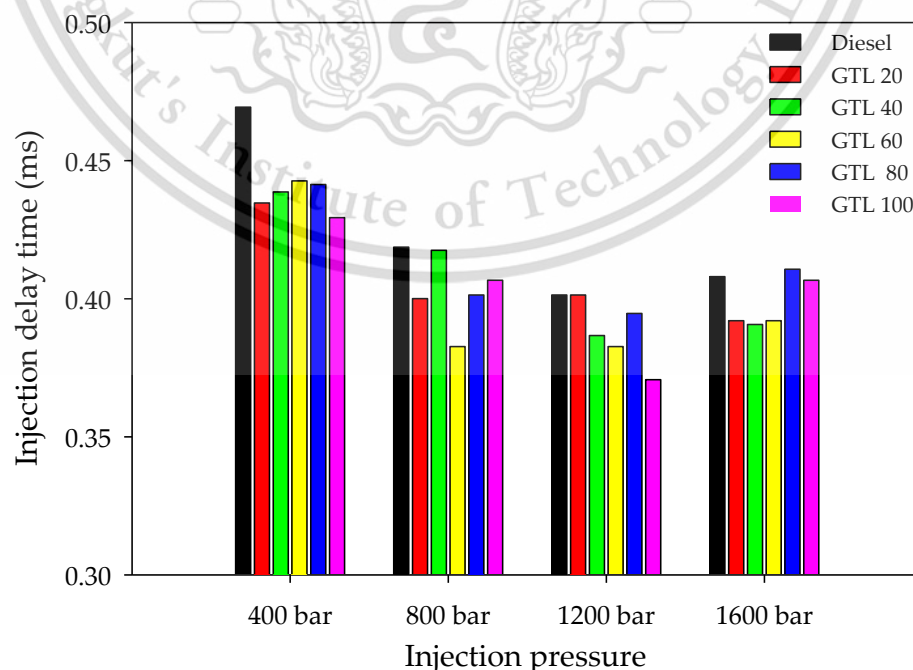


Figure 4.19 Injection delay for set of test fuels at different injection pressure

This material is reserved for educational use only, not allowed for commercial use.

Forbidden to modify the content, and cite the document when use.

4.2.3. Fuel injection quantity (mass)

For better understanding on the effect of fuel properties to injection behavior, the amount of fuel injection has been measured and compared for all test fuels under the same experimental condition. Figure 4.20, Figure 4.21 and Figure 4.22 illustrate the result of injection quantity for all test fuels at injector energizing duration of 0.5, 1.0 and 2.5 ms respectively. In spite of having lower fuel density of GTL, the amount of fuel injection is higher as compared to the rest fuel for identical condition. Diesel fuel shows the lower injection amount for all test condition regardless of injection pressure and injector energizing duration. Previous study presented by Boudye et al [43] concluded that at single main injection, viscosity has greater impact on fueling compared to density, which may be the reason to have higher injection mass of GTL. For rest of the blended fuel, the amount of injection is getting higher with higher GTL fraction in the blends. But, GTL 80 shows quite uneven pattern.

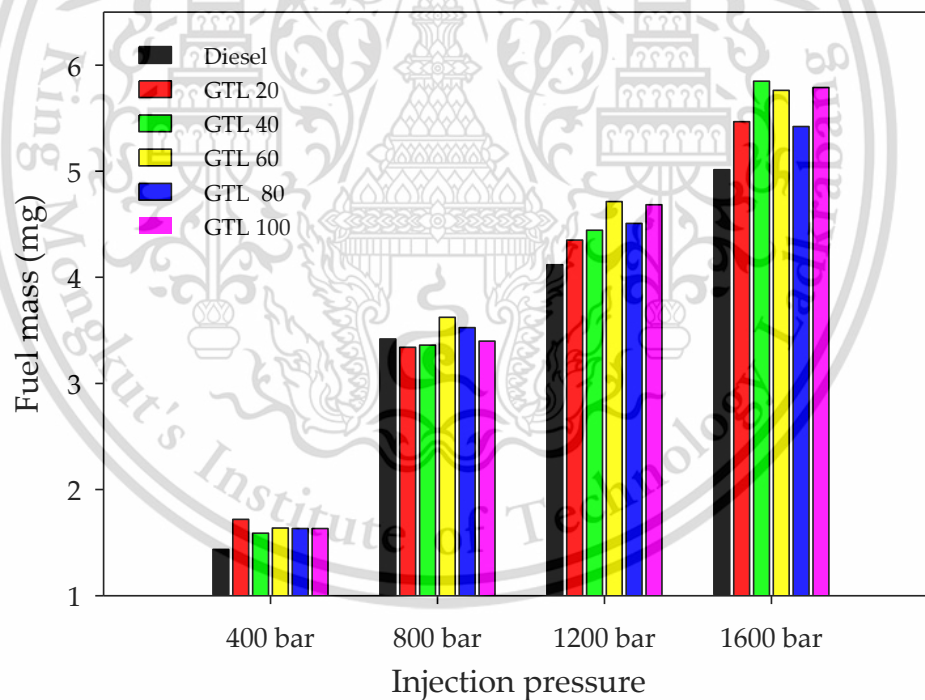


Figure 4.20 Amount of fuel injection with different injection pressure at $T_e = 0.5$ ms

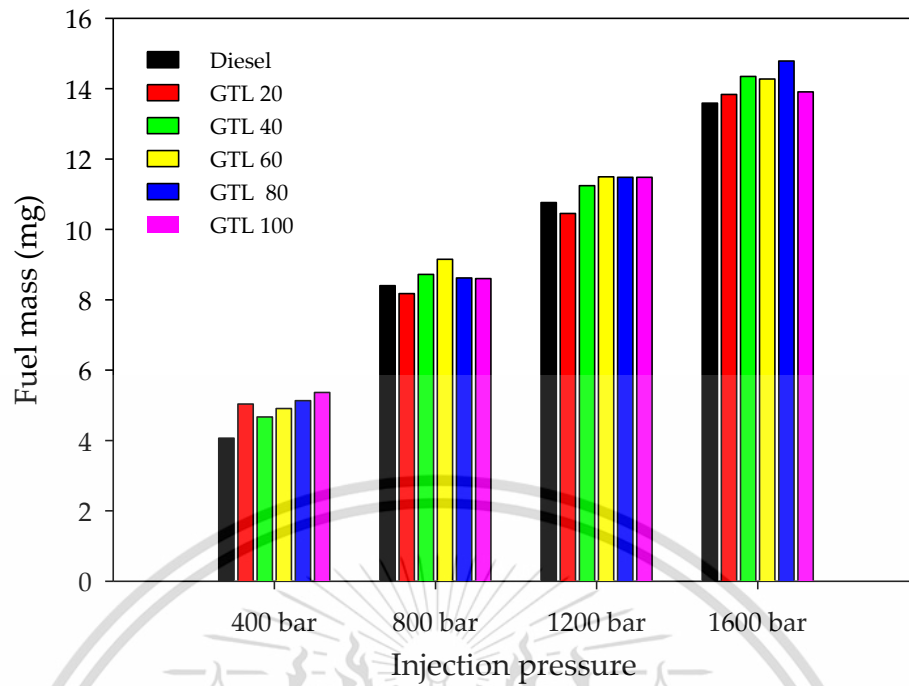


Figure 4.21 Amount of fuel injection with different injection pressure at $T_e = 1.0$ ms

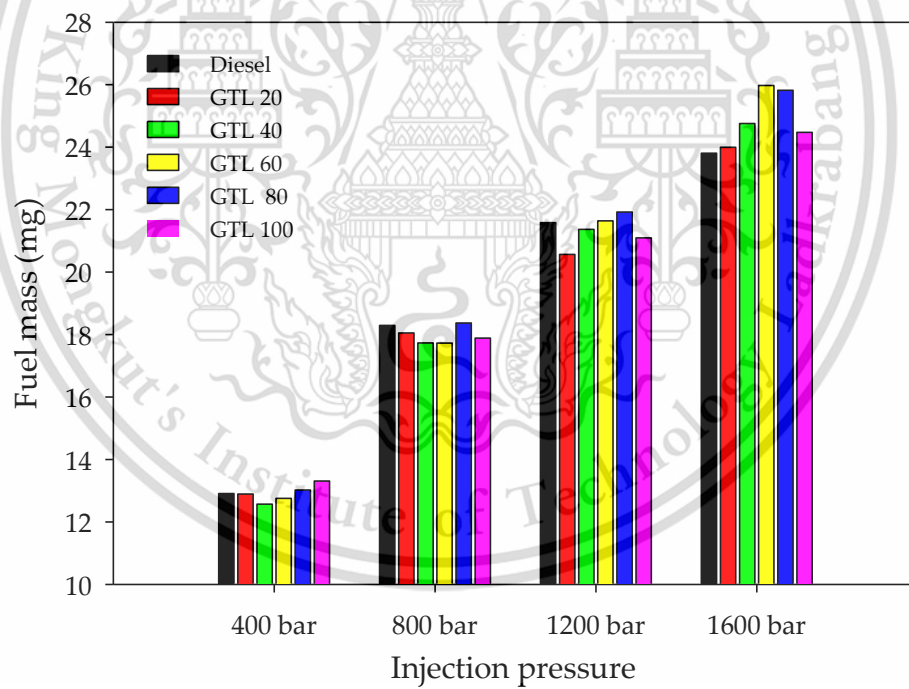


Figure 4.22 Amount of fuel injection with different injection pressure at $T_e = 2.5$ ms

4.2.4. Coefficient of discharge

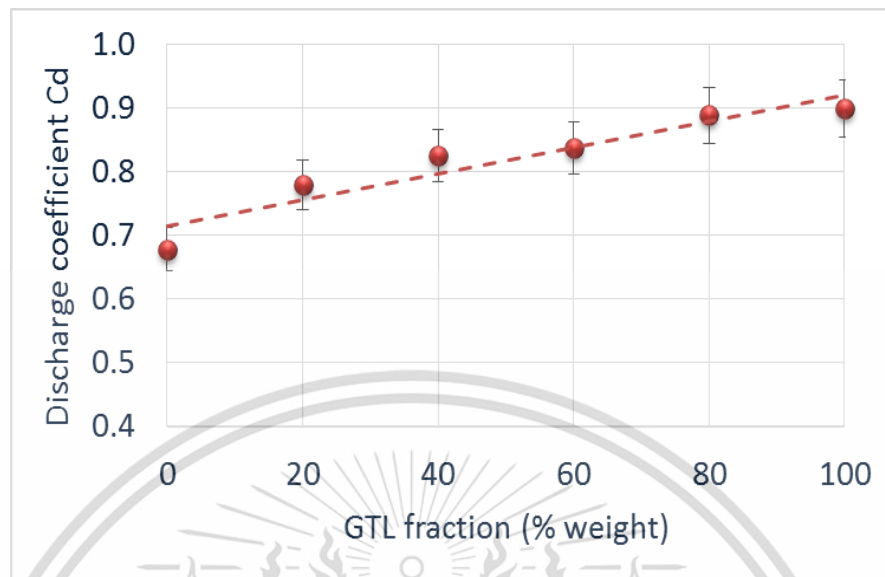


Figure 4.23 Coefficient of discharge vs GTL fraction

Coefficient of discharge is an important factor for diesel engine combustion. It has a major effect on the amount of fuel injected per cycle into the combustion chamber. The discharge coefficient value has been calculated using Equation 3.4. Figure 4.23 illustrates the coefficient of discharge measured during this experimental study. The result shows that with increasing of GTL fraction in blended fuels, the value of discharge coefficient is increasing linearly. Since coefficient of discharge is a flow property, in which mass gets higher with higher density and higher viscosity value effect on flow causing the lower mass. However, in spite of having lower density and higher viscosity value GTL showed larger injection mass. This result contradicts with result reported by Dernote et al [23] in which Cd is lower with increased fuel viscosity.

4.3. Spray analysis

The macroscopic spray behavior has been studied for all test fuels in order to understand effect of fuel properties. As the air-fuel mixing process is a key event in diesel combustion, a good knowledge of the formation of the spray help a lot to improve mixing efficiency. In general, the spray penetration length and spray angle are the parameters used to judge fuel spray performance in macroscopic level. The merits of high or low penetration/angel largely depend on engine design and geometry. For example, shorter spray penetration may be of an advantage where it reduces fuel impingement, but in larger engines may need longer spray penetration for maximum air utilization. Thus, the obtained results of spray penetration, spray angle, spray velocity and spray volume for different fuel blends in different measurement conditions are reported in this work. Figure 4.24 shows the raw images of spray evolution of GTL and diesel fuel.

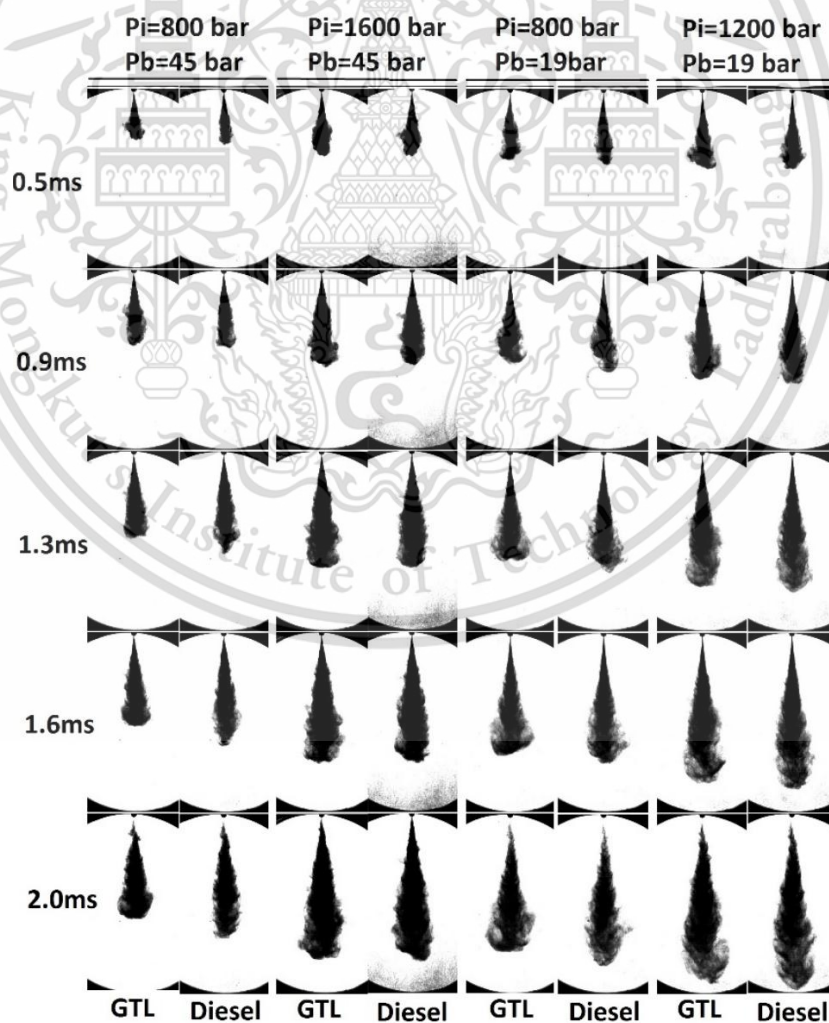


Fig.4.24 Spray images of GTL and diesel at different test condition

This material is reserved for educational use only, not allowed for commercial use.

Forbidden to modify the content, and cite the document when use.

4.3.1. Spray penetration

Spray tip penetrations of all the fuels at different injection pressure are measured. In this section, the obtained results are divided in to two subsections based on two back pressure selected in the experiments.

4.3.1.1 Spray penetration at $P_b=19$ bar

The spray penetration length for all studied fuels, performed with injection pressures of 800 and 1200 bar and injector energizing duration of 0.5 and 1.0 ms at back pressure of 19 bar. The results have been compared and illustrated from Figure 4.25 to Figure 4.28.

The result shows that pure diesel fuel has longer spray penetration than the rest of blended fuel. At initial phase of injection, there is no significant difference in penetration length for all fuel. This could be due to higher density of diesel fuel [44]. Increase in GTL fraction in blended fuel leads to decreasing in penetration length. Azimov et al [33] also concluded that diesel showed longer penetration than GTL for identical test condition. The spray penetration pattern is similar for both injection energizing duration. However, when the injection pressure increases from 800bar to 1200bar, the spray penetration also becomes longer. Similarly, the result shows that spray penetration is longer for all test fuel when injector energizing duration changed from 0.5ms to 1.0ms.

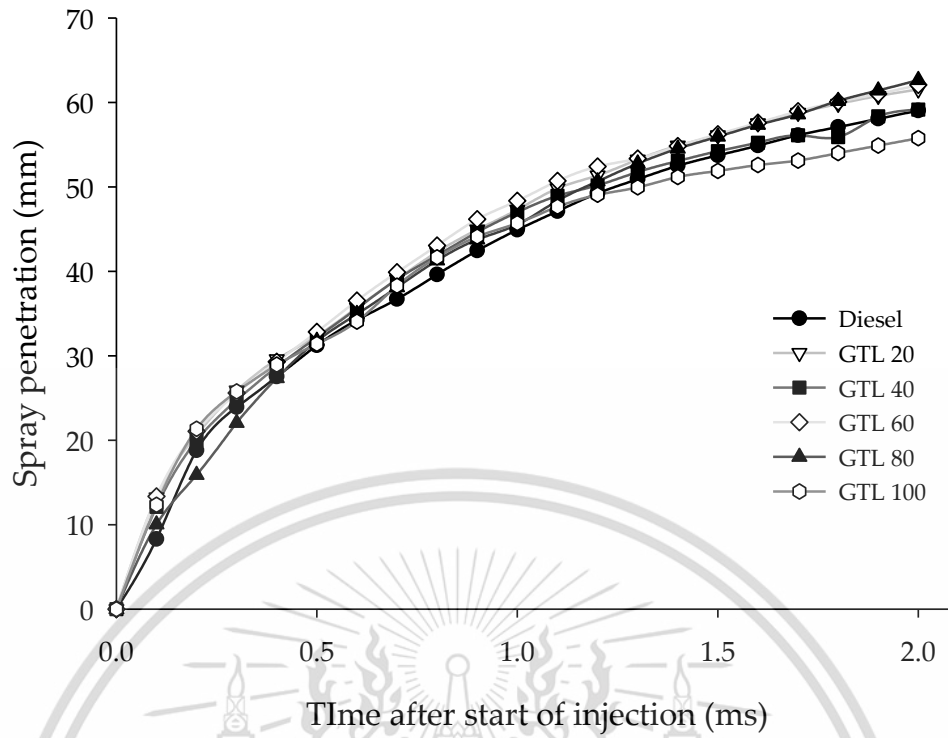


Figure 4.25 Spray penetration at $P_b = 19$ bar, $P_i = 800$ bar, and $T_e = 0.5$ ms

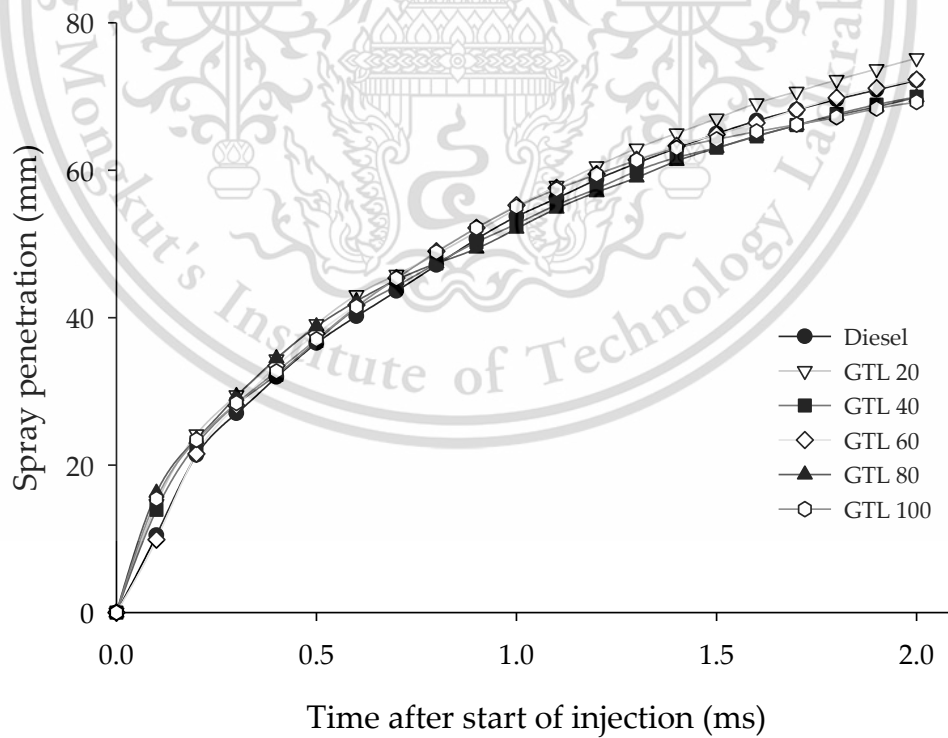


Figure 4.26 Spray penetration at $P_b = 19$ bar, $P_i = 1200$ bar, and $T_e = 0.5$ ms

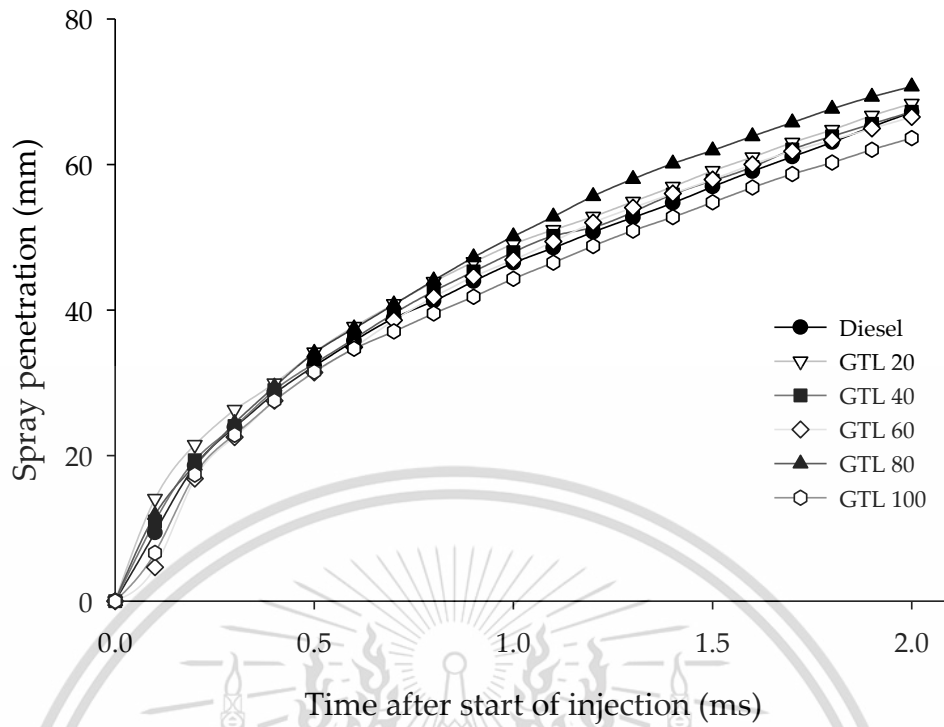


Figure 4.27 Spray penetration at $P_b = 19$ bar, $P_i = 800$ bar, and $T_e = 1.0$ ms

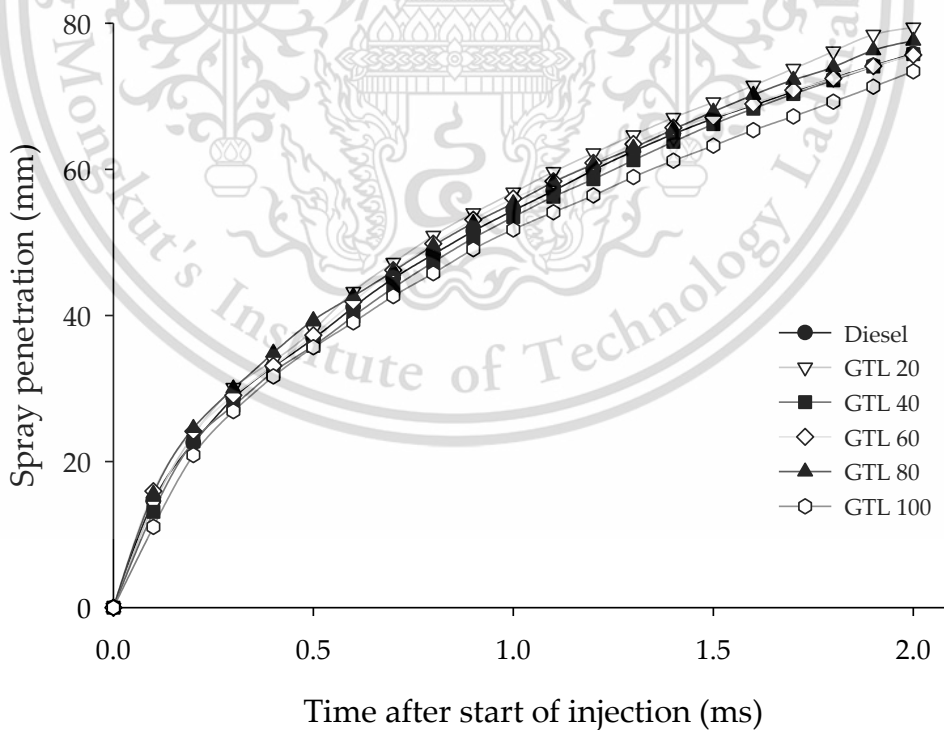


Figure 4.28 Spray penetration at $P_b = 19$ bar, $P_i = 1200$ bar, and $T_e = 1.0$ ms

4.3.1.2 Spray penetration at $P_b=45$ bar

At back pressure of 45bar, the spray penetration length has been studied under injection pressure of 400, 800, 1200 and 1600 bar and injector energizing duration has been varied from 0.5 ms to 1.0 ms. The observed results are illustrated from Figure 4.29 to Figure 4.35 below.

Here also, the diesel shows longer penetration than the rest of tested fuels. In general, the similar patterns could be seen clearly as the penetration is getting shorter with increasing of GTL fraction in blended fuels at all injection pressure condition. The obtained result shows a good agreement with the work reported by Kitano et al [27] and Azimov et al [33]. Moreover, it is also quite near to the result reported by Pyari et al [26]. However, the overall penetration for all blended fuels is increased with increase in injection pressure. It also getting longer with increasing in injector energizing duration from 0.5 to 1.0 ms. The most probable reason behind increasing in penetration length with increase of injection pressure could be, the increase in injection pressure results higher mass flow rate, which results longer penetration length. In other hand at the lower injection pressure where back pressure dominate after injection stop, thus causes momentum loss a lot leading to shorter penetration. The result agrees with the numerical study performed by Shervani-Tabar et al [45] who investigate effect of injection pressure on spray penetration. The result also clearly shows the effect of back pressure on spray penetration. The penetration length becomes shorter while back pressure was increased from 19bar to 45bar.

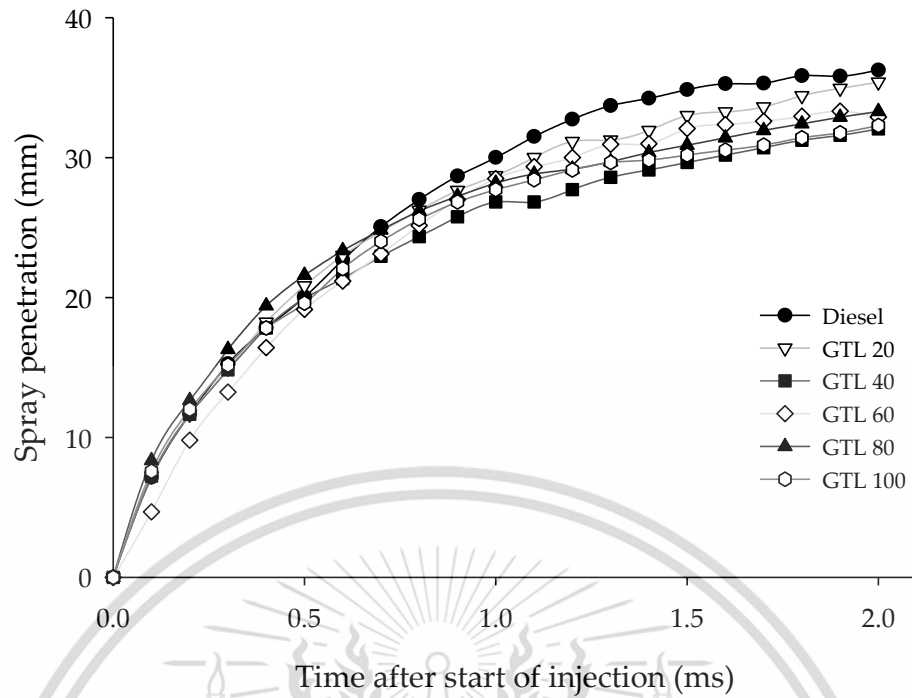


Figure 4.29 Spray penetration at $P_b = 45$ bar, $P_i = 400$ bar, and $T_e = 0.5$ ms

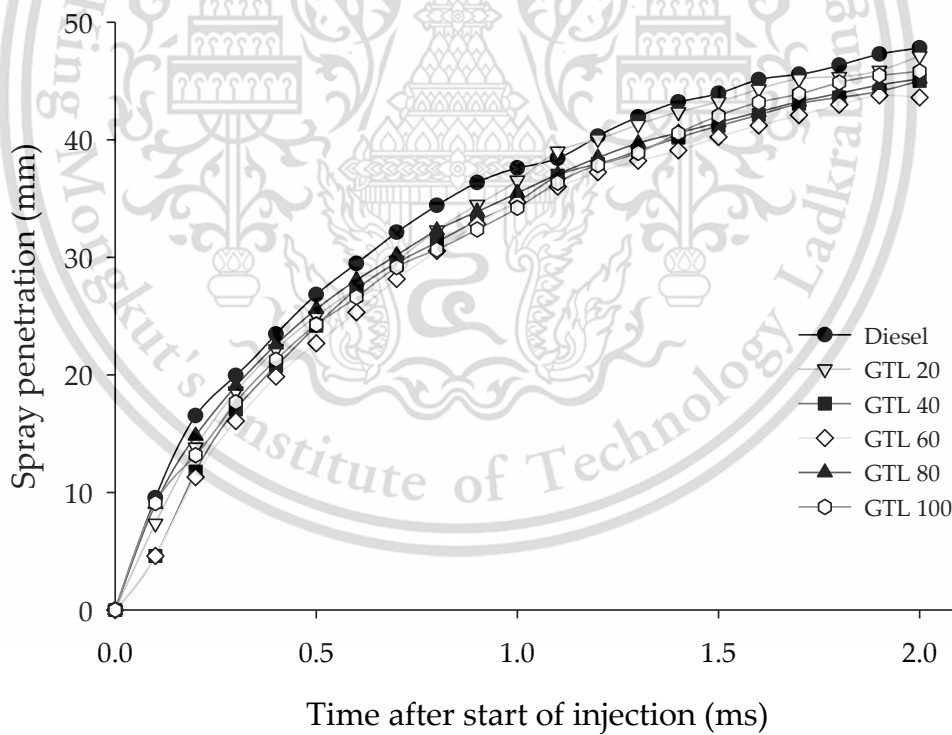


Figure 4.30 Spray penetration at $P_b = 45$ bar, $P_i = 800$ bar, and $T_e = 0.5$ ms

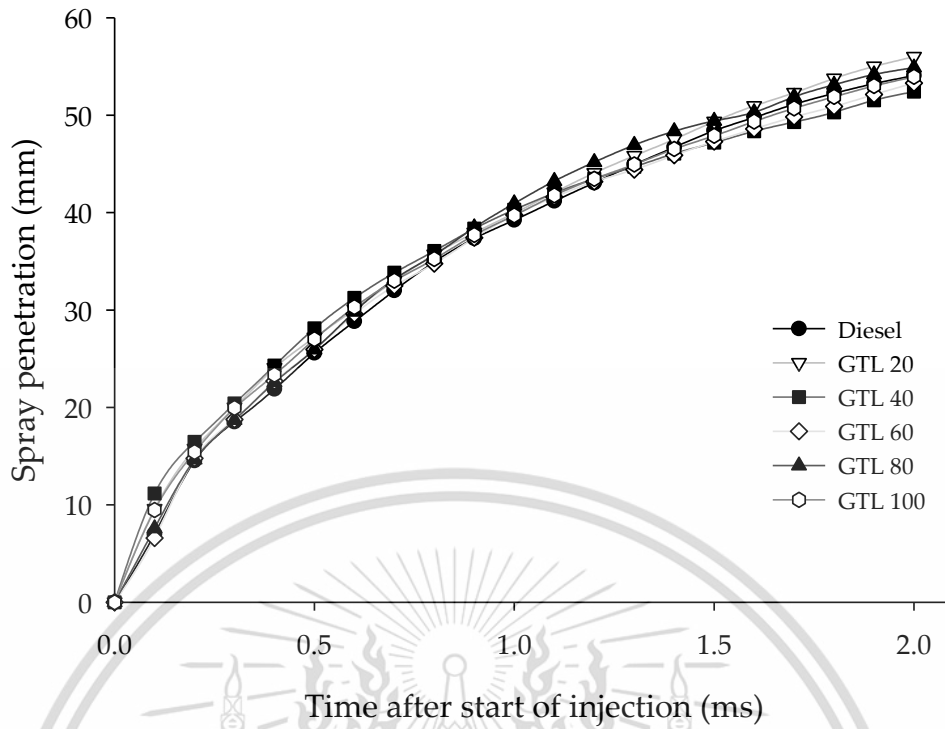


Figure 4.31 Spray penetration at $P_b = 45$ bar, $P_i = 1200$ bar, and $T_e = 0.5$ ms

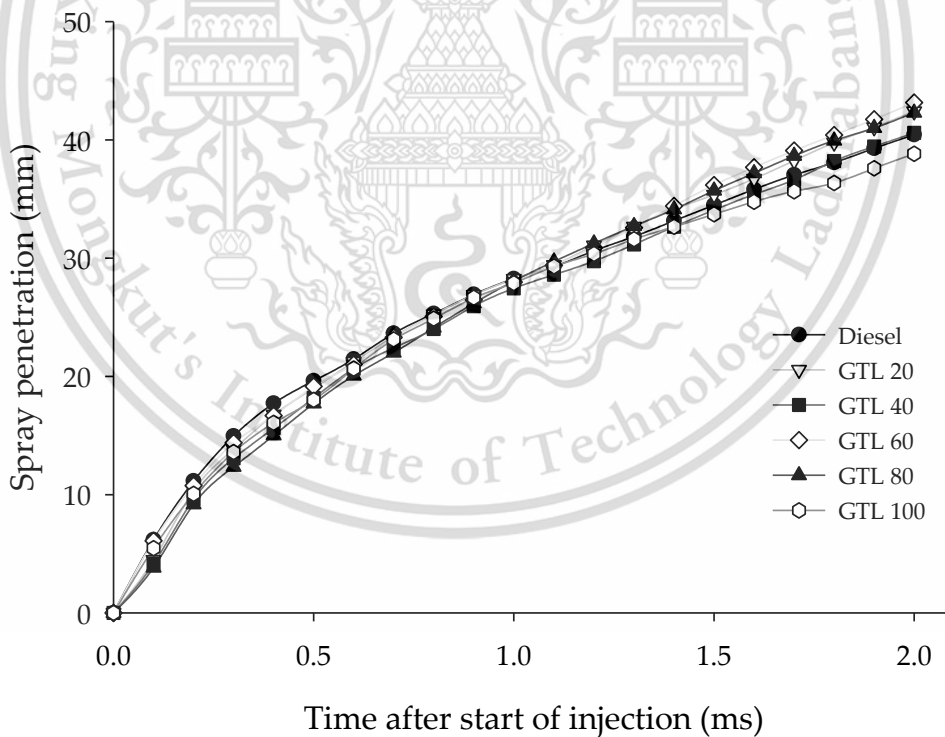


Figure 4.32 Spray penetration at $P_b = 45$ bar, $P_i = 400$ bar, and $T_e = 1$ ms

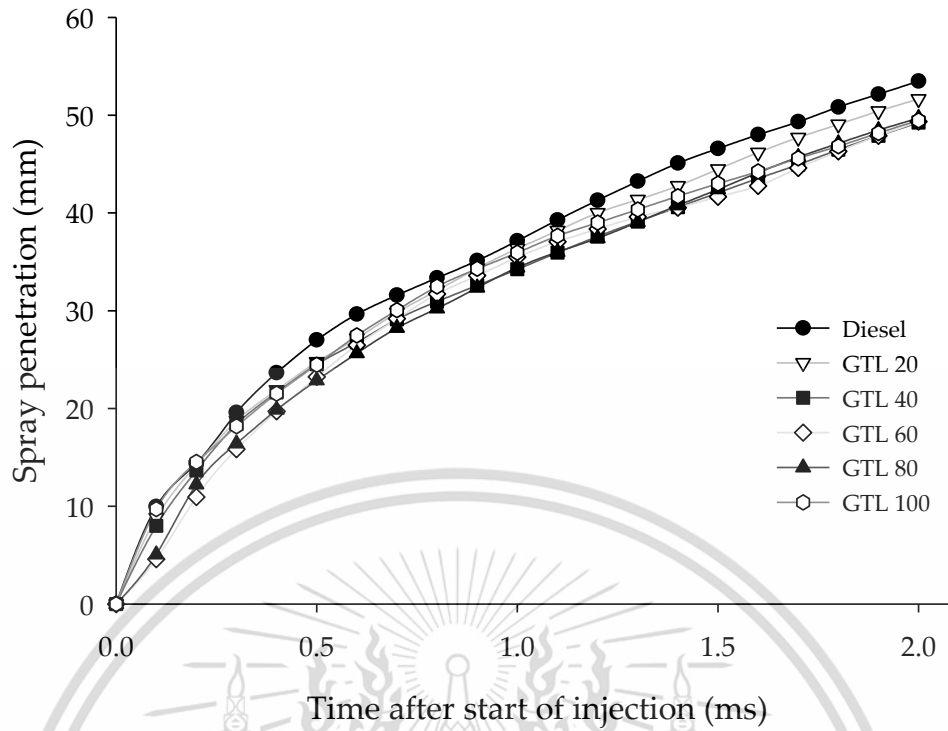


Figure 4.33 Spray penetration at $P_b = 45$ bar, $P_i = 800$ bar, and $T_e = 1$ ms

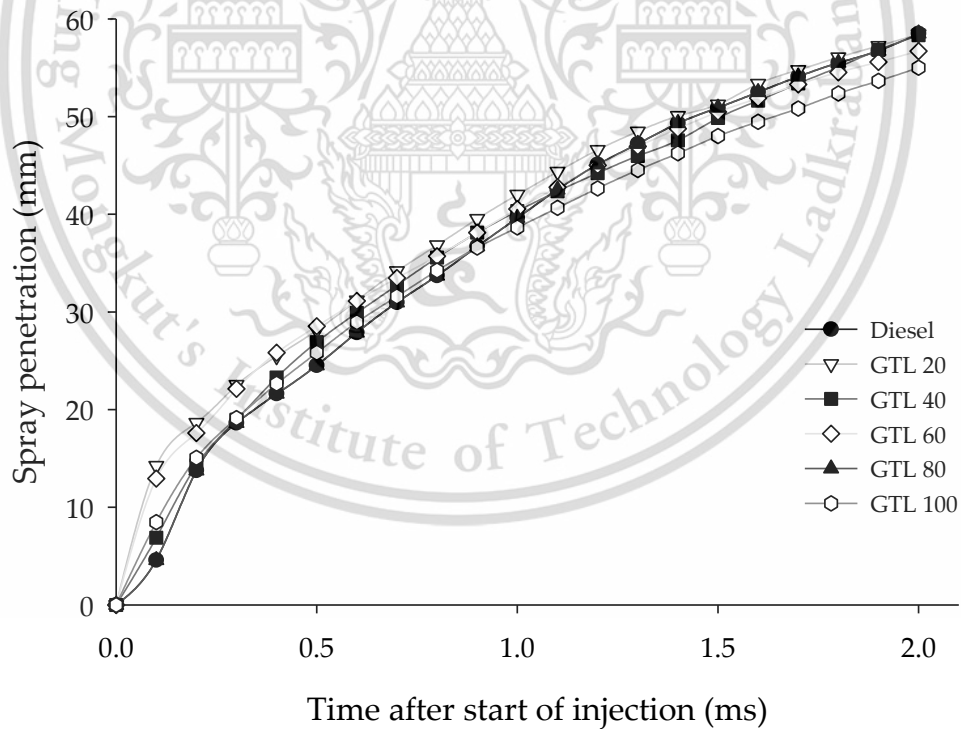


Figure 4.34 Spray penetration at $P_b = 45$ bar, $P_i = 1200$ bar, and $T_e = 1$ ms

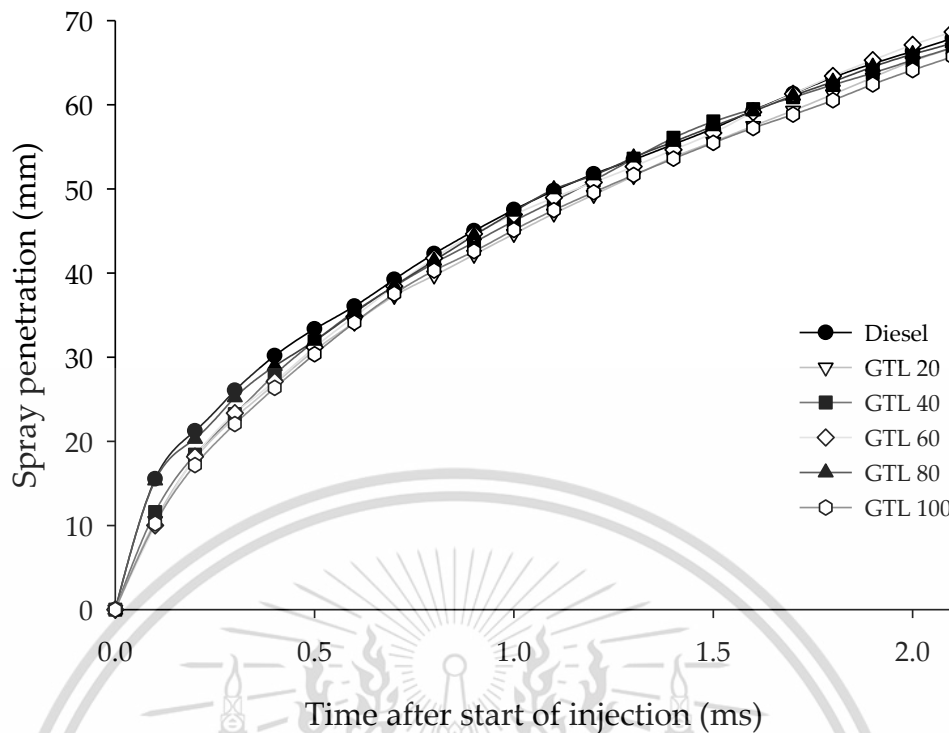


Figure 4.35 Spray penetration at $P_b = 45$ bar, $P_i = 1600$ bar, and $T_e = 1$ ms

4.3.2. Spray angle

The spray angle for all blended fuels, performed with different injection pressure of 400, 800, 1200 and 1600 bar and injector energizing duration of 0.5 and 1.0 ms at back pressure of 19 and 45 bar are compared and illustrated from Figure 4.36 to Figure 4.46.

Result shows the spray angle for diesel fuel decreased rapidly at the beginning and goes constant after a while whereas GTL has higher spray angle at initial stage and lower at later stage. Irrespective of injection pressure and injector energizing duration, the spray angle value for GTL is higher at the initial phase of injection. At later stage, diesel shows higher value in most of the cases. However, its not clear difference for all fuel types at later stages for same measurement conditions.

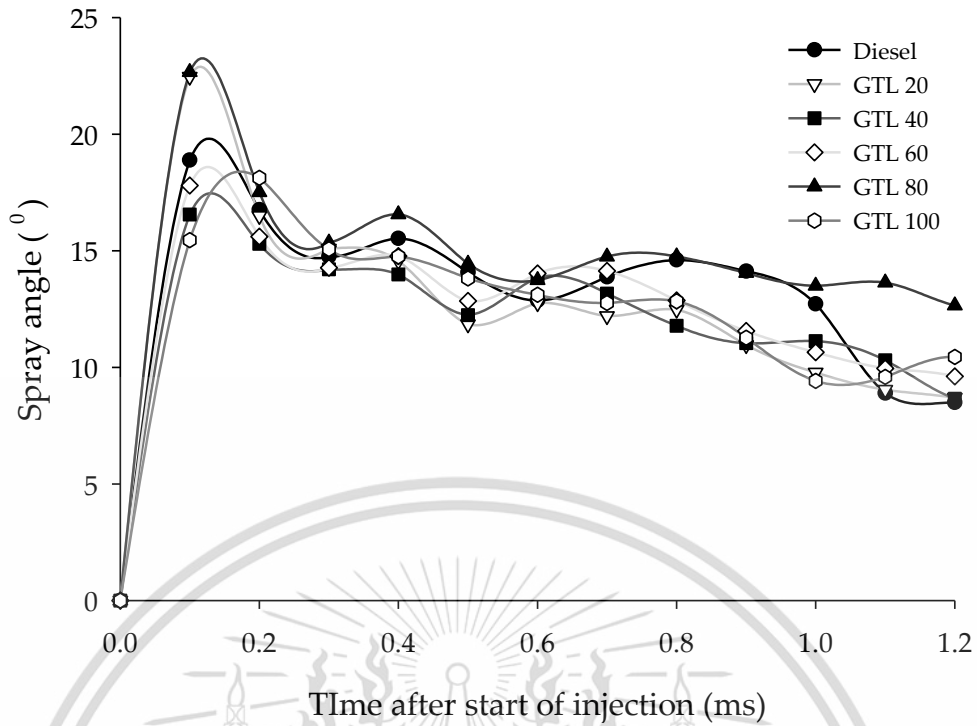


Figure 4.36 Spray angle at $P_b = 19$ bar, $P_i = 800$ bar, and $T_e = 0.5$ ms

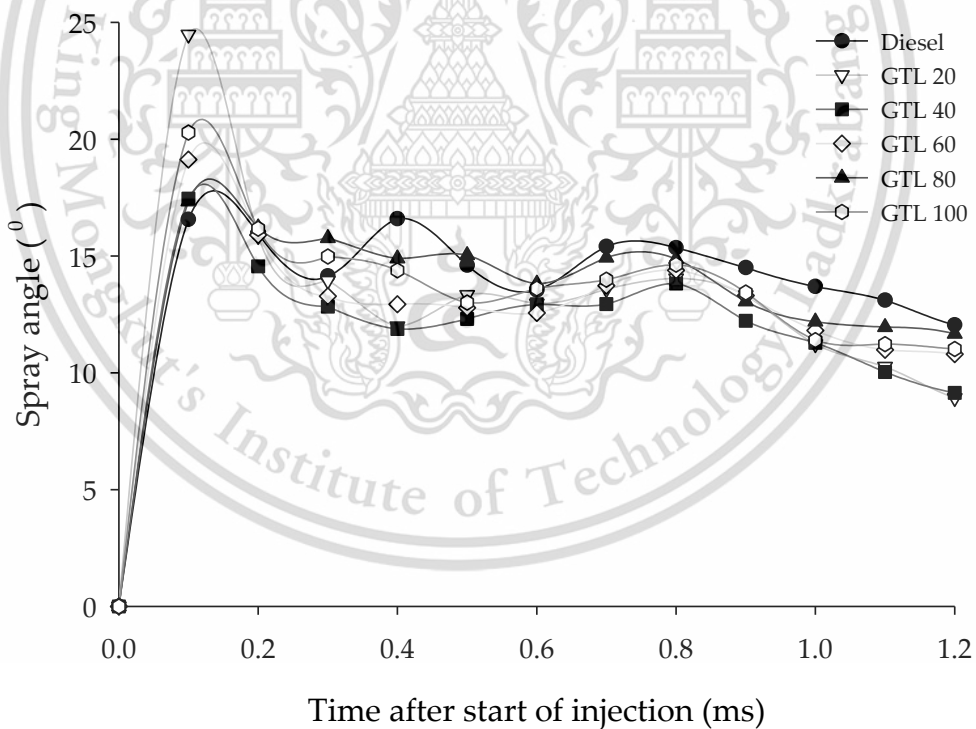


Figure 4.37 Spray angle at $P_b = 19$ bar, $P_i = 1200$ bar, and $T_e = 0.5$ ms

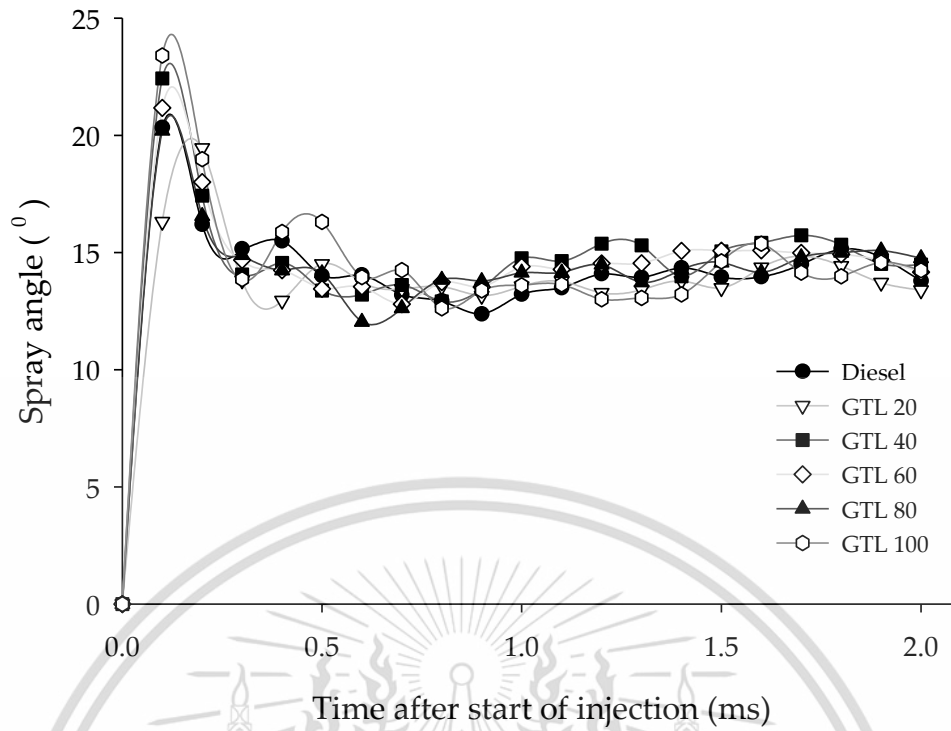


Figure 4.38 Spray angle at $P_b = 19$ bar, $P_i = 800$ bar, and $T_e = 1.0$ ms

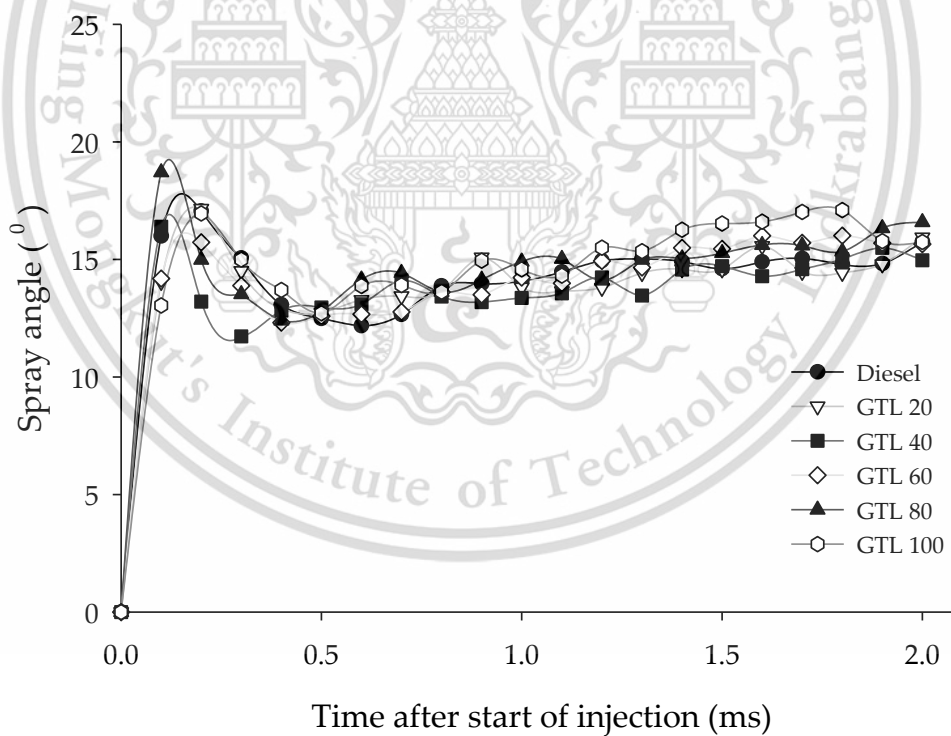


Figure 4.39 Spray angle at $P_b = 19$ bar, $P_i = 1200$ bar, and $T_e = 1.0$ ms

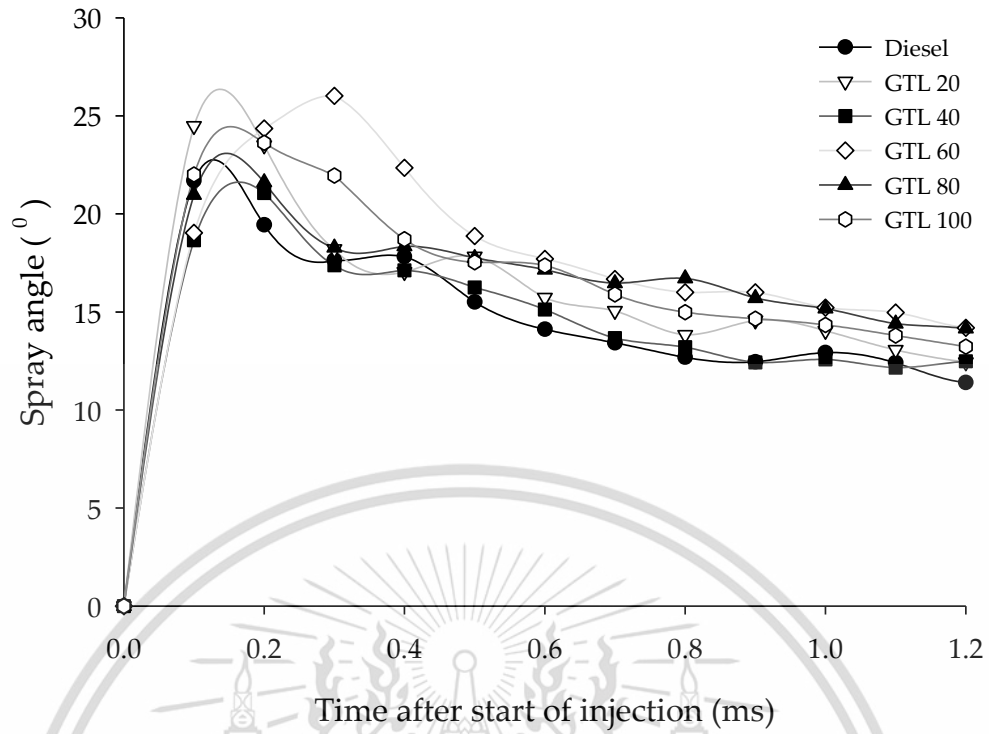


Figure 4.40 Spray angle at $P_b = 45$ bar, $P_i = 400$ bar, and $T_e = 0.5$ ms

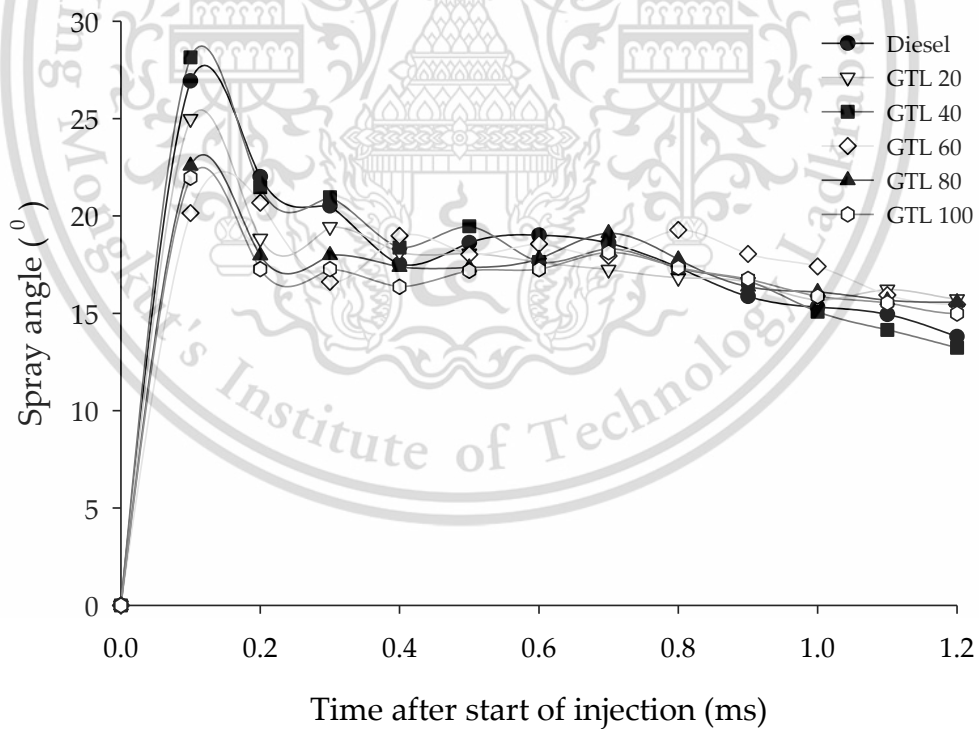


Figure 4.41 Spray angle at $P_b = 45$ bar, $P_i = 800$ bar, and $T_e = 0.5$ ms

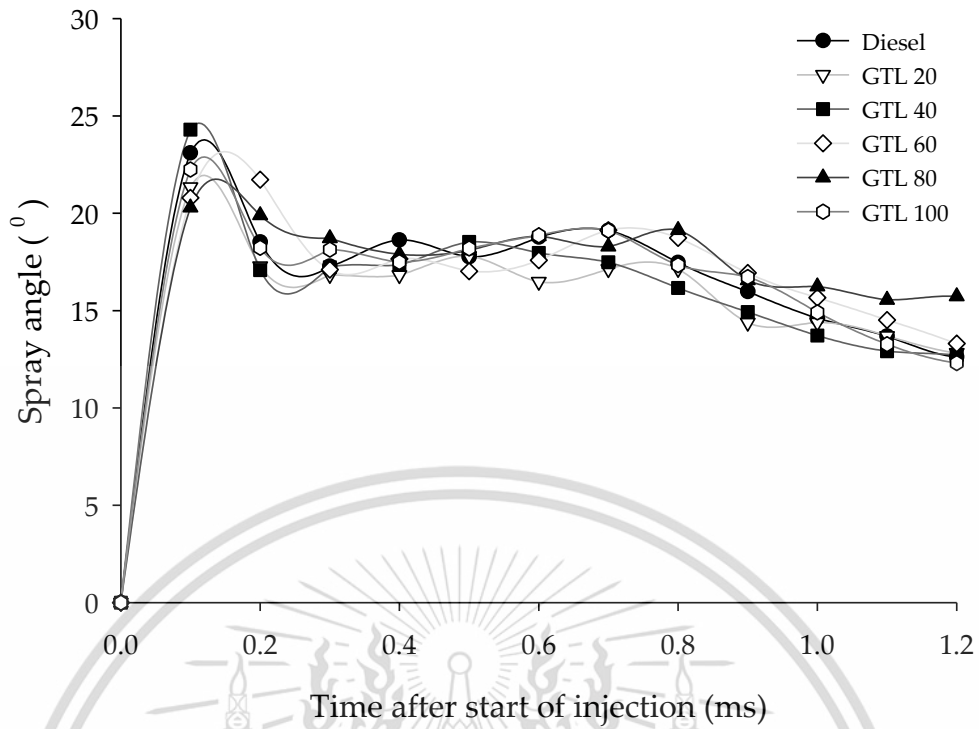


Figure 4.42 Spray angle at $P_b = 45$ bar, $P_i = 1200$ bar, and $T_e = 0.5$ ms

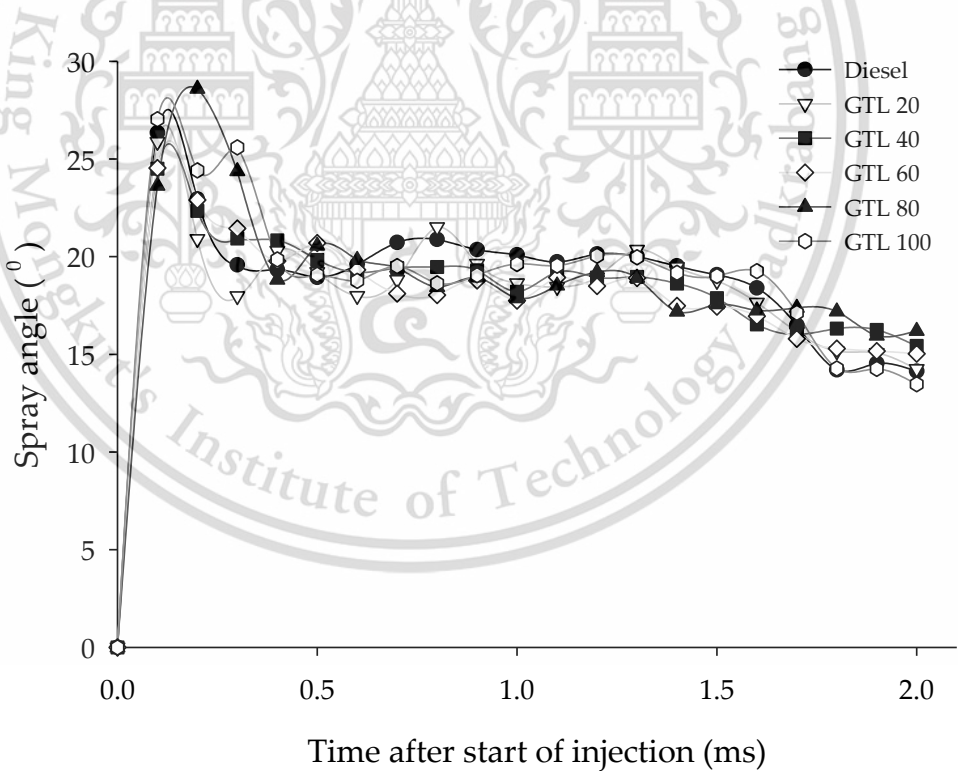


Figure 4.43 Spray angle at $P_b = 45$ bar, $P_i = 400$ bar, and $T_e = 1.0$ ms

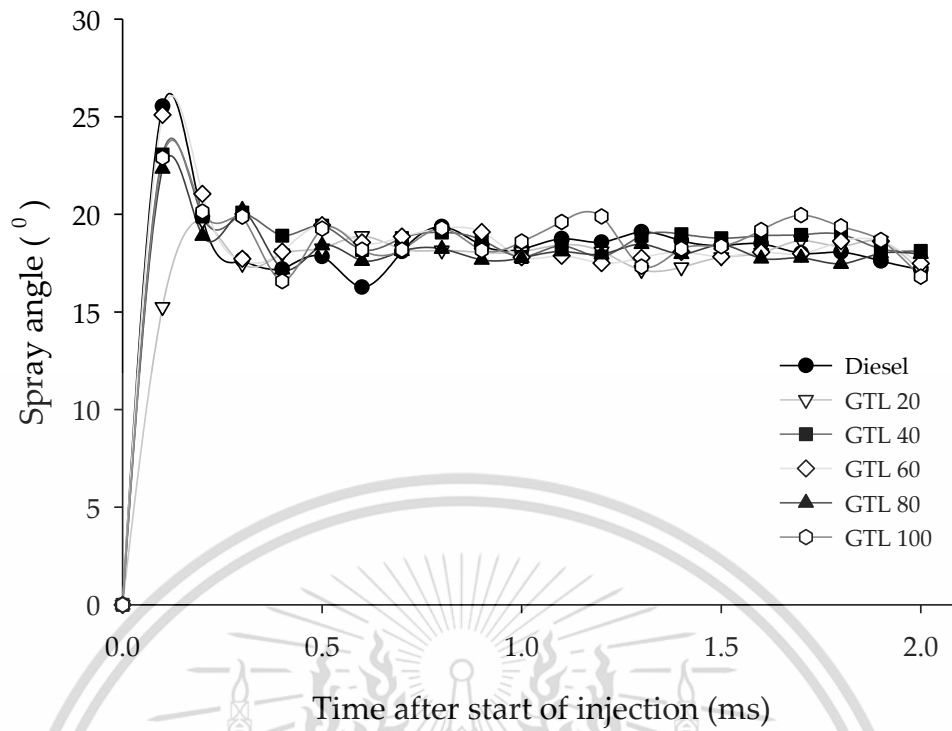


Figure 4.44 Spray angle at $P_b = 45$ bar, $P_i = 800$ bar, and $T_e = 1.0$ ms

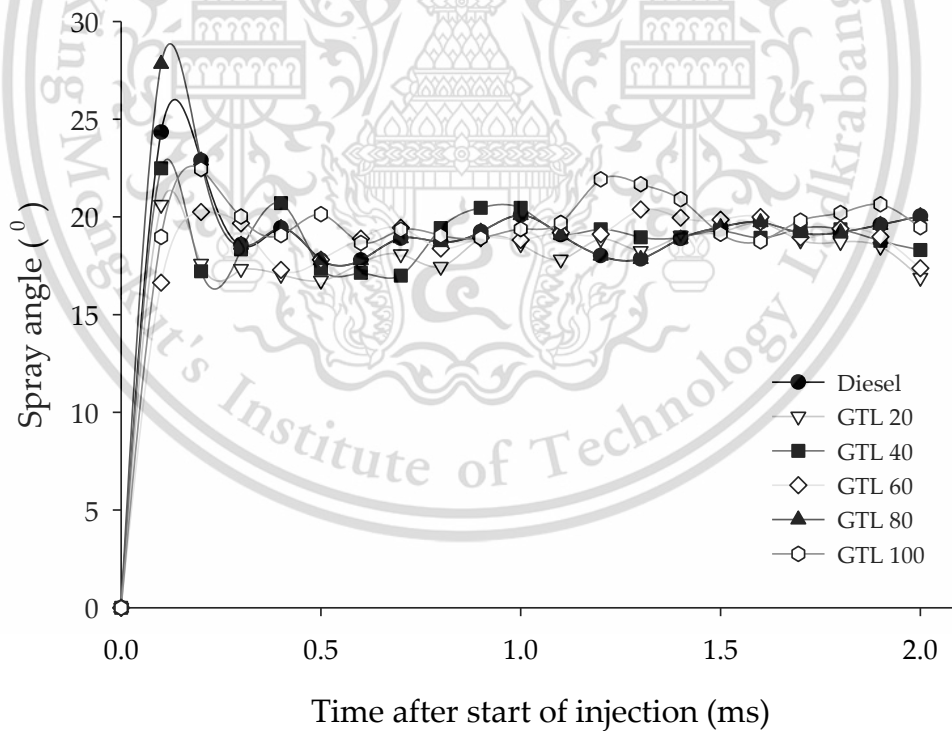


Figure 4.45 Spray angle at $P_b = 45$ bar, $P_i = 1200$ bar, and $T_e = 1.0$ ms

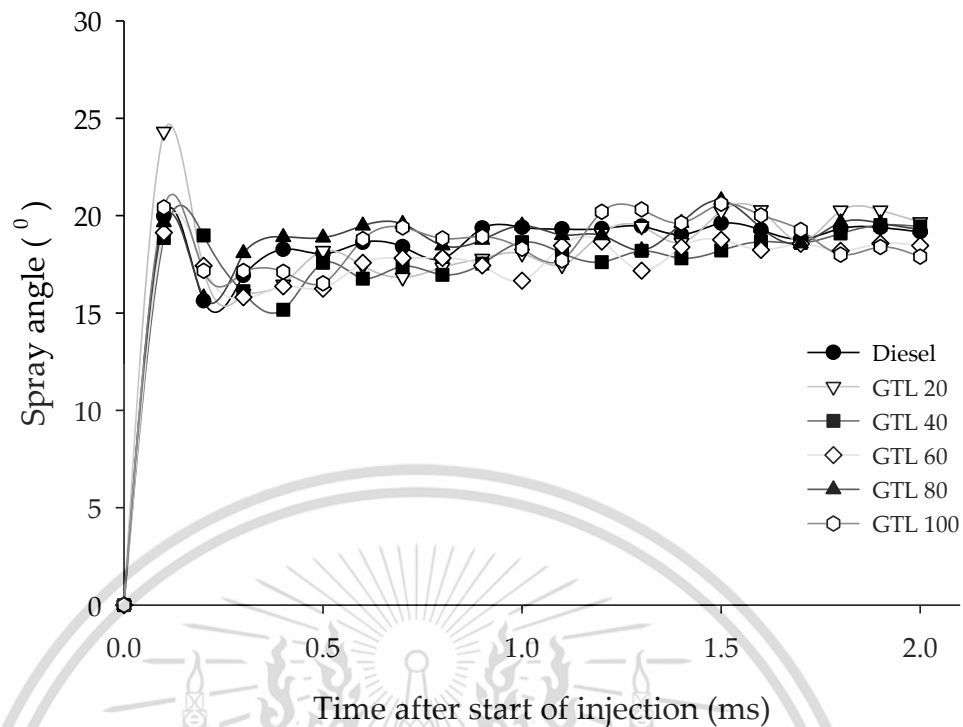


Figure 4.46 Spray angle at $P_b = 45$ bar, $P_i = 1600$ bar, and $T_e = 1.0$ ms

4.3.3. Spray velocity

The spray velocity for all studied fuels, performed under different injection pressure of 400, 800, 1200 and 1600 bar and injector energizing duration of 0.5 and 1.0 ms at back pressure of 19 and 45 bar are compared and illustrated from Figure 4.47 to Figure 4.57.

Result shows the spray velocity for all tested fuel is very high at the beginning and rapidly slows down. There is no any significant pattern at the initial stage to make comparison for all fuel types. Whereas, at later stage diesel fuel diesel shows higher spray velocity as compared to that of other test fuels.

Purpose of velocity measurement was to find different characteristics between compared fuels. It is supposed to be, better combustion and atomization higher velocity is preferred in real combustion [46]. Its also noticed that spray velocity gets higher with increasing of injection pressure.

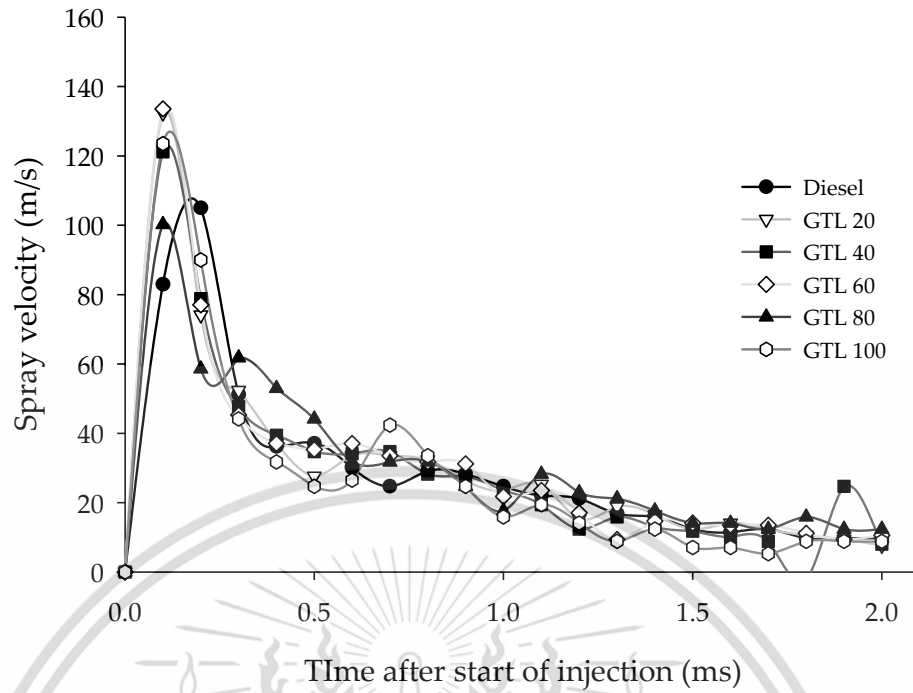


Figure 4.47 Spray velocity at $P_b = 19$ bar, $P_i = 800$ bar, and $T_e = 0.5$ ms

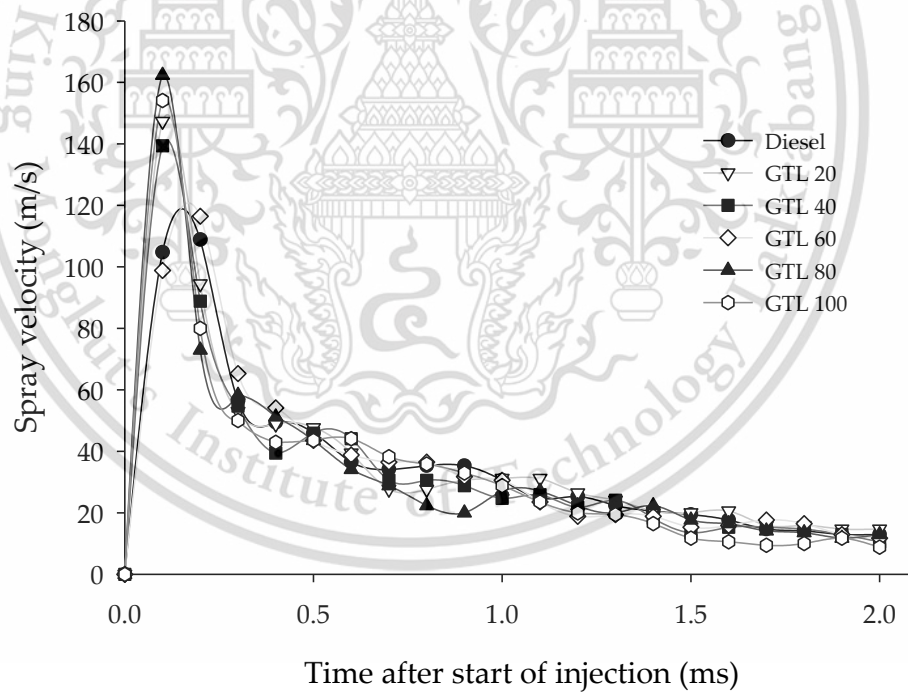


Figure 4.48 Spray velocity at $P_b = 19$ bar, $P_i = 1200$ bar, and $T_e = 0.5$ ms

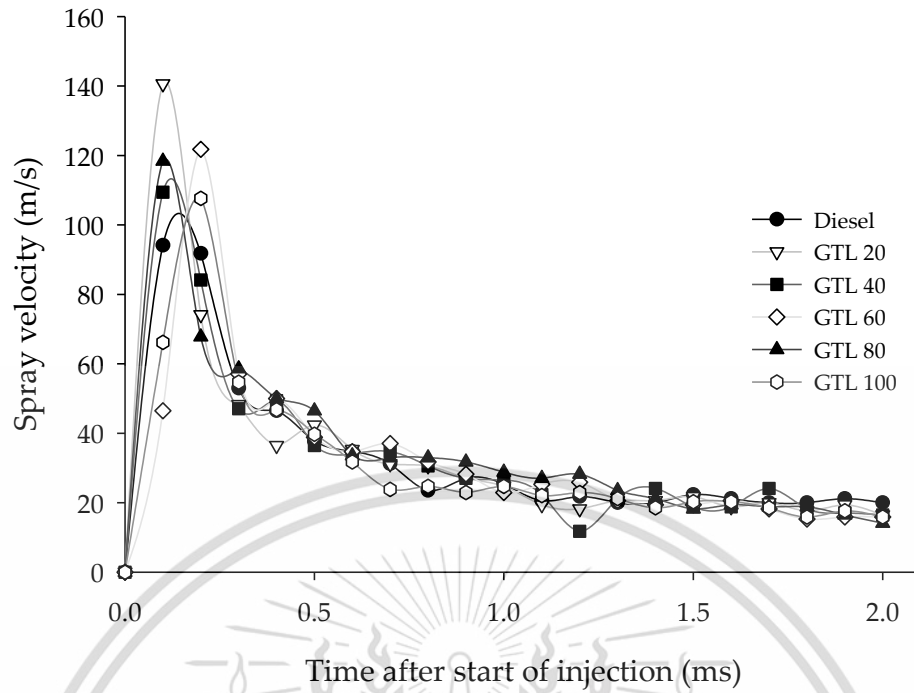


Figure 4.49 Spray velocity at $P_b = 19$ bar, $P_i = 800$ bar, and $T_e = 1.0$ ms

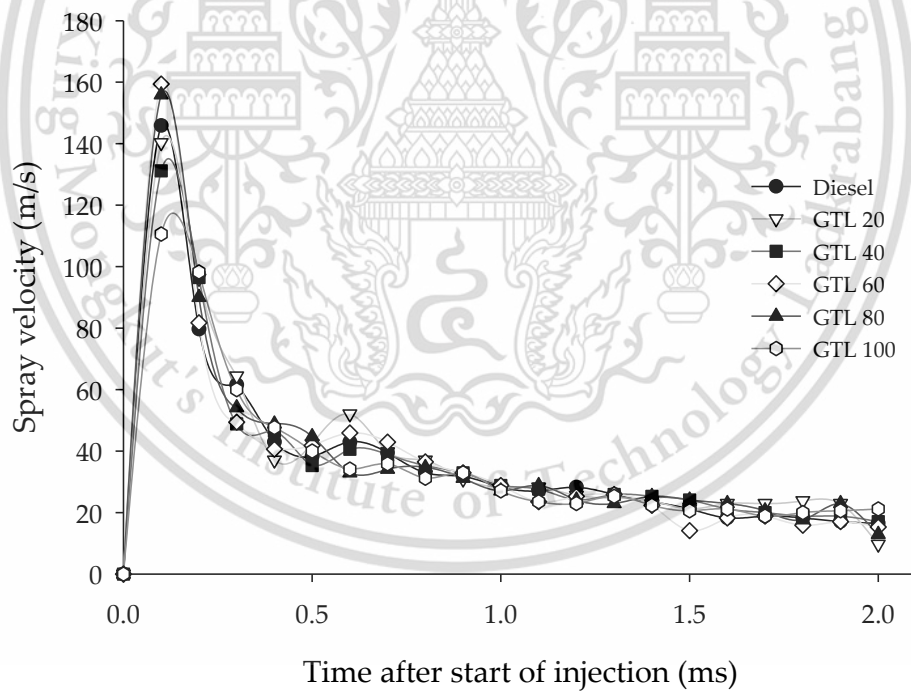


Figure 4.50 Spray velocity at $P_b = 19$ bar, $P_i = 1200$ bar, and $T_e = 1.0$ ms

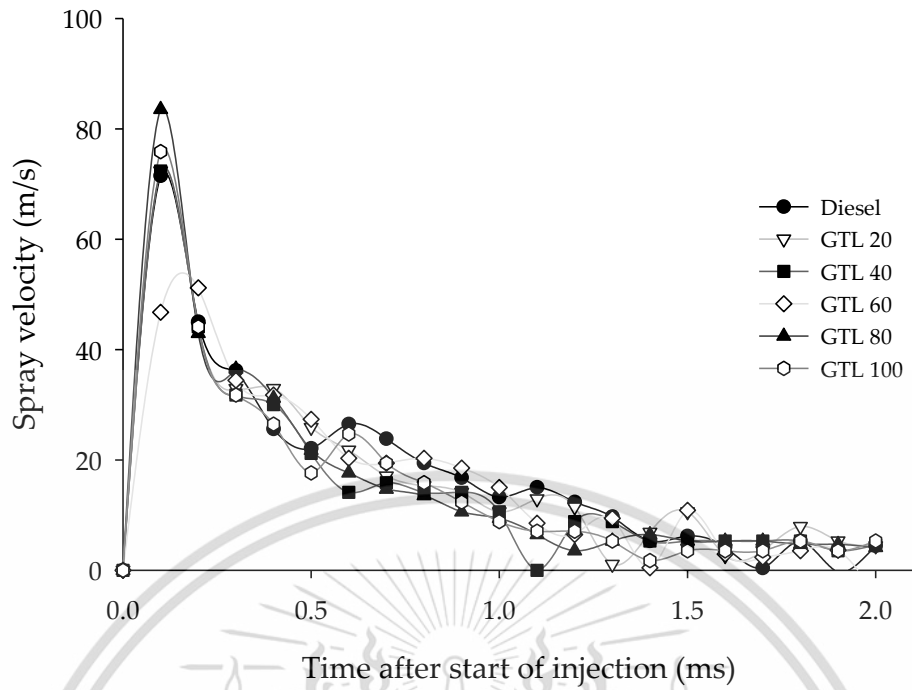


Figure 4.51 Spray velocity at $P_b = 45$ bar, $P_i = 400$ bar, and $T_e = 0.5$ ms

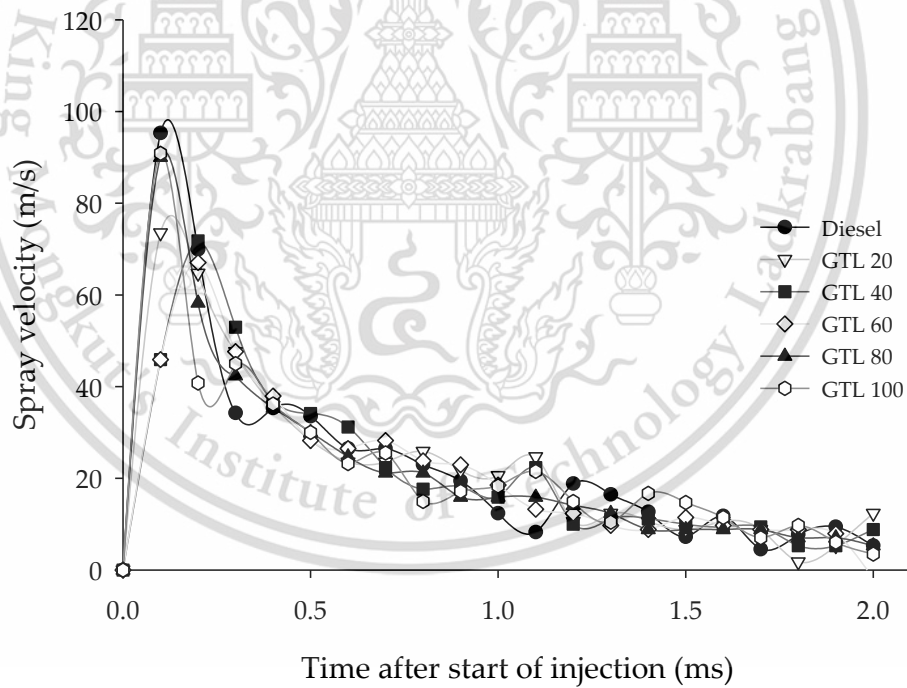


Figure 4.52 Spray velocity at $P_b = 45$ bar, $P_i = 800$ bar, and $T_e = 0.5$ ms

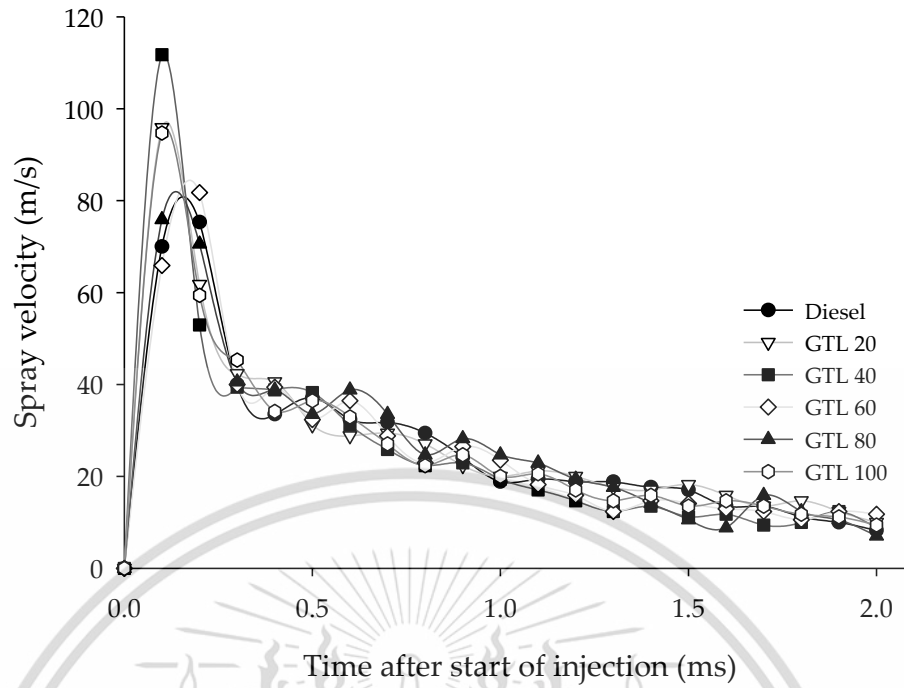


Figure 4.53 Spray velocity at $P_b = 45$ bar, $P_i = 1200$ bar, and $T_e = 0.5$ ms

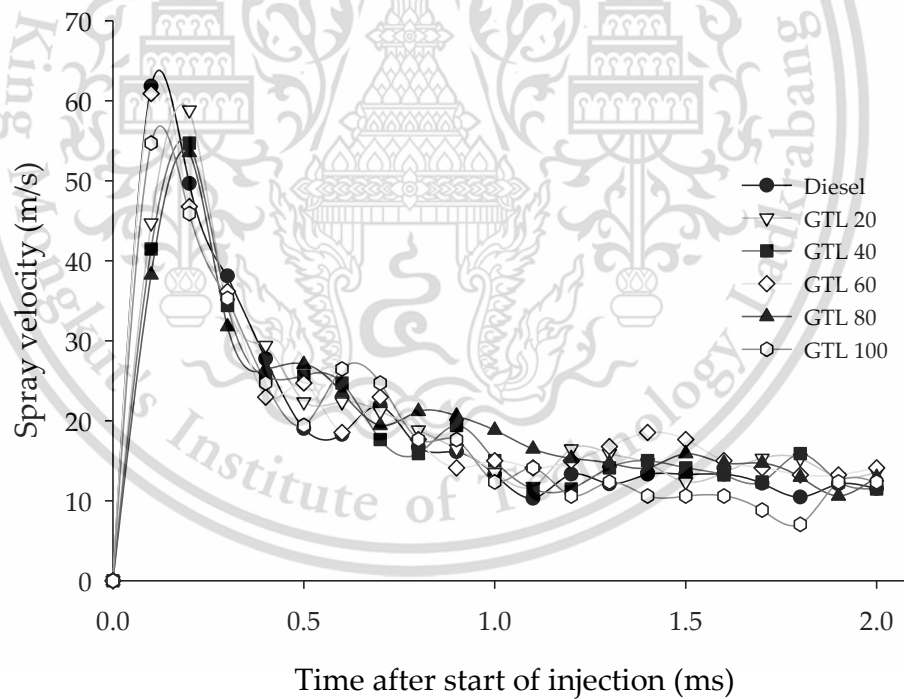


Figure 4.54 Spray velocity at $P_b = 45$ bar, $P_i = 400$ bar, and $T_e = 1.0$ ms

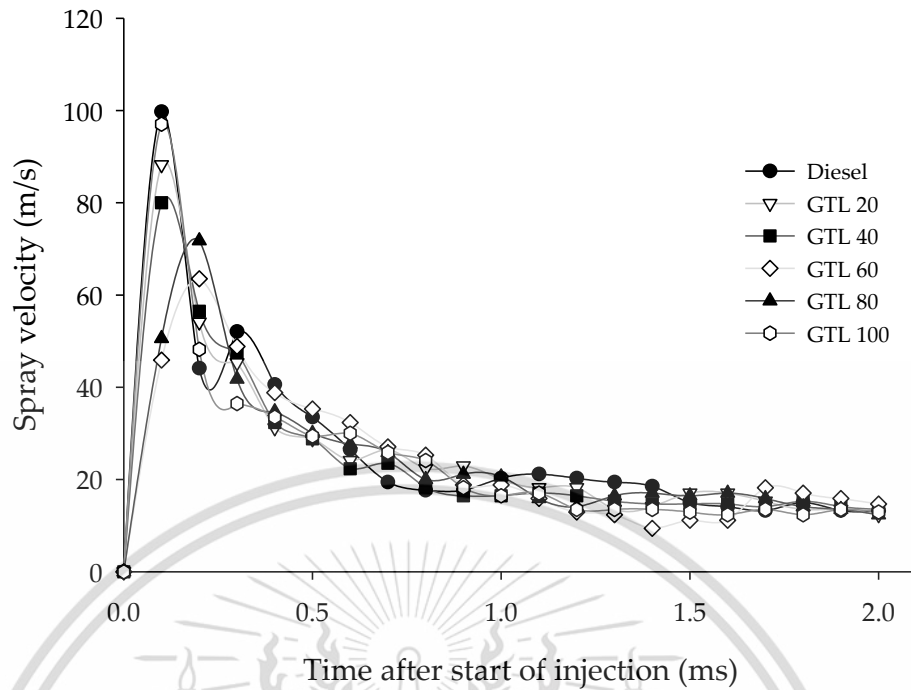


Figure 4.55 Spray velocity at $P_b = 45$ bar, $P_i = 800$ bar, and $T_e = 1.0$ ms

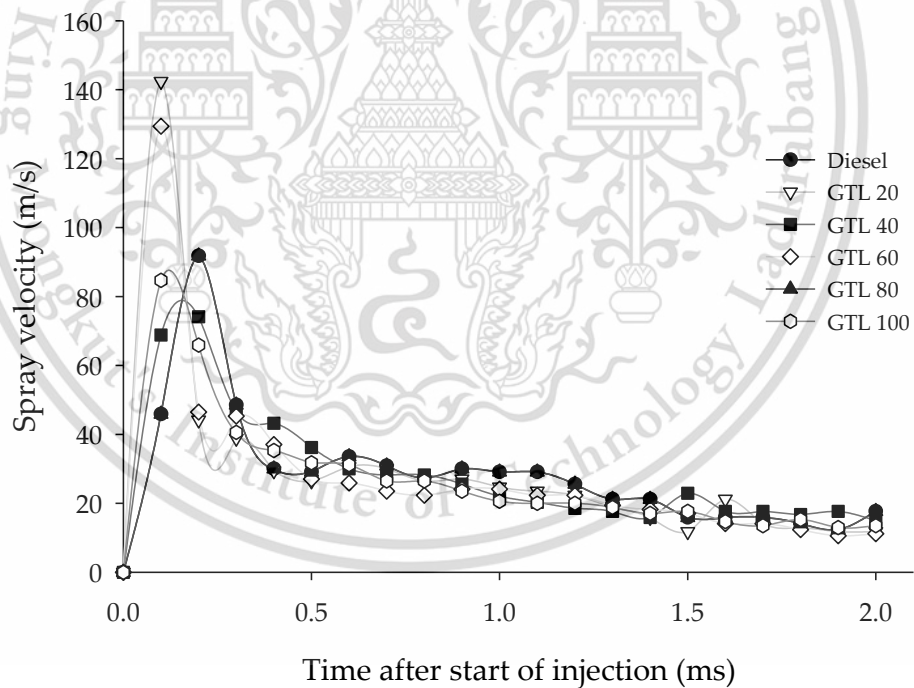


Figure 4.56 Spray velocity at $P_b = 45$ bar, $P_i = 1200$ bar, and $T_e = 1.0$ ms

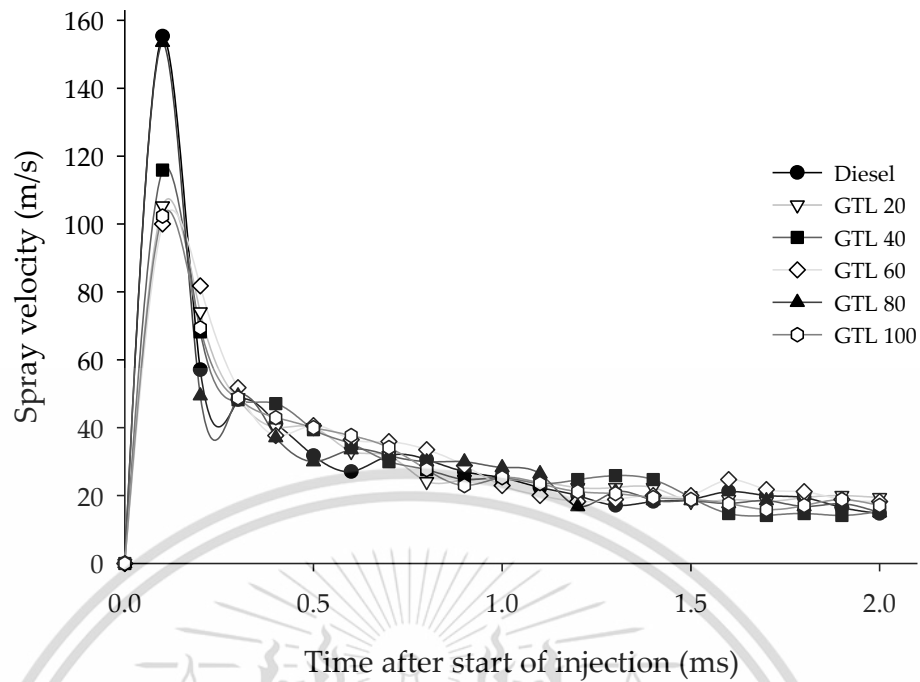


Figure 4.57 Spray velocity at $P_b = 45$ bar, $P_i = 1600$ bar, and $T_e = 1.0$ ms

4.3.4. Spray volume

The results of spray volume in different test condition has been obtained using the Equation 3.6., it reflects the mass of air entrained by the spray and global fuel/air concentration [31]. From Figure 4.58 to 4.61, the results show spray volume graph obtained with identical back pressure and injection energizing duration, while injection pressure is increased from 400 to 1600 bar. Presented spray volume can be termed as “equivalent spray volume” [47], which is measured from spray tip penetration and visible cone angle. For all injection pressure condition, diesel fuel shows slightly higher spray volume. It clears that, spray volume has higher effect of spray tip penetration, in which diesel fuel with longer spray tip penetration showed larger spray volume.

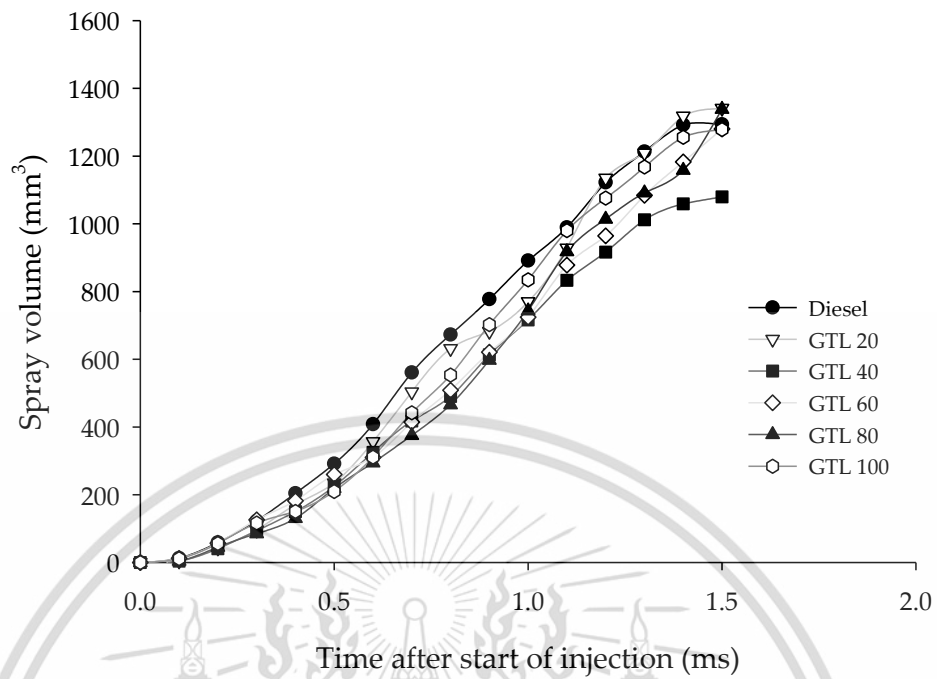


Figure 4.58 Spray volume at $P_b = 45$ bar, $P_i = 400$ bar, and $T_e = 1.0$ ms

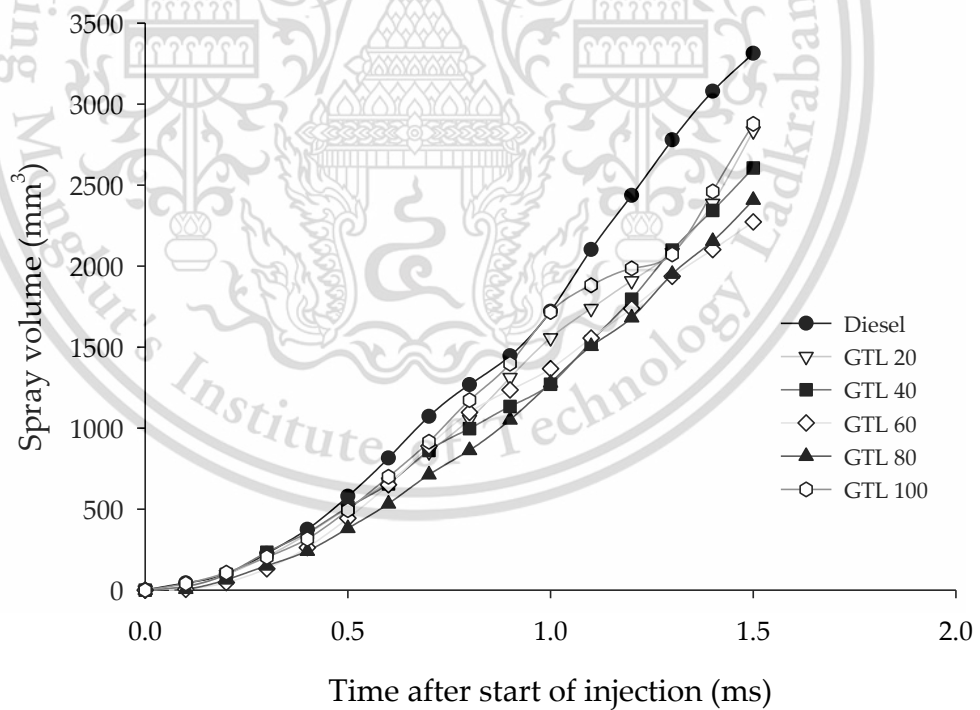


Figure 4.59 Spray volume at $P_b = 45$ bar, $P_i = 800$ bar, and $T_e = 1.0$ ms

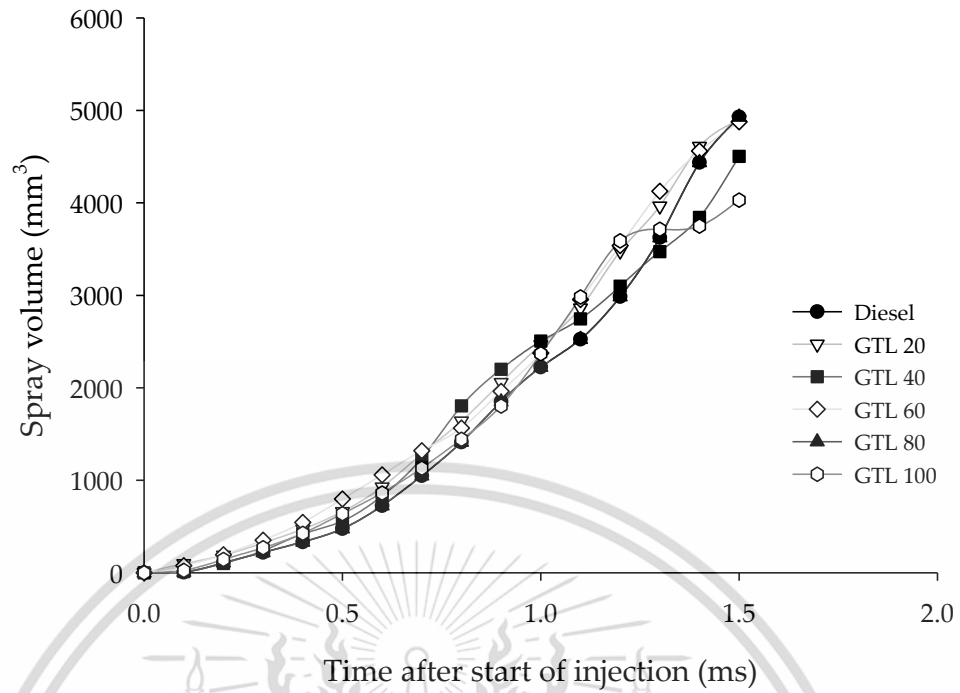


Figure 4.60 Spray volume at $P_b = 45$ bar, $P_i = 1200$ bar, and $T_e = 1.0$ ms

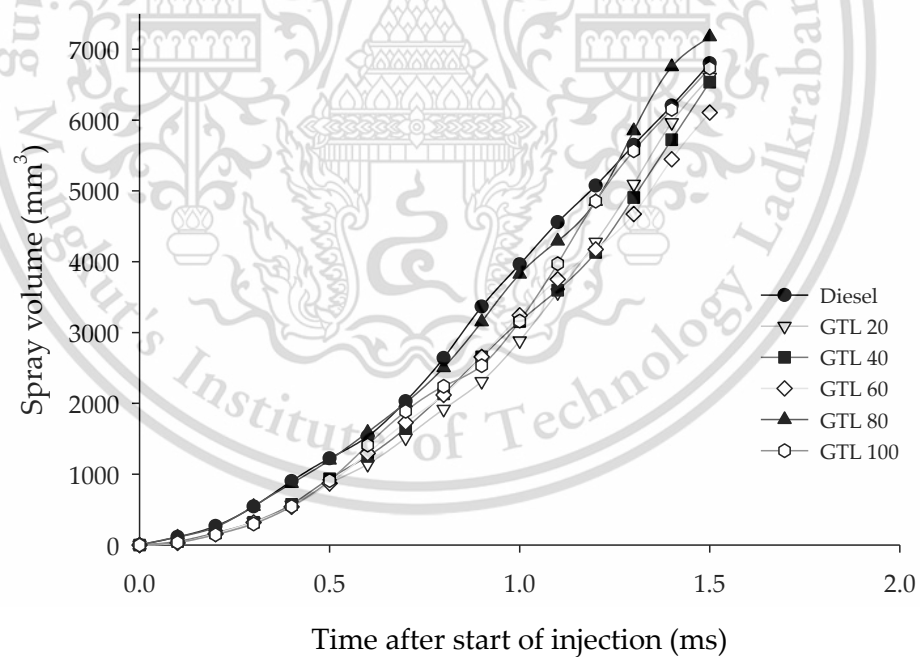


Figure 4.61 Spray volume at $P_b = 45$ bar, $P_i = 1600$ bar, and $T_e = 1.0$ ms

4.4. Effect of GTL-Diesel fuel blends on Diesel combustion

Injection pressure is an important parameter of an injection system, which affects the mixture formation, performance, and exhaust gas emissions of diesel. This material is reserved for educational use only, not allowed for commercial use.

Forbidden to modify the content, and cite the document when use.

engines. In recent diesel engines, fuel injection system is normally designed to attain a high injection pressure. A change in injection pressure causes a varying injection rate, which influences the atomization, vaporization, and mixing process. A low injection pressure produces large fuel mean drop sizes, and thus, it causes an increase in the ignition-delay values [48]. In this research, the effects of injection pressure on common rail fuel injection system were investigated by varying the values of 400, 800, 1200 and 1600 bar. However, experiment to study combustion phenomenon wasn't performed. This discussion is based on the literature relating the spray behavior shown by the test fuel blends in above experiment.

The fuel properties result of blended fuels showed, change in properties in proportion to respective blending ration of GTL and diesel fuel. Higher value of cetane number measured for GTL signifies benefit over diesel fuel in CI engine combustion. Higher cetane value is very crucial to determine ignition delay period. In diesel fuel combustion, the soot emission may increase due to the decrease in the ignition delay period. However, it is different for GTL fuel. Although the GTL has higher cetane value than that of diesel fuel, means that ignition delay period is shorter, the soot emission level tends to decrease as well [49]. It is explained that, very low sulfur and aromatic contents in GTL fuel make it possible to reduce soot emission [50-52]. In other hand lower T90 distillation temperature of GTL shows, volatility of GTL fuel is higher than diesel fuel, which increases the evaporation rate during the mixing process. In real diesel engine, increasing the temperature also increases the evaporation rate with higher volatility. However, if there is no adhesion of unevaporated fuel on cylinder liner wall and piston bowl, the ambient gas temperature may have a greater effect on soot formation than fuel volatility does [53].

Most of the researches revealed lower NO_x emission of GTL fuel than diesel and biodiesels [54]. Higher CN and lower aromatic contents of GTL assist in maintaining the combustion temperature which provides significant NO_x reduction. GTL–diesel blends demonstrated higher NO_x decrement with the higher fraction of GTL in blends. GTL–biodiesel blends showed lower NO_x reduction compared to neat GTL, diesel and GTL–diesel blends. High EGR rate can be utilize very well in GTL combustion to reduce significant level of NO_x however, soot emission increases dramatically. Tsujimura et al. [55] reported that advancing in injection timing can be preferred to reduce both NO_x

and soot with application of higher EGR rate. Thus, the result obtained in this research, short injection delay time with higher injection mass and also the higher cetane value which shortens the ignition delay time, could help to advance in injection timing in GTL combustion.

The result obtained in spray characteristics shows, diesel shows longer spray penetration and larger spray volume while, GTL showed wider spray angle. This result supports better mixture formation in case of diesel fuel due to its larger spray volume. However, GTL spray penetrates slightly advanced flame front propagation [33]. This may be due to the fact that GTL fuel has a higher vapor pressure and therefore higher volatility than diesel fuel, contributing to a certain extent to better mixture formation, increased combustion speed and further flame front propagation [53].



CHAPTER 5

CONCLUSIONS

5.1. Conclusions

In this research physical and chemical properties of four mixtures of GTL and commercial diesel along with pure GTL and pure diesel fuels have been analyzed and then experimental investigation on injection characteristics and spray behavior has been performed. Study of Injection characteristics has been accomplished by using the Zeuch method and result has been discussed in terms of injection rate profile, injection delay time, amount of fuel injected and coefficient of discharge. Furthermore, the macroscopic Spray behavior has been studied by capturing video of the fuel injection inside optically accessible high pressure chamber using a high speed video camera. Macroscopic characteristics resemble spray penetration, spray angle, spray velocity and spray volume of the fuels during the fuel injection process.

After completion of this work, the following conclusion has been drawn.

- a. Heating value, discharge coefficient and kinematic viscosity of tested fuel increases with increasing of GTL fraction in the GTL-diesel fuel blends.
- b. Density, injection delay time and bulk modulus of elasticity of tested fuel decreases with increasing of GTL fraction in fuel blends.
- c. Irrespective of fuel type and measured conditions, observed injection rate profiles are of rectangular shape.
- d. For shorter injector energizing duration, the initiation of injection starts earlier and closes later with increased GTL fraction. This effect has been clearly observed in lower injection pressure, whereas, it's not so much difference in higher injection pressure condition.
- e. For longer injector energizing duration, the initiation of injection starts earlier and also closes earlier with increasing of GTL fraction in low injection pressure condition. However, the initiation of fuel injection is quite similar for higher injection pressure condition, whereas, it's clearly noticeable at closing for all injection pressure range.
- f. For the same test condition, diesel fuel has higher spray penetration than GTL fuel. Increasing in GTL fraction in blended fuel shortens the spray penetration.

This material is reserved for educational use only, not allowed for commercial use.

Forbidden to modify the content, and cite the document when use.

- g. As we know larger spray angle is preferred for better combustion efficiency. At lower injection pressure, the result shows higher spray angle with increase GTL fraction in blended fuels at early stages up to 0.7 ms and for later condition its fluctuates unevenly. At higher injection pressure, spray angle variation is barely observed throughout the investigated period. GTL blends with diesel shows improvement in spray angle.
- h. Spray velocity is mostly dependent on injection pressure. It is found that the spray velocity gets higher with increased injection pressure for all tested fuels. At the beginning of start of injection, GTL shows higher spray velocity compared to other fuel blends. However, it looks similar at the later stage.

It can be concluded that, from the result obtained in this research and previous literature, GTL has shown better mixture formation and flame propagation, which may yield better combustion efficiency. In other hand, the shorter injection delay time, larger injection mass for same injector energizing duration, higher cetane number which is prone to reduce ignition delay time, may help to advance in injection timing in case of GTL combustion. Advanced injection timing is favorable for utilizing higher EGR rate and subsequently reduces both NO_x and soot.

5.2. Recommendation for further work

In this work, it has been focused on physical fuel properties and its effects on spray characteristics and injection behavior in direct injection common rail. Spray test has been done in non-vaporizing condition at room temperature. So, it can be suggested that, it would be beneficial to study those experiment considering temperature inside the spray chamber.

There are various factors effecting on injection phenomenon of diesel engine, physical properties of fuel effects highly prior to combustion and chemical properties becomes more dominant after starting of combustion. Thus, it is suggested to observe effect on combustion using the same fuel matrix for better understand of combustion efficiency and emission for GTL-diesel fuel blend.

In present days, multiple injection strategy is being implemented on most of diesel engine. So, it could be more reliable if further study is done with consideration of multiple injection strategy.

REFERENCES

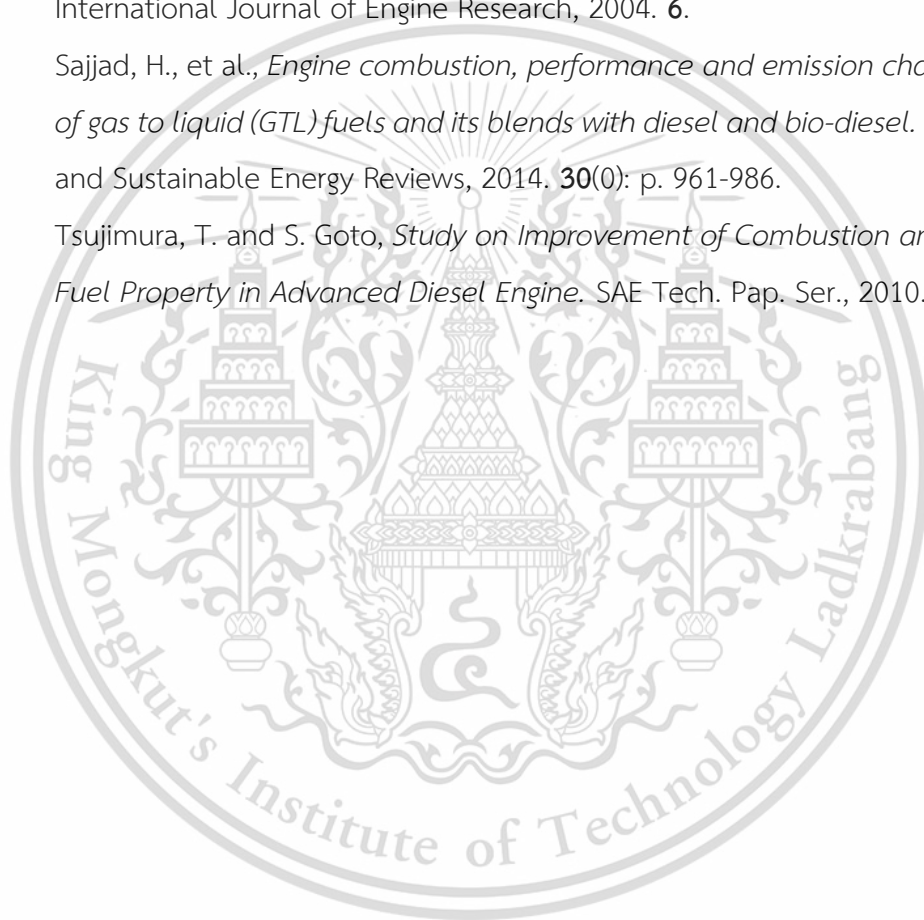
1. Brownstein, A.M., *Renewable Motor Fuels: The Past, the Present and the Uncertain Future*. 2014: Elsevier Science.
2. Union, E., *European emission standards for light commercial vehicle*, in *Compression Ignition (Diesel)*. 2007.
3. Tanabe, K., S. Kohketsu, and S. Nakayama, *Effect of Fuel Injection Rate Control on Reduction of Emissions and Fuel Consumption in a Heavy Duty DI Diesel Engine*. 2005, SAE Technical Paper.
4. Heywood, J.B., *Internal Combustion Engine Fundamentals*. 1988: McGraw-Hill.
5. Li, Y., et al., *Comparative Experimental Study on Microscopic Spray Characteristics of RME, GTL and Diesel*. 2010, SAE Technical Paper.
6. Dernotte, J., et al., *Influence of Fuel Properties on the Diesel Injection Process in Nonvaporizing Conditions*. 2012. **22**(6): p. 461-492.
7. Bauer, H. and H. Robert Bosch Gmb, *Diesel-engine management*. Bosch handbook series. 2004, Plochingen : Bury St. Edmunds: Robert Bosch ; Professional Engineering. 489 p.
8. Kegl, B., M. Kegl, and S. Pehan, *Introduction*, in *Green Diesel Engines*. 2013, Springer London. p. 1-3.
9. Tschöke, H. and R.B. G.m.b.H., *Diesel Distributor Fuel-injection Pumps VE*. 1994: Robert Bosch GmbH, Automotive Equipment Business Sector, Department for Technical Information.
10. Hiroyasu, H., M. Arai, and S.o.A. Engineers, *Structures of Fuel Sprays in Diesel Engines*. 1990: Society of Automotive Engineers.
11. Kegl, B., M. Kegl, and S. Pehan, *Green Diesel Engines: Biodiesel Usage in Diesel Engines*. 2013: Springer.
12. Merker, G., et al., *Simulating Combustion: Simulation of combustion and pollutant formation for engine-development*. 2005: Springer Berlin Heidelberg.
13. Bruneaux, G., *Liquid and Vapor Spray Structure in High Pressure Common Rail Diesel Injection* 2001. **11**(5): p. 24.

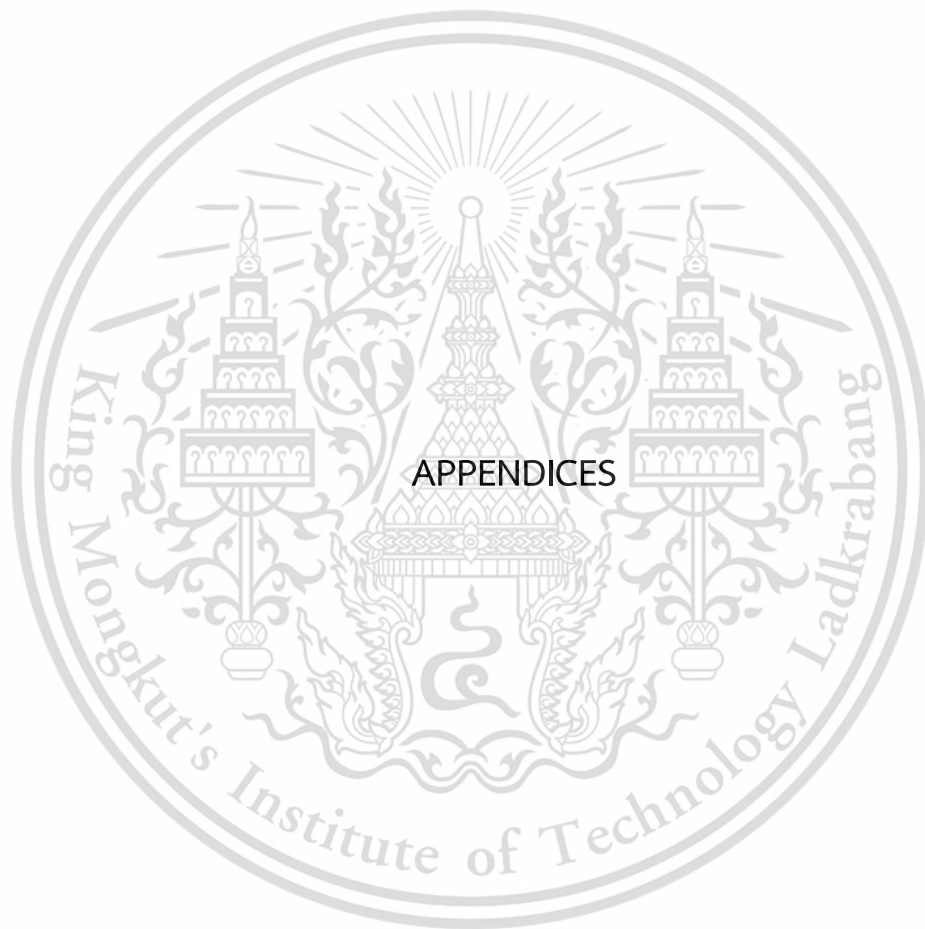
14. Çelikten, İ., *An experimental investigation of the effect of the injection pressure on engine performance and exhaust emission in indirect injection diesel engines*. Applied Thermal Engineering, 2003. **23**(16): p. 2051-2060.
15. Hwang, J.W., et al., *Effect of fuel injection rate on pollutant emission in DI diesel engine*. 1999, SAE Technical paper Series.
16. Jayashankara, B. and V. Ganesan, *Effect of fuel injection timing and intake pressure on the performance of a DI diesel engine – A parametric study using CFD*. Energy Conversion and Management, 2010. **51**(10): p. 1835-1848.
17. Juneja, H., Y. Ra, and R.D. Reitz, *Optimization of injection rate shaping using active control of fuel injection*. SAE technical paper series, 2004.
18. Desantes, J.M., et al., *The modification of the fuel injection rate in heavy-duty diesel engines. Part 1: Effects on engine performance and emissions*. Applied Thermal Engineering, 2004. **24**(17–18): p. 2701-2714.
19. Elkotb, M.M., *Fuel Atomization for Spray Modelling*. Progress in Energy and Combustion Science, 1982. **8**.
20. Lefebvre, A.H. *Atomization and Sprays*. 1989. Hemisphere, New York.
21. Shoba, T.T., et al., *Optical Characterization of Diesel, RME and Kerosene Sprays by Microscopic Imaging, in 24th European Conference on Liquid Atomization and Spray System*. 2011, ILASS: Estoril, Portugal
22. Siebers, D.L., *Scaling Liquid-Phase Fuel Penetration in Diesel Sprays Based on Mixing-Limited Vaporization*. SAE Tech. Pap. Ser., 1999.
23. Dernotte, J., et al., *Influence of physical fuel properties on the injection rate in a Diesel injector*. Fuel, 2012. **96**(0): p. 153-160.
24. Han, D., et al., *Experimental study on injection characteristics of fatty acid esters on a diesel engine common rail system*. Fuel, 2014. **123**(0): p. 19-25.
25. Kim, K.S., et al., *Experimental Investigation and Comparison of Spray and Combustion Characteristics of GTL and Diesel Fuels*. International Journal of Automotive Technology, 2007. **8**(3).
26. Payri, F., et al., *Characterisation of Injection-Combustion Process in a Common-rail DI Diesel Engine Running with Sasol Fischer-Tropsch Fuel*. SAE Tech. Pap. Ser., 2000(01).

27. Kitano, K., I. Sakata, and R. Clark, *Effects of GTL fuel properties on DI diesel combustion*. SAE technical paper series, 2005(2005-01-3763).
28. Desantes, J.M., et al., *Development and validation of a theoretical model for diesel spray penetration*. Fuel, 2006. **85**(7–8): p. 910-917.
29. Desantes, J.M., et al., *A contribution to the understanding of isothermal diesel spray dynamics*. Fuel, 2007. **86**(7–8): p. 1093-1101.
30. Ejim, C.E., B.A. Fleck, and A. Amirfazli, *Analytical Study for Atomization of Biodiesels and Their Blends in a Typical Injector: Surface Tension and Viscosity Effects*. Fuel, 2007. **86**.
31. Arregle, J., J.V. Pastor, and S. Ruiz, *The influence of injection parameters on diesel spray characteristics*. SAE Technical paper series, 1999(1999-01-0200).
32. Delacourt, E., B. Desmet, and B. Besson, *Characterisation of very high pressure diesel sprays using digital imaging techniques*. Fuel, 2005. **84**(7–8): p. 859-867.
33. Azimov, U.B., et al., *Instantaneous 2-D visualization of spray combustion and flame luminosity of GTL and GTL-biodiesel fuel blend under quiescent ambient conditions*. International Journal of Automotive Technology, 2011. **12**(2): p. 159-171.
34. Settles, G.S., *Schlieren and Shadowgraph Techniques: Visualizing Phenomena in Transparent Media*. 2001: Springer Berlin Heidelberg.
35. Otsu, N., *A Threshold Selection Method from Gray-Level Histograms*. IEEE Transactions on Systems, Man and Cybernetics, 1979. **9**(1): p. 62–66.
36. Delacourt, E., *Caracterisation experimentale des jets d'injection Diesel a tres hautes presions*. 2003, Valenciennes University: France.
37. Arbab, M.I., et al., *Fuel properties, engine performance and emission characteristic of common biodiesels as a renewable and sustainable source of fuel*. Renewable and Sustainable Energy Reviews, 2013. **22**: p. 133-147.
38. Wu, T., et al., *Physical and Chemical Properties of GTL–Diesel Fuel Blends and Their Effects on Performance and Emissions of a Multicylinder DI Compression Ignition Engine*. Energy & Fuels, 2007. **21**(4): p. 1908-1914.
39. Mancaruso, E. and B.M. Vaglieco, *Premixed combustion of GTL and RME fuels in a single cylinder research engine*. Applied Energy, 2012. **91**(1): p. 385-394.

40. Soltic, P., et al., *Experimental investigation of mineral diesel fuel, GTL fuel, RME and neat soybean and rapeseed oil combustion in a heavy duty on-road engine with exhaust gas aftertreatment*. Fuel, 2009. **88**(1): p. 1-8.
41. Ryan, T. and R. Maly, *Fuel Effects on Engine Combustion and Emissions*, in *Flow and Combustion in Reciprocating Engines*, C. Arcoumanis and T. Kamimoto, Editors. 2009, Springer Berlin Heidelberg. p. 381-420.
42. Tat, M.E. and J.H.V. Gerpen, *Measurement of Biodiesel Speed of Sound and Its Impact on Injection Timing*. 2003, Iowa State University: National Renewable Energy Laboratory.
43. Boudy, F. and P. Seers, *Impact of physical properties of biodiesel on the injection process in a common-rail direct injection system*. Energy Conversion and Management, 2009. **50**(12): p. 2905-2912.
44. Guohong, G., S. Chonglin, and L. Lidong. *Spray characteristics of diesel fuel, Fishch-Tropsch diesel fuel and their blend*. in *Electrical and Control Engineering (ICECE), 2011 International Conference on*. 2011.
45. Shervani-Tabar, M.T., M. Sheykhvazayefi, and M. Ghorbani, *Numerical study on the effect of the injection pressure on spray penetration length*. Applied Mathematical Modelling, 2013. **37**(14–15): p. 7778-7788.
46. Hultkonen, T., et al. *Spray Studies and Diesel Fuel Comparison in Swedish-Finnish Flame Days 2011*. 2011. Piteå, Sweden: The Swedish and Finnish National Committees of the International Flame Research Foundation.
47. Kuniyoshi, H., et al., *Investigation on the Characteristics of Diesel Fuel Spray*. SAE Tech. Pap. Ser., 1980.
48. Bakar, R.A., A.R. Ismail, and Semin, *Fuel Injection Pressure Effect on Performance of Direct Injection Diesel Engines Based on Experiment*. American Journal of Applied Science, 2008. **5**(3).
49. Azimov, U. and K.-S. Kim, *Visualization of Gas-to-Liquid Fuel Liquid Length and Soot Formation in The Constant Volume Combustion Chamber*. Journal of Thermal Science and Technology, 2008. **08**(0002).
50. Tanaka, S. and e. al., *Effect of Fuel Compositions on PAH in Particular matter from DI Diesel Engine*. SAE Tech. Pap. Ser., 1998.

51. Lim, M.C.H., *Effect of Fuel Composition and Engine Operating Conditions on Polycyclic Aromatic Hydrocarbon Emissions from a Fleet of Heavy Duty Diesel Buses*. Atmospheric Environment, 2005. **39**(40).
52. Lim, M.C.H., *The Effect of Fuel Characteristics and Engine Operating Conditions on the Elemental Composition of Emissions from Heavy Duty Diesel Buses*. Fuel, 2007. **86**.
53. Sakai, A., et al., *Improvements in Premixed Charge Compression Ignition Combustion and Emission with Lower Distillation Temperature Fuels*. International Journal of Engine Research, 2004. **6**.
54. Sajjad, H., et al., *Engine combustion, performance and emission characteristics of gas to liquid (GTL) fuels and its blends with diesel and bio-diesel*. Renewable and Sustainable Energy Reviews, 2014. **30**(0): p. 961-986.
55. Tsujimura, T. and S. Goto, *Study on Improvement of Combustion and Effect of Fuel Property in Advanced Diesel Engine*. SAE Tech. Pap. Ser., 2010.





This material is reserved for educational use only, not allowed for commercial use.

Forbidden to modify the content, and cite the document when use.

Appendix-A. Standard required for diesel fuel oils

A.1 Requirements for Diesel Fuel Oils (ASTM D 975-97)

Property	Grade				
	LS #1	LS #2	No. 1-D	No. 2-D	No. 4-D
Flash point °C, min	38	52	38	52	55
Water and sediment, % vol, max.	0.05	0.05	0.05	0.05	0.50
Distillation temp., °C, 90%					
Min.	--	282	--	282	--
Max.	288	338	288	338	--
Kinematic Viscosity, mm ² /s at 40°C					
Min.	1.3	1.9	1.3	1.9	5.5
Max.	2.4	4.1	2.4	4.1	24.0
Ramsbottom carbon residue on 10%, %mass, max.	0.15	0.35	0.15	0.35	--
Ash, % mass, max.	0.01	0.01	0.01	0.01 0.10	
Sulfur, % mass, max	0.05	0.05	0.50	0.50 2.00	
Copper strip corrosion, Max 3 hours at 50°C	No. 3	No. 3	No. 3	No. 3	--
Cetane Number, min.	40	40	40	40	30
One of the following Properties must be met:					
(1) cetane index	40	40	--	--	--
(2) Aromaticity, % vol, max	35	35	--	--	--

A.2 Requirements for Diesel Fuel Oils (EN 590)

Property	Unit	lower limit	upper limit
Cetane index		46,0	-
Cetane number		51,0	-
Density at 15°C	kg/m ³	820	845
Polycyclic aromatic hydrocarbons	%(m/m)	-	11
Sulphur content	mg/kg	-	350 (until 2004-12-31) or 50,0
			10,0 (on the 01-01-2009)
Flash point	°C	Above 55	-
Carbon residue (on 10% distillation residue)	%m/m	-	0,30
Ash content	% (m/m)	-	0,01
Water content	mg/kg	-	200
Total contamination	mg/kg	-	24
Copper strip corrosion (3 hours at 50 °C)	rating	Class 1	Class 1
Oxidation Stability	g/m ³	-	25
Lubricity, corrected wear scar diameter (wsd 1,4) at 60 °C	µm	-	460
Viscosity at 40 °C	mm ² /s	2,00	4,50
Distillation recovered at 250 °C, 350 °C	%V/V	85	<65
95%(V/V) recovered at	°C	-	360
Fatty acid methyl ester content	% (V/V)	-	7

This material is reserved for educational use only, not allowed for commercial use.

Forbidden to modify the content, and cite the document when use.

Appendix-B. Specifications of measurement devices used

B.1 Dynamic pressure sensor

Pressure

KISTLER
measure. analyze. innovate.

High-Temperature Pressure Sensor for Engine Measuring Technology

Type 6052C...

High-temperature pressure sensor with very small dimensions are ideal for use in internal combustion engines with complex structural geometry of the cylinder head. The sensor is installed with front sealing in an M5x0,5 bore.

- Good temperature stability of the sensitivity
- High sensitivity
- Low thermal shock error
- Long service life due to front seal

Description

Type 6052C... uses a piezoelectric crystal which achieves high sensitivity in conjunction with an extremely small sensor structure. This sensitivity varies by not more than $\pm 1,0\%$ in the operating temperature range. The passive acceleration compensation patented by Kistler keeps the influence of engine vibrations to a minimum.

The front seal allows very good heat dissipation and thus briefly a maximum operating temperature of 400 °C. The diaphragm, optimized by finite element calculation, produces good measuring results and ensures a long service life.

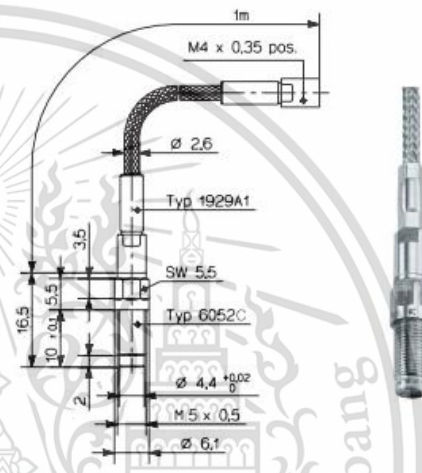
Application

The sensor Type 6052C... is an excellent all-rounder. Its rugged construction makes it suitable for measurements at the knock limit as well as for thermodynamic investigations. This sensor is used mainly on multi-valve engines, motor cycle and other small engines and for combustion analysis.

For applications mainly in the knocking range or at very high peak pressures, use of Type 6052C...U20 with reinforced diaphragm (heavy duty version) is recommended.

Type 6052C...U40 is provided with additional damping and is suitable for applications on engines with extremely high vibrations, e.g. racing engines.

These sensors are always provided with an integrated cable. For standard applications, a rugged cable with steel braiding Type 1929A1 is used. If the sensor connector is exposed directly to engine oil, e.g. when installed through the valve cover, the oil proof cable (IP67) Type 1983AA1 is recommended.



Technical Data

Type 6052C...

Measuring range	bar	0 ... 250
Calibrated partial ranges	bar	0 ... 50, 0 ... 100, 0 ... 150
Overload	bar	300
Sensitivity	pC/bar	≈ 20
Natural frequency (measuring element)	kHz	≈ 160
Linearity, all ranges (at 23 °C)	%/FSO	$\leq \pm 0,4$
Acceleration sensitivity		
axial	bar/g	$< 0,0002$
radial	bar/g	$< 0,0005$
Operating temperature range	°C	-20 ... 350
Temperature min./max.		-50 ... 400
Sensitivity change		
200 °C ± 50 °C	%	$\leq \pm 0,5$
23 ... 350 °C	%	$\leq \pm 2$
Thermal shock error		
(at 1500 1/min, $p_m = 9$ bar)		
Δp (short time drift)	bar	$\leq \pm 0,5$
Δp_m	%	$\leq \pm 2$
Δp_{max}	%	$\leq \pm 1,5$
Insulation resistance at 23 °C	Ω	$\geq 10^{14}$
Shock resistance	g	2 000
Tightening torque	N·m	1,5
Capacitance, without cable	pF	5
Weight with cable	g	30
Connector, ceramic insulator	-	M4 x 0,35

Page 1/3

This information corresponds to the current state of knowledge. Kistler reserves the right to make technical changes. Liability for consequential damage resulting from the use of Kistler products is excluded.

©2006, Kistler Instrumente AG, PO Box, Eulachstr. 22, CH-8408 Winterthur
Tel +41 52 224 11 11, Fax +41 52 224 14 14, info@kistler.com, www.kistler.com

This material is reserved for educational use only, not allowed for commercial use.

Forbidden to modify the content, and cite the document when use.

B.2 Static pressure sensor



- 27 -

01041
Revised 07-27-10
Section 05

Pressure Transmitters PXT Series



Features

- 4-20 mA Output Signal
- Precision Etched Silicon Sensor
- Corrosion Resistant Construction
- High Stability



The PXT Series pressure transmitter is a state-of-the-art instruments providing 4 to 20 mA outputs. It features a precision micro-machined silicon diaphragm with fully welded stainless steel pressure port for greater accuracy, stability and a wide range of compatibility.

Silicon technology is used to provide a miniature micro-machined diaphragm which is electrostatically bonded to a glass substrate and is then stitch-bonded within a glass to metal seal assembly to provide exceptional thermal and stress isolation. This technology assures you of high accuracy and stability over a wide range of operating conditions.

The enclosure is made of 316 stainless steel and all wetted parts are 316L stainless steel or HASTELLOY C276.

Applications

The PXT can be used in applications such as Compressors, Engines, Process Control, Liquid Level and Pumps.

Specifications

Accuracy (Full Scale, Best Straight Line):

±0.25% including non-linearity, hysteresis and repeatability. Long term stability better than 0.2% FS over twelve (12) months.

Zero Setting: ±0.5% of full scale (0.25% typical).

Span Setting: ±0.5% of full scale BSL (RSS).

Overpressure/Proof Pressure: 400% for up to 500 psi (3.45 MPa) [34 Bar]. 200% for higher ranges.

Burst Pressure: Ranges 0-1000 psi = 600% of full scale or 4000 psi whichever is lower. Ranges 2000 psi [13.79 MPa] [137 Bar]= 20,000 psi (27.5 MPa) [275 Bar].

Response Time: Frequency response better than 2 kHz.

Storage Temperature: -65 to 200°F (-54 to 93°C).

Operating Temperature: -40 to 180°F (-40 to 82°C).

Compensated Temperature: -20 to 160°F (-29 to 71°C).

Total Thermal Effects Over Compensated Range: ±2% FS TEB.

Physical:

Enclosure: Weather Resistant.

Body: 316 stainless steel. Meets NACE MR01-75.

Wetted Parts: 316L stainless steel or HASTELLOY C276.

Process Connection: 1/4 NPT female.

Electrical Cable: Integral: 60 in. (914 mm); vented: 1/2 in. NPT male conduit connection

Environmental Effect:

Humidity: No effect.

Mounting: Position/orientation has negligible effect.

Reverse polarity protected

Shock: 1000g 1ms Half sine Pulse in each of 3 mutually perpendicular axis will not affect performance.

Vibration: Effect on output response is less than 0.05% FS/g at 30g Peak 10Hz to 2kHz, limited by 0.05 in double amplitude. (MIL STD 810C Proc. 514.2-2 curve L). PXT Power Requirements: Typically 24 VDC is required, using the Loop Resistance Graph, 9-30 VDC.

PXT Series Transmitter Output: 4-20 mA, 2-wire.

Insulation: Greater than 10 Mohms @ 500 VDC.

RFI Protection: To the European standards of BS EN 50082-2:1991 in accordance with IEC 801 parts 1 to 6 for susceptibility to EMC and to BS EN 50081-1992 for emissions.

Voltage Surge/Spike: Protected against a 600 V spike to IEC 60-2. Reverse polarity protected.

Sealed: Sealed at one atmosphere at sea level for ranges > 1000 psi (6.89 MPa) [68 Bar].

Vented: Vented for ranges <= 1000 psi (6.89 MPa) [68 Bar].

UL Certification: Class I, Division 2, Groups A, B, C and D; Class II, Groups E, F and G. Pressure transmitter, Model PXT. Intrinsically safe when installed per system, Diagram No. 05-08-0754. UL File #E169675

Shipping Weight: 0.90 lb. (408 g).

Shipping Dimensions: 5 x 5 x 5 inches (127 x 127 x 127 mm).

This material is reserved for educational use only, not allowed for commercial use.

Forbidden to modify the content, and cite the document when use.

B.3 High speed video camera



FASTCAM Mini UX100

COMPACT HIGH-SPEED CAMERA SYSTEM

Real Power in a Compact Package

The Photron FASTCAM Mini UX100, high speed camera packs a lot of performance in such a small package, providing 1,280 by 1,024 pixel resolution to 4,000 frames per second (fps) and reduced resolution operation all the way to 800,000 fps, with 1,280(H) by 720 (V), equivalent to 720 HD video resolution, to 6,400 fps. This makes the UX100 a small and lightweight camera ideally suited for applications as varied as fluidics, life sciences or ballistic testing. A global shutter provides blur free imagery with a minimum shutter speed of 1 μ s with 12-bit pixel depth (36-bit for the color version) from the CMOS pixels 10 μ m square pixel providing an ISO 12232 Ssat certified light sensitivity of 10,000 ISO for the monochrome version.

Benefits

- Frame Rate Performance examples:
 - 4,000 fps at 1,280 x 1,024 pixel resolution
 - 5,000 fps at 1,280 x 1,000 pixel resolution
 - 6,250 fps at 1,280 x 800 pixel resolution
 - 10,000 fps at 896 x 488 pixel resolution
 - 25,000 fps at 1,280 x 200 pixel resolution
 - 200,000 fps at 1,280 x 24 pixel resolution
 - 800,000 fps at 640 x 8 pixel resolution
- Self-contained, compact and lightweight camera 120mm (4.7")H x 120mm (4.7")W x 90mm (3.6")D and 1.5Kg
- Sensitivity: ISO 12232 Ssat standard
 - ISO 10,000 monochrome
 - ISO 5,000 color
- Suitable for operation in High-G environments. Operation tested to 100G, 10ms, 6 axis
- 4GB, 8GB and 16GB memory options and high performance GigaBit Ethernet interface to PC

Target applications include:

- Biomechanics
- Life sciences
- Fluid dynamics
- Off board automotive safety testing
- Defense and aerospace research
- Material science

Photron
www.photron.com

This material is reserved for educational use only, not allowed for commercial use.

Forbidden to modify the content, and cite the document when use.

FASTCAM Mini UX100

COMPACT HIGH-SPEED CAMERA SYSTEM

Specifications: Partial Frame Rate / Recording Duration Table

FRAME RATE (fps)	MAXIMUM RESOLUTION		RECORD DURATION (12-BIT)					
			TIME (Sec.)			FRAMES		
			4GB	8GB	16GB	4GB	8GB	16GB
1,000	1,280	1,024	2.18	4.37	8.73	2,180	4,365	8,734
2,000	1,280	1,024	1.09	2.18	4.37	2,180	4,365	8,734
4,000	1,280	1,024	0.55	1.09	2.18	2,180	4,365	8,734
5,000	1,280	1,000	0.45	0.89	1.79	2,232	4,469	8,943
6,250	1,280	800	0.45	0.89	1.79	2,791	5,587	11,179
6,400	1,280	720	0.48	0.97	1.94	3,101	6,208	12,421
8,000	1,280	616	0.45	0.91	1.81	3,624	7,256	14,519
10,000	896	488	0.65	1.31	2.62	6,536	13,084	26,181
16,000	1,280	312	0.45	0.90	1.79	7,156	14,326	28,665
20,000	1,280	248	0.45	0.90	1.80	9,009	18,023	36,063
40,000	1,280	120	0.47	0.93	1.86	18,607	37,248	74,531
80,000	1,280	56	0.59	1.05	2.09	39,872	79,818	159,709
100,000	1,280	32	0.70	1.40	2.79	69,777	139,682	279,492
200,000	1,280	24	0.47	0.93	1.86	93,036	186,072	372,656
800,000	640	8	0.70	1.40	2.79	558,216	1,117,457	2,235,938

Sensor	1,280 x 1,024 pixels, 10um pixel size, 12-bit ADC (Bayer system color, 36 bit single sensor)	Trigger Modes	Start, Center, End, Manual, Random
Shutter	Global electronic shutter from 20ms to 1 μs dependent on frame rate	Saved Image Formats	JPEG, AVI, TIFF, BMP, RAW, PNG, MOV and FTIF. Images can be saved with or without image or comment data
Memory	4GB (2,180 frames @ maximum resolution) or 8GB (4,365 frames @ maximum resolution) memory options 16GB (8,734 frames @ maximum resolution) memory options	Data Display	Frame Rate, Shutter Speed, Trigger Mode, Date or Time, Status (Playback/Record), Real Time, Frame Count and Resolution
Camera Control	High speed Gigabit Ethernet	Cooling	Actively cooled using external fans
Low Light Mode	Low light mode drops the frame rate and shutter time to their maximum values, while maintaining other set parameters, to enable users to position and focus the camera	Hi-G Operation	Tested to 100G, 10ms, 6 axis
Triggering	Selectable positive or negative TTL SVP-p or switch closure	Operating Temperature	0 - 40 degrees (32 - 104 degree F)
Timing	Internal clock or external source	Mounting	4 x 1/4-20UNC
I/O	Input: Trigger (TTL/Switch), Sync, Ready, Event, IRIG Output: Trigger, Sync, Ready, Rec, Expose	Dimensions	120mm (4.7")H x 120mm (4.7")W x 90mm (3.6")D
Phase Lock	Enables cameras to be synchronized precisely together or to a master camera or external source.	Weight	1.5 kg (3.4 lbs)
		Power Requirements	100V-240V AC 40W, 50-60Hz DC operation 22-32 VDC, 40VA

Specifications subject to change without notice

PHOTRON USA, INC.
9520 Padgett Street, Suite 110
San Diego, CA 92126-4446
USA
Tel: 858.684.3555 or 800.585.2129
Fax: 858.684.3558
Email: image@photron.com
www.photron.com

PHOTRON (EUROPE) LIMITED
The Barn, Bottom Road
West Wycombe, Bucks, HP14 4BS
United Kingdom
Tel: +44 (0) 1494 481011
Fax: +44 (0) 1494 487011
Email: image@photron.com
www.photron.com

PHOTRON LIMITED
Fujinri 1-1-8
Chiyoda-Ku, Tokyo 102-0071
Japan
Tel: +81 (0) 3 3238 2107
Fax: +81 (0) 3 3238 2109
Email: image@photron.co.jp
www.photron.co.jp

Photron
SLOW MOTION IMAGING SOLUTIONS

Appendix-C. Detail of control program/mechanism

C.1 Injector energizing and camera actuating

Figure A.1 shows schematic diagram of injector energizing duration control and camera operation control mechanism. Arduino software is used to write the program in an ET-EASY328 programmable micro controller. An USB interface is used to connect computer and micro controller to write the programmed code in Arduino software. After finishing the writing of program, the trigger/switch becomes the input device where to connect the injector driver and camera for output signal, a converter is used. The injector which is connected to injector driver is then gets energized.

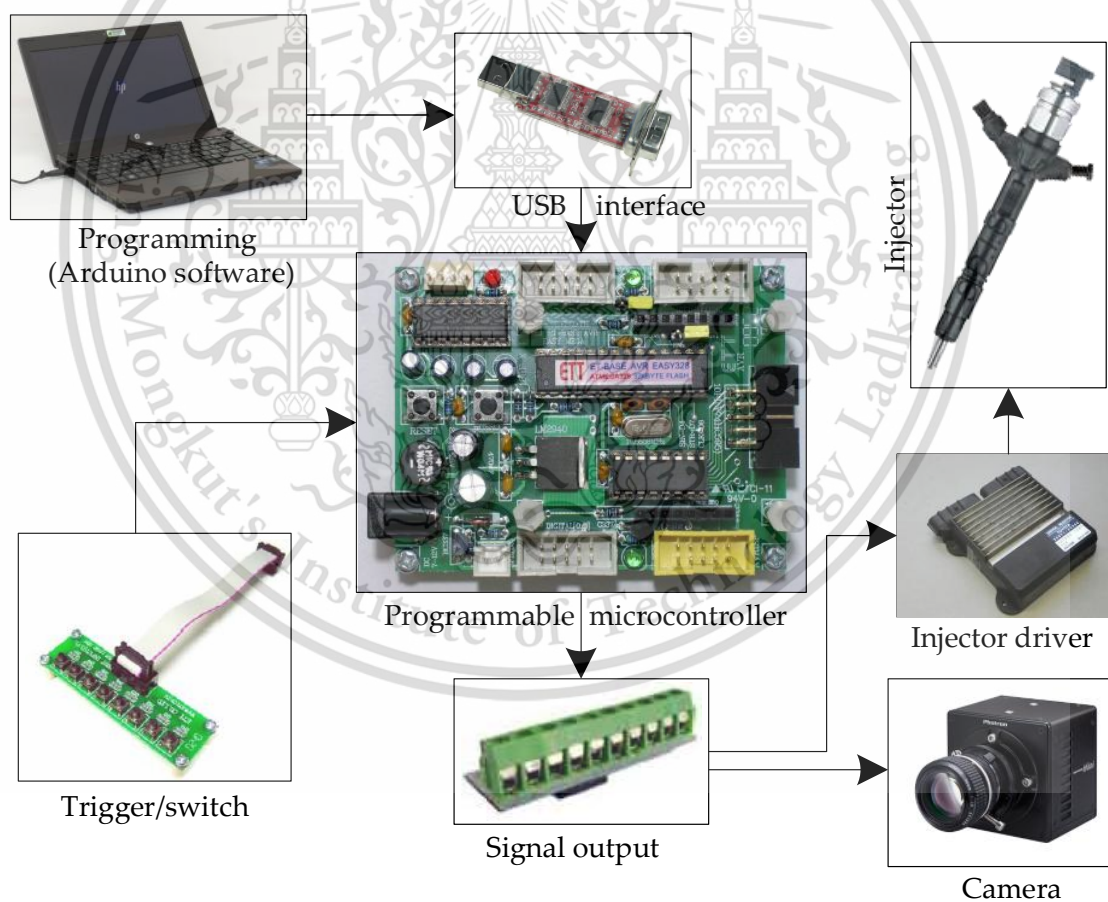


Figure A.1 Schematic of injector energizing and camera actuating mechanism

The graphical representation of concept used to control injector energizing duration and capturing of spray video is shown in Figure A.2 below. To avoid voltage fluctuation, a small time delay was set up initially and then camera has been triggered on then after a small time delay was provided again and injector has been energized as per the injector energizing duration used throughout this experiment.

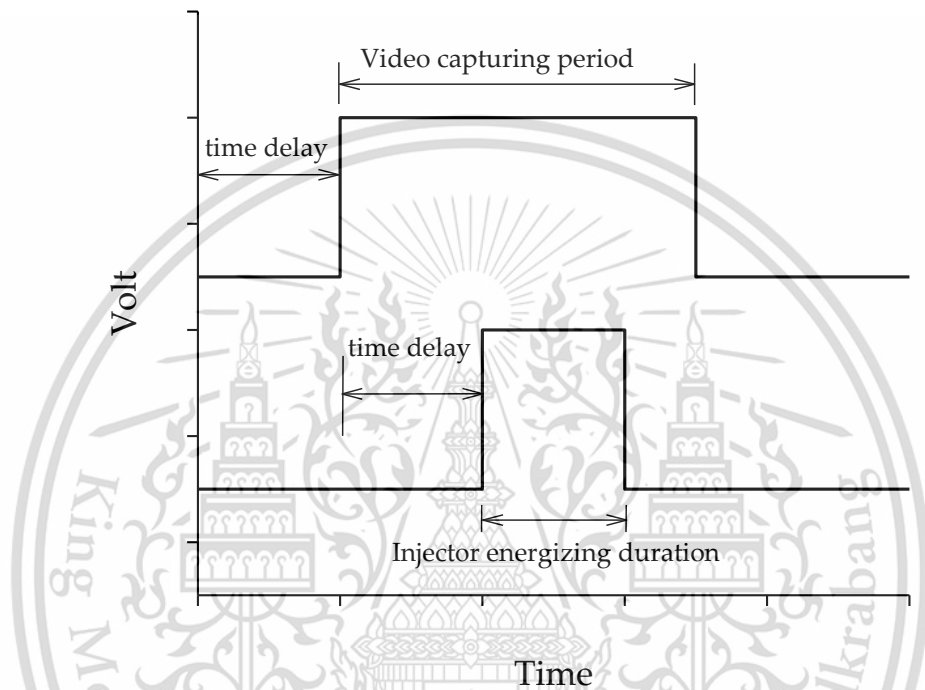


Figure A.2 Graphical representation of injector energizing and video capturing duration

The Arduino code used to control the injector energizing duration and camera actuation is shown below.

```
#define camera 9
#define injector 8
#define swt 0
int sw;
void setup ()
{
  pinMode (swt, INPUT);
  pinMode (camera, OUTPUT);
  pinMode (injector, OUTPUT);
```

This material is reserved for educational use only, not allowed for commercial use.

Forbidden to modify the content, and cite the document when use.

```

}
void loop ()
{
sw=digitalRead (swt);
if(sw==0)
{
Delay(50); // delay in millisecond.//
digitalWrite(camera, HIGH); //camera 9//
delayMicroseconds(3000); // delay in microseconds.//
digitalWrite(camera,LOW);
digitalWrite(injector,HIGH); //injector 8. Begin of injector energizing duration.//
delayMicroseconds(1000); //This time is the injection duration in microsecond.
The injector energizing duration can be change by altering the value given inside the
bracket. In this case the injection energizing duration is 1.0 ms.//
digitalWrite(injector,LOW); //injector 8. End of injector energizing.//
}
Else
{
}
}

```

C.2 Injection pressure controlling

A LabVIEW program is used and interfaced to NI 6221 device. The voltage is supplied to the motor via inverter which is signaled from NI device. The motor is coupled to injection pump using pulley system. The required injection pressure should be typed in front panel of Labview program first, then the inverter adjusts itself to get that pressure and controls the motor speed accordingly. A pressure sensor used in common rail gives feedback to the system about the pressure value then the program use that gives signal to the inverter which then controls the motor speed accordingly. Figure A.3 shows the schematic of injection pressure control mechanism used in this thesis work.

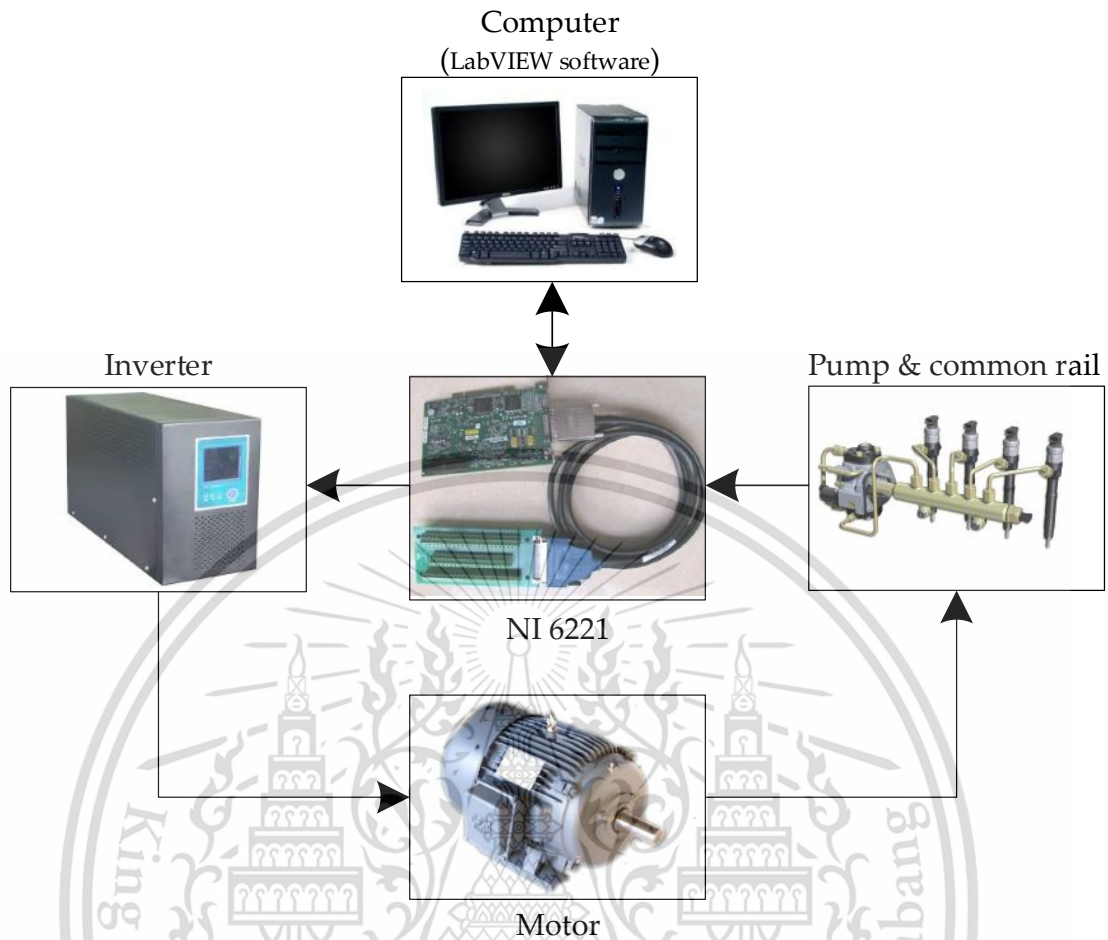
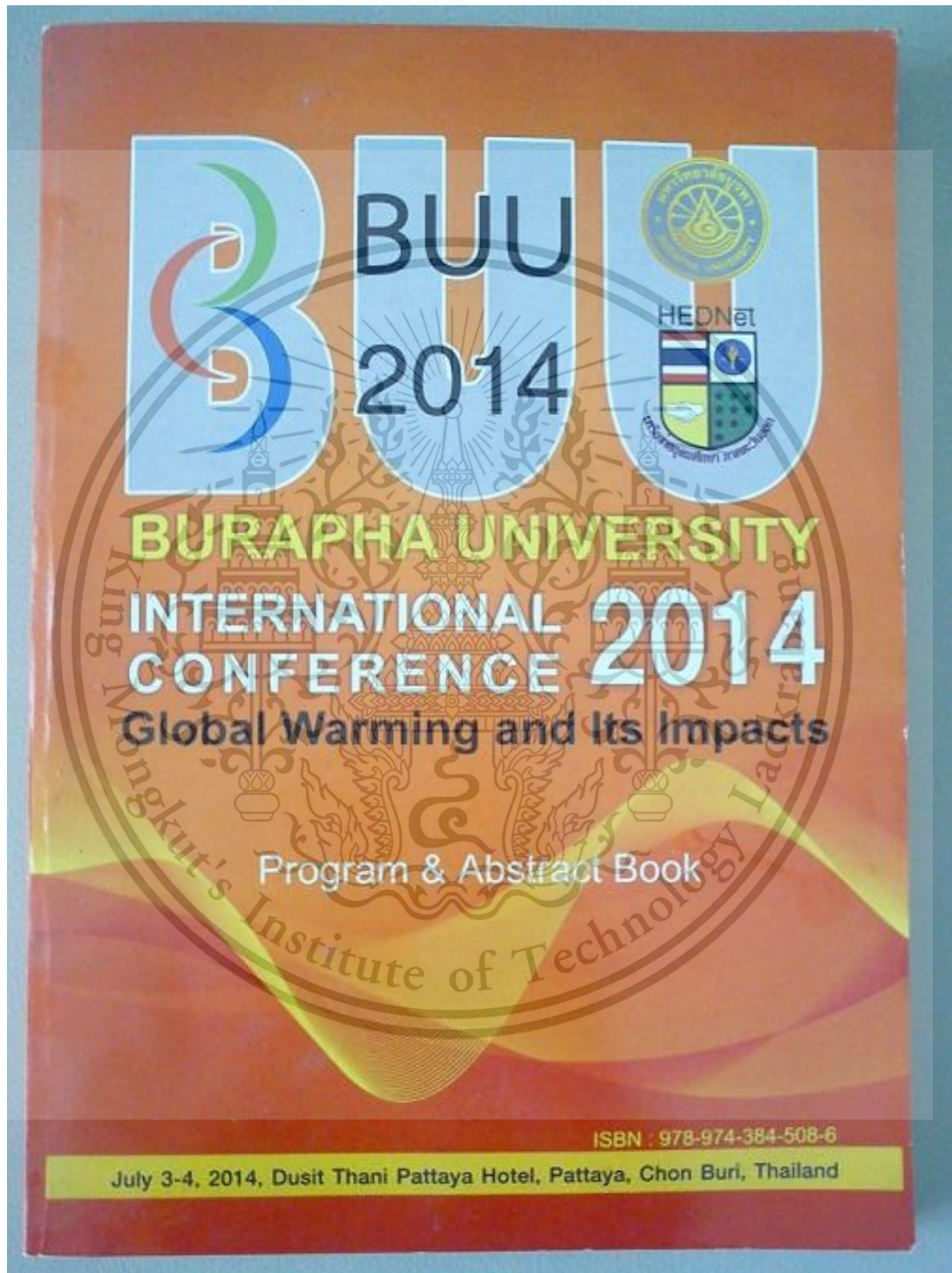


Figure A.3 Injection pressure control mechanism

Appendix-D Proceedings

D.1 Burapha university international conference 2014



This material is reserved for educational use only, not allowed for commercial use.

Forbidden to modify the content, and cite the document when use.

Experimental Study of Physical/Chemical Properties of GTL-Diesel Fuel Blends on Injection Rate

Santosh Paudel¹, Prathan Srichai², Peerawat Saisirirat^{3*}, Preechar Karin¹,
 Chinda Charoenphonphanich², Nuwong Chollacoop³, Hidenori Kosaka⁴

1. *International College, King Mongkut's Institute of Technology Ladkrabang
 Ladkrabang, Bangkok, 10520, Thailand*

2. *Faculty of Engineering, King Mongkut's Institute of Technology Ladkrabang
 Ladkrabang, Bangkok, 10520, Thailand*

3. *National Metal and Materials Technology Center (MTEC), National Science and Technology
 Development Agency (NSTDA), Klong Luang, Pathumthani, 12120, Thailand*

4. *Department of Mechanical and Aerospace Engineering, Tokyo Institute of Technology
 1-44-18 Hayamiya, Nerima-ku, Tokyo, 179-0085, Japan*

E-mail: peerawat.saisirirat@mtec.or.th

ABSTRACT

The Gas to Liquid (GTL) fuel has been taken as promising high quality alternative diesel fuel to mitigate fossils fuel crisis in the near future for diesel engine. In this paper, the fuel physical and chemical properties were analyzed for the GTL/commercial diesel blends. Then, the experimental study has been performed to measure fuel injection rate by using the Zeuch method. Six fuels were tested, e.g. diesel fuel, four GTL-diesel blends: 20% (G20), 40% (G40), 60% (G60), 80% (G80) and pure GTL (G100). The experiment has been carried out using a diesel common rail fuel injection system with a six-hole solenoid injector. The test conditions were ambient temperature initiation, 0.75 ms injection duration, 45 bar back pressure and 605 bar rail pressure. The result showed that all analyzed fuel properties have good linear relationship with the GTL weight fraction. With lower density of 6.86% and higher viscosity of 6.86% than commercial diesel fuel, the GTL has higher injection rate than the commercial diesel fuel.

Keywords: Gas to Liquid (GTL), Injection rate, Zeuch method, Diesel common rail

INTRODUCTION

With higher thermal efficiency, lower specific fuel consumption and lower carbon dioxide (CO₂) emission, the diesel engine have been widely used in light- and heavy-duty vehicle for years. However, the exhaust emission regulations of diesel engine have become stricter in many countries. In recent years, GTL fuel has attracted considerable attention as alternative diesel fuel (Wu et al, 2007). GTL process technology is one promising approach to fulfill energy crisis in the near future. The GTL fuel can be synthesized via Fischer-Tropsch (F-T)

catalytic conversion process using natural gas as feedback. Compared with conventional fossil based diesel fuel, the GTL fuel has attractive fuel properties with high cetane number, high heating value, no sulfur and aromatic contents. Hence, it has some potential to reduce engine exhaust emissions (Tsuji-mura, et al, 2007).

To reduce the exhaust emissions, it is necessary to understand fuel injection characteristics, which play a great role in diesel combustion. To further improve the engine efficiency and reduce the environmental impacts of diesel combustion, the operation of direct injection system is crucial (Tanabe et al, 2005). Many involved processes, e.g. the fuel metering accuracy, the rate of fuel introduction into the combustion chamber, the consequence of spray evolution, fuel atomization and mixing with surrounding air, have determined the combustion development and decided the engine performance with its limited pollutants (Heywood, J.B, 1988).

The physical properties of fuel affect the injection and flow characteristics inside the injector. Density and viscosity are considered as major affecting factors in injection rate and flow characteristics. In addition, the injector geometry, injection pressure, injection duration and operating principle of injector are also major components affecting fuel injection (Dernotte et al, 2012).

In the present study, the fuels chosen were diesel fuel, diesel fuel blended with 20%, 40%, 60% and 80% of GTL and the GTL fuel. The fuel properties were measured according to respective ASTM standard. The effect of GTL and diesel fuel blends on the injection rate was investigated by using Zeuch injection method. Fuel mass flow rate, discharge coefficient, injection delay has been measured using the solenoid diesel injector.

MATERIALS AND METHODS

Zeuch measuring method

In Zeuch's measuring method, the fuel is injected into a chamber filled with tested fuel at a certain pressure. As the mass of fuel in the chamber increases due to the injected fuel, the chamber pressure increases in proportion to the injected mass. Through the fuel bulk modulus of elasticity, the derivative of the chamber pressure with respect to volume provides the injection rate signal. The fuel bulk modulus of elasticity is

$$K = V \frac{dp}{dv} \quad (1)$$

Where, K is the fuel bulk modulus of elasticity, V the chamber volume, p the pressure inside chamber. From the definition, bulk modulus of elasticity is the differential change in pressure due to a finite volume of injected fuel multiplied by the initial chamber volume. The Zeuch injection rate measuring method is derived based on the conservation of mass. By inserting the fuel bulk modulus in time derivative of mass, the equation becomes

$$\frac{dm}{dt} = \rho \frac{V}{K} \frac{dp}{dt} \quad (2)$$

Here, m is the mass of fuel and ρ is the fuel density.

Experimental setup

The schematic diagram of experimental apparatus is shown in Figure 1. In this work, a cubic Zeuch chamber (1) of 40 cc capacity was used, in which a six-hole solenoid diesel injector (2) with 0.14 mm injection diameter was installed inside the chamber to inject the test fuel. In order to provide back pressure, the chamber was filled with the test fuel by a hand pump (5). The static pressure sensor (3) and dynamic pressure sensor (4) were installed to measure back pressure and dynamic chamber pressure, respectively, which were then recorded by a data acquisition system (16). For fuel system, the high pressure pump was driven by three-phase electric motor controlled by an inverter. The pressure was kept constant by controlling the electric motor revolution. The injection duration and trigger time was controlled by a programmable microcontroller (12), which then actuated the EDU (14) to inject fuel into the test chamber. To measure the bulk modulus, high pressure nitrogen was used to push a pneumatic cylinder (6) located with a dial gauge to measure the displacement volume.

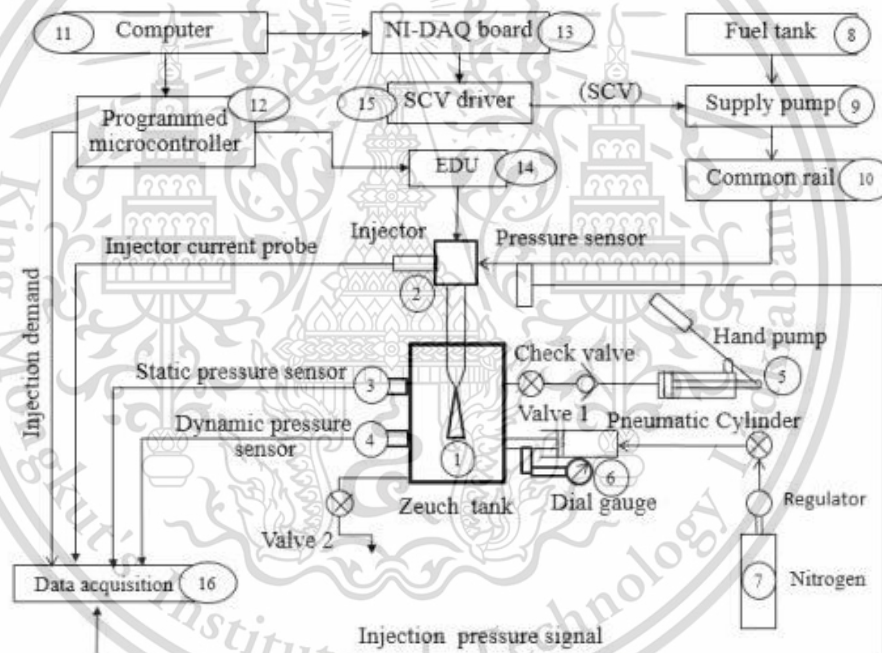


Fig. 1 Schematic diagram of experimental setup

The experimental test condition and fuel properties of neat GTL and diesel fuel are shown in Table 1 and Table 2, respectively.

Table 1. Experimental test condition

Variables	Test conditions
Test fuel	Diesel, G20, G40, G60, G80, G100
Back pressure	45 bar
Injection duration	0.75 ms
Rail pressure	605 bar

Table 2. Fuel properties

Fuel analysis	GTL	Diesel	Unit	Test standard
Heating value	47.3	45.13	MJ/kg	ASTM D240
Density @15 ⁰ C	785.1	837.2	kg/m ³	ASTM D4052
Flash point	102.5	65	⁰ C	ASTM D93
Pour point	-1.6	-11.2	⁰ C	ASTM D5951
Kinematic Viscosity	3.433	3.205	mm ² /s	ASTM D445
Copper corrosion	1a	1a	-	ASTM D130
Cloud point	4.1	7.8	⁰ C	ASTM 5773

Injection rate analysis

In this calculation, the measured mass of injected fuel, m_{measured} , was calculated from the area covered by the injection rate curve. The discharge coefficient C_d is a ratio between measured mass of injected fuel and the theoretical injected mass, m_{th} .

$$C_d = \frac{m_{\text{measured}}}{m_{\text{th}}} \quad (3)$$

The theoretical mass of injected fuel, m_{th} , was calculated from a combination of continuity equation.

$$m_{\text{th}} = n_{\text{orifice}} \cdot A \cdot \sqrt{2 \cdot \Delta P \cdot \rho} \quad (4)$$

Where n_{orifice} is the number of orifices, A the cross-sectional area, ΔP the pressure difference (injection pressure - back pressure), and ρ the fuel density at operating temperature.

RESULTS

GTL-diesel blends fuel properties

With increasing GTL fraction, density of the mixtures decreases proportionally, as shown in Figure 2(a). From Figure 2(b), it can be seen that the heating value increases with GTL fraction. The blended fuel properties are in accordance with pure fuel properties that the density of pure GTL is 6.86% lower and its heating value is 4.58% higher than that of diesel fuel. The reason of lower density of GTL is due to presence of low densities paraffinic hydrocarbons as its major constituents.

From Figure 2(c)-(d), the results show that with increasing GTL blended fraction, the kinematic viscosity increases but the bulk modulus decreases. Compare to diesel fuel properties, the kinematic viscosity of GTL fuel is 6.64% higher and bulk modulus is 16.66% lower than the diesel fuel, in the test condition of ambient temperature, 45 bar of chamber pressure.

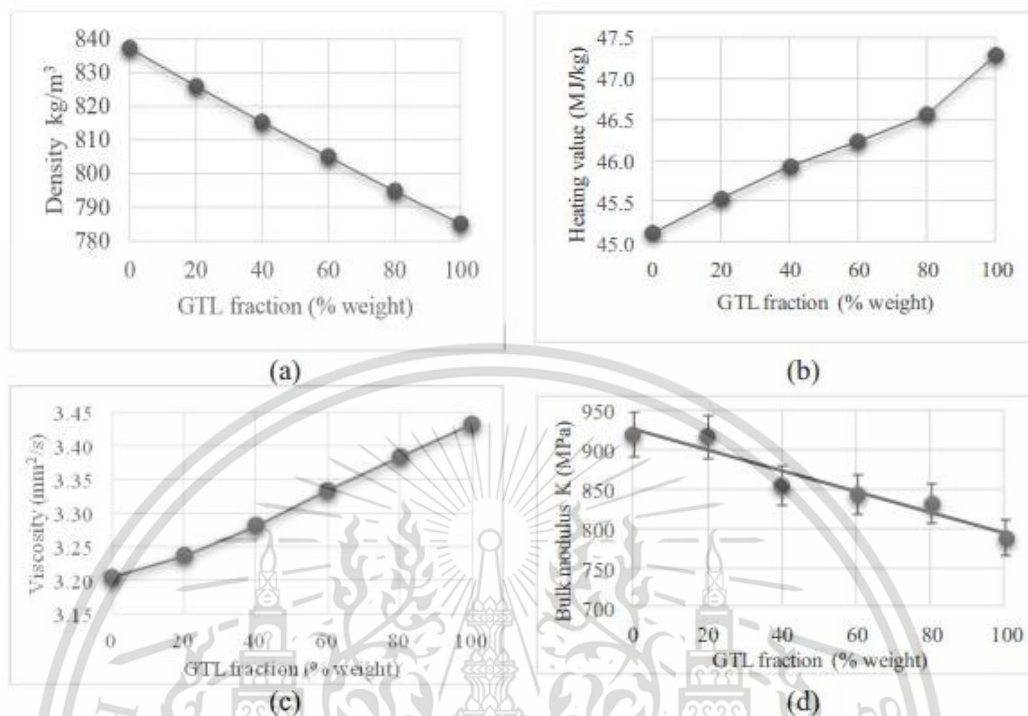


Fig. 2 Effects of GTL fraction on (a) density, (b) heating value, (c) viscosity and (d) bulk modulus

Injection rate

Figure 3 shows the observed injected rate, calculated from Eq. 2. The test fuel is injected with the same actuated commands through the programmed microcontroller. With different fuel properties (e.g. density, viscosity and bulk modulus) varied by GTL fraction, the injection rate profile changes proportionally. It can be seen that the injection rate initiates faster but ends slower when the GTL fraction increases. In other words, the results show that with increasing GTL fraction, the injection rate increases proportionally.

The results of discharge coefficient calculated from Eq. 3 are shown in Figure 4(a). It can be seen that the diesel fuel exhibits lowest discharge coefficient at the test condition; whereas, the discharge coefficient increases proportionally to the GTL blended fraction. Figure 4(b) shows the comparison of injection delay time after the programmed microcontroller actuated. It is the time lag between start of ignition signal to the start of injection, which can be seen from injection profile curve. Hence, injection delay are reduced with GTL blended fraction.

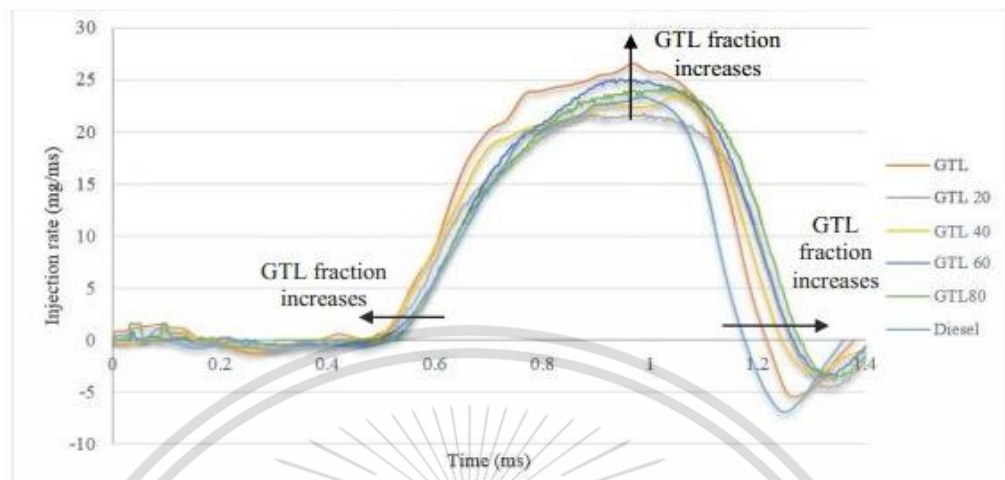


Fig. 3 Comparison of injection rate between GTL blends fuel,
 $P_{inj}=605\text{bar}$, $P_{back}=45\text{bar}$, $T_{inj}=0.75\text{ms}$



Fig. 4. Effects of GTL fraction on (a) Discharge coefficient
 and (b) Injection delay at $P_{inj}=605\text{bar}$, $P_{back}=45\text{bar}$, $T_{inj}=0.75\text{ms}$

CONCLUSION

In this work, the fuel properties of GTL-diesel blends have been analyzed, and the experimental investigation on injection rate has been done by using the Zeuch method. For six different fuels, injection rate analysis was done in terms of injection rate profile, discharge coefficient and injection delay time. Increasing of GTL blended fraction increases viscosity, heating value and discharge coefficient; whereas, density, injection delay time and bulk modulus are decreased. The result shows low density GTL fuel has higher measured mass flow rate from high density diesel fuel. Thus, it can be concluded that density is not only parameter to affect mass flow. Rather, the injector type and operation principle also have effects on injection quantity.

ACKNOWLEDGEMENT

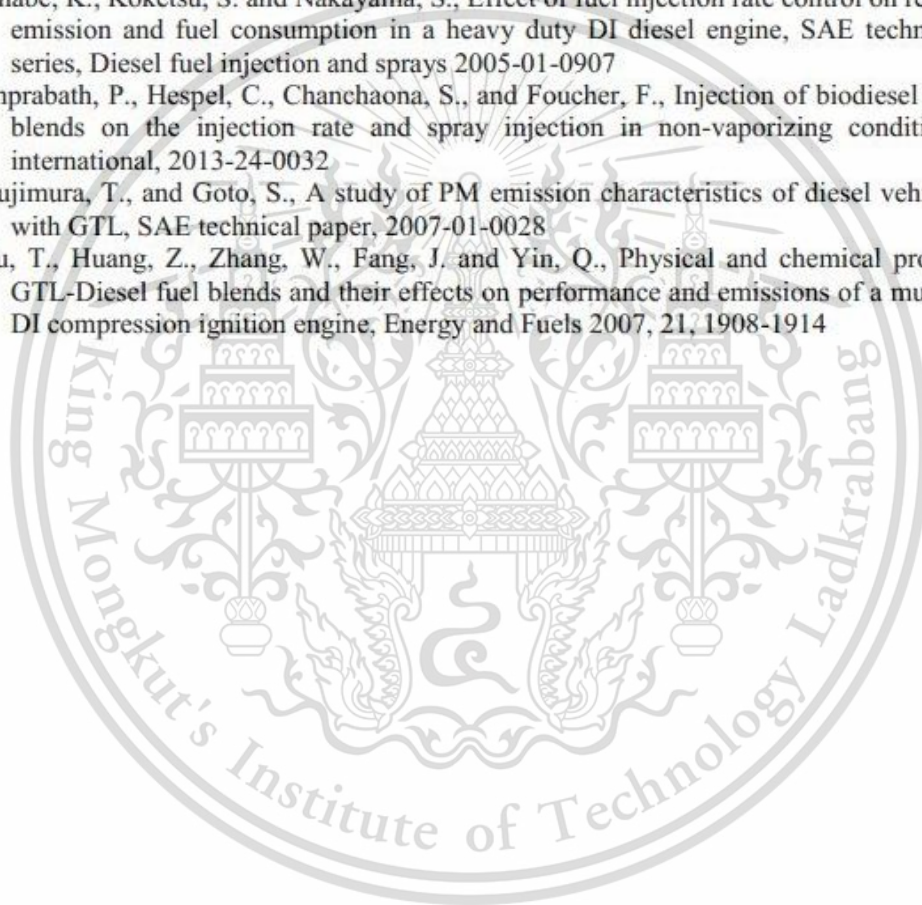
The authors would like to thank TAIST (Thailand Advanced Institute of Science and Technology) Tokyo Tech Program, Combustion and Engine Research Laboratory, King

Burapha University International Conference 2014
Burapha University, Thailand
July 3-4, 2014

Mongkut's University of Technology Thonburi (KMUTT) and National Metal and Material Technology Center (MTEC) for providing financial and technical supports to conduct this work.

REFERENCES

- Dernotte, J., Hespel, C., Foucher, F., Houille, S., and Mounaim-Rousselle, C., Influence of physical fuel properties on injection rate on a diesel injector, *Fuel* 96 (2012), 153-160
- Heywood, J.B., *Internal combustion engine fundamentals*, McGraw hill international editions 1988, 621.43 87-15251
- Tanabe, K., Koketsu, S. and Nakayama, S., Effect of fuel injection rate control on reduction of emission and fuel consumption in a heavy duty DI diesel engine, SAE technical paper series, Diesel fuel injection and sprays 2005-01-0907
- Tinprabath, P., Hespel, C., Chanchaona, S., and Foucher, F., Injection of biodiesel and diesel blends on the injection rate and spray injection in non-vaporizing conditions, SAE international, 2013-24-0032
- Tsujimura, T., and Goto, S., A study of PM emission characteristics of diesel vehicle fueled with GTL, SAE technical paper, 2007-01-0028
- Wu, T., Huang, Z., Zhang, W., Fang, J. and Yin, Q., Physical and chemical properties of GTL-Diesel fuel blends and their effects on performance and emissions of a multicylinder DI compression ignition engine, *Energy and Fuels* 2007, 21, 1908-1914



D.2 International conference on science, technology and innovation for sustainable well-being



This material is reserved for educational use only, not allowed for commercial use.

Forbidden to modify the content, and cite the document when use.



หนังสือรับรองการตีพิมพ์บทความ

วารสาร มทร.อีสาน

ขอรับรองว่าบทความวิจัย

เรื่อง Spray Visualization of GTL-Diesel Fuel Blends in High Pressure Chamber

โดย Santosh Paudel, Prathan Srichai, Peerawat Saisirirat, Chinda Charoenphonphanich, Preechar Karin, Nuwong Chollacoop and Hidenori Kosaka

ได้ผ่านการประเมินจากคณะกรรมการผู้ทรงคุณวุฒิ

และตีพิมพ์ใน RMUTI Journal Special Issue 1 2015

The 6th International Conference on Science, Technology and Innovation for Sustainable Well-Being (STISWB VI)

(นางสาวอุบล สุริพล)

บรรณาธิการ วารสาร มทร.อีสาน

มหาวิทยาลัยเทคโนโลยีพระจอมเกล้าอีสาน



The 6th International Conference on Science, Technology and Innovation for Sustainable Well-Being (STISWB VI 2014)
August 28-30 2014, Apsara Angkor Resort & Conference,
Siem Reap, Kingdom of Cambodia

Spray Visualization of GTL-Diesel Fuel Blends in High Pressure Chamber

Santosh Paudel^{1*}, Prathan Srichai², Peerawat Saisirirat³,
Chinda Charoenphonphanich², Preechar Karin¹, Nuwong Chollacoop³ and
Hidenori Kosaka⁴

¹ International College, ² Faculty of Engineering,
King Mongkut's Institute of Technology Ladkrabang, Bangkok, Thailand, 10520

³ National Metal and Materials Technology Center (MTEC),
National Science and Technology Development Agency (NSTDA),
Pathumthani, Thailand, 12120

⁴ Department of Mechanical and Aerospace Engineering,
Tokyo Institute of Technology, Tokyo, Japan 179-0085

*Corresponding Author: santospaudel@gmail.com, +66 (0)89-373-5257

Abstract

Gas to Liquid (GTL) fuel has been taken as an alternative clean diesel fuel with promising fuel properties. It has high cetane rating, low aromatic and sulfur contents compared to conventional diesel fuels. To meet the stringent emission rules developed in recent years, it is essential to have a notion of fuel injection behaviors e.g., the spray evolution, fuel atomization and mixing inside the combustion chamber for combustion process optimization. In this work, the effects of injection pressure and the blended fractions of GTL fuel on fuel spray pattern in terms of spray penetration, spray angle and spray velocity have been investigated. Six different fuels (commercial diesel fuel, various blends of GTL-diesel as GTL20, GTL40, GTL60, GTL80 and pure GTL100) were chosen. The experiment has been carried out using a common rail system with a solenoid operated injector with injection pressure of 400 and 1,600 bar. The ambient pressure inside the chamber was maintained at 45 bar, and injection duration was 1ms. The series of fuel jet images were captured by shadowgraph photography technique using a high speed camera with 10,000 frames per second. The result showed that the spray penetration is higher at higher injection pressure for all fuel types. In addition, the GTL blended fuels show shorter spray penetration and larger spray angle with increasing of fraction of GTL fuels, during the beginning phase of fuel injection duration.

Keywords: Gas to Liquid, Shadowgraph photography technique, Spray characteristics

1. Introduction

Due to high fuel efficiency of compression-ignition engine and high energy density and transportability of liquid fossils fuel, diesel became attractive power source for industrial and commercial purposes. However, the diesel engine emits large amount of NOx and particular matter despite the fact that the emission regulation is being

stricter in many countries. Furthermore, fossil fuel reserves are being depleted due increasing of energy demands. Alternative fuels with properties defined for diesel engine must be utilized to meet both emission regulation and dependency on fossil fuels [1, 2]. The Gas to Liquid (GTL) fuels, which are synthesized from natural gas by means of Fischer-Tropsch process, can play a

promising role as clean alternative fuel. GTL fuel has several beneficial properties as an alternative fuel compared to conventional fossils diesel including high cetane rating, low sulfur content, negligible amount of aromatics and high hydrogen-carbon ratio [3, 4].

The physical and chemical properties of fuel, such as density, viscosity, surface tension, heating value, distillation temperature, strongly affect fuel injection process and spray characteristics in the diesel engine. The fuel spray plays a very important role in diesel engine process since it is concerned with fuel atomization, air-fuel mixing, ignition process, combustion and subsequent emission. Thus, since GTL fuel has some different fuel properties as compared to conventional diesel fuel, it is necessary to investigate spray characteristics of GTL fuel [5-7].

In this paper, the comparative study of spray characteristics between GTL-diesel fuels blends (GTL100, GTL80, GTL60, GTL40, GTL20, and diesel) in terms of spray penetration, spray angle and spray velocity are presented for injection pressure of 400 bar and 1,600 bar.

2. Material and Methods

2.1 Experimental setup

In this experiment, the constant volume chamber has a cylindrical shape of 80 mm diameter with observation window. To visualize spray characteristics, quartz disc, being transparent and high strength, were used as optical accessible windows to both sides of the chamber. The spray images were captured according to the shadowgraph photography technique. The single hole solenoid type injector with injector diameter of 0.14 mm was installed to supply fuel to the high pressure chamber. Series of image were captured using HSV (high speed video) camera at captured rate of 10,000 frames per second with resolution of 640x480 pixel and 1/64,000 sec shutter speed.

The schematic diagram of experimental setup is shown in Fig 1, consisting four major systems as follows. First is the high pressure chamber, in which nitrogen is supplied

through a nitrogen cylinder fitted with pressure gauge and regulator to maintain required ambient pressure. Second is the fuel system, where a feed pump is used to deliver test fuel to the high pressure pump. The high pressure pump, which is coupled with 5hp motor and 3 phase inverter, was used to control rotational speed of motor. Third is the DAQ National Instrument model NI-6221 with LabVIEW, which were used to control constant rail pressure by PID control with closed loop from rail pressure sensor and a limit of rail pressure by suction control valve (SCV). The injection duration and trigger timing were controlled by a programmable microcontroller, which then actuates injector driver to inject fuel to the high pressure chamber and turns on high speed video (HSV) camera. Fourth is the high speed video camera, Photorn FASTCAM Mini UX100, which was used to capture the spray characteristics with shadowgraph imaging method.

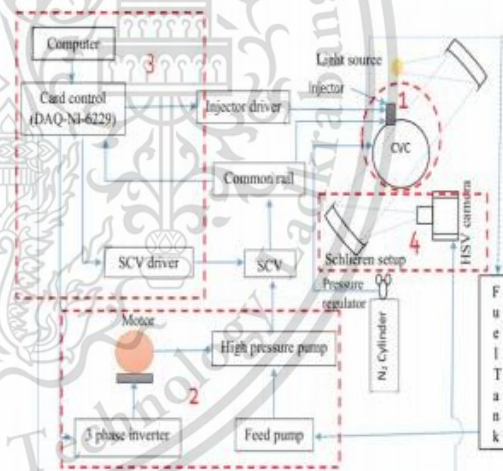


Fig. 1 Schematic of experimental setup

2.2 Test fuel

In this work GTL (labeled GTL100) and diesel were blended in various proportions. Blends of these two fuels, GTL20, GTL40, GTL60 and GTL80, represent GTL fractions of 20%, 40%, 60% and 80% by weight. Fuel properties of neat GTL and diesel fuels with respective test methods used is shown in Table 1.



Table 1. Test fuel properties

Properties	Method	GTL	Diesel
Heating value (MJ/kg)	ASTM D240	47.3	45.1
Density@15°C (kg/m ³)	ASTM D4052	785.1	837.2
Kinematic viscosity (mm ² /s)	ASTM D445	3.433	3.205
Surface tension (mN/m)	ASTM D1590	23.3	28.7

2.3 Experimental condition

Experimental condition for this work is shown in Table 2.

Table 2. Experimental test condition

Experimental variables	Test conditions
Test fuels	Diesel, GTL20, GTL40, GTL60, GTL80, GTL100
Back pressure	45 bar
Injection duration	1 ms
Rail pressure	400 bar and 1,600 bar

2.4 Spray image analysis

Raw images were analyzed using a digital image processing program to determine spray tip penetration and spray angle. The spray penetration (S) is defined as a distance of

spray tip from the injector tip in axial direction; whereas, spray angle is defined as maximum angle in each side of spray at a distance $S/2$ from the injector tip. Spray velocity is calculated from spray penetration in each frame divided by time [8]. The specific code in MATLAB is used to measure spray penetration and spray angle in each image by following the definition. In this work, the experimental results were averaged from three repeated tests.

3. Result and Discussion

The raw shadowgraph images of neat GTL and diesel are shown in Fig. 2 at various stages after the start of injection.

3.1 Spray characteristics at injection pressure of 400 bar

3.1.1 Spray penetration

Figure 3(a) shows the spray penetration of all experimented fuels at same test condition with 400 bar injection pressure, 45 bar back pressure and 1 ms injection duration. Result shows that diesel has longer spray penetration than GTL. At initial phase of injection, there is no significant difference in penetration length for all fuels. Between 0.2 and 0.8 ms after start of injection, as shown in Fig. 3(b), it can be seen that diesel has longer penetration than GTL due to higher density of diesel fuel [9]. Increase in

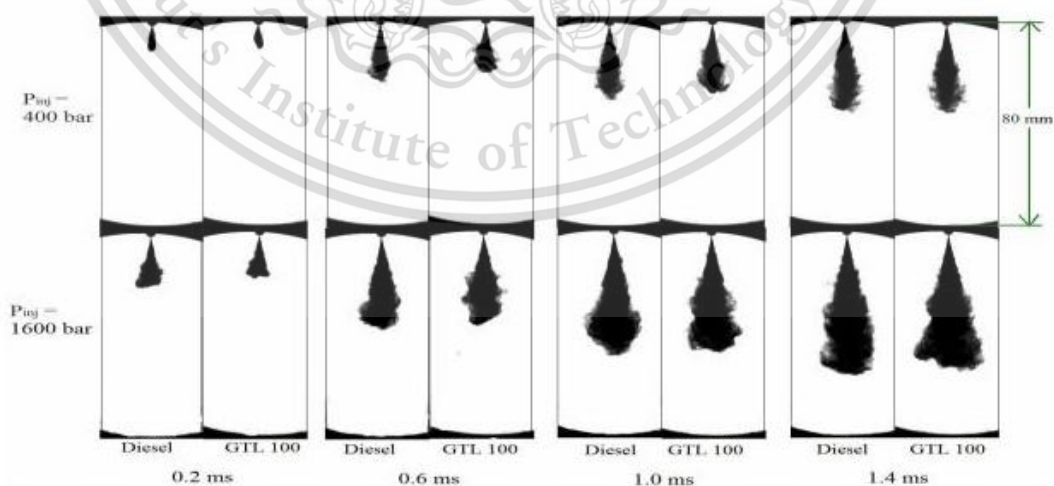


Fig. 2 Raw images of GTL100 and diesel spray at different time (ms) after start of injection ($P_{back}=45$ bar, $T_{inj}=1$ ms)

GTL fraction in blended fuel leads decreasing in penetration length; while at later stage of injection period, the penetration is quite same for all kind of fuels. In previous study, Azimov et al also presented longer penetration for diesel than GTL for identical test condition [10]. The most probable reason is that at the lower injection pressure, back pressure dominate after injection stop causing momentum lost leading to shorter penetration.

3.1.2 Spray angle

Figure 3(c) shows the spray angle for all tested fuels. The tested data are displayed by scatter dots with two points moving average line superimposed. It can be seen that initially all fuels have almost same angle value. The spray angle for diesel fuel decreased rapidly at the beginning and reaches constant after a while; whereas, GTL has higher spray angle at initial stage and lower at later stage. Similar results were observed by Guohong Gong [9].

3.1.3 Spray velocity

Figure 3(d) shows spray velocity of all tested fuels with injection pressure of 400 bar. The test result shows spray velocity is higher initially and reduces with time. For better combustion and atomization, higher velocity is preferred in real combustion [11].

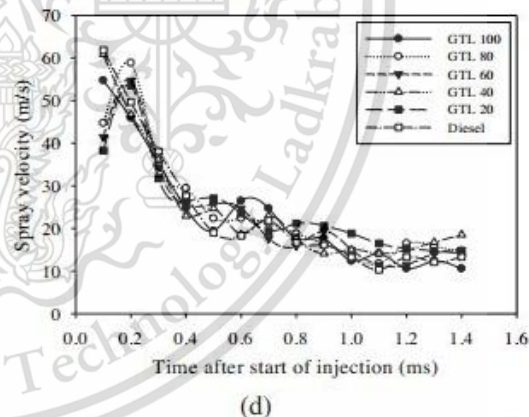
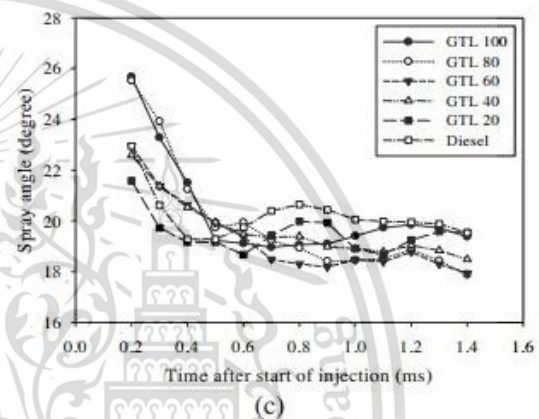
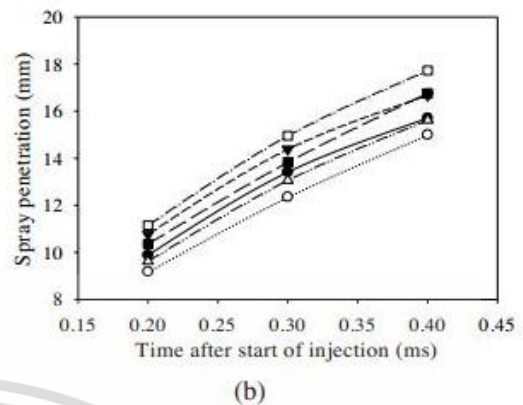
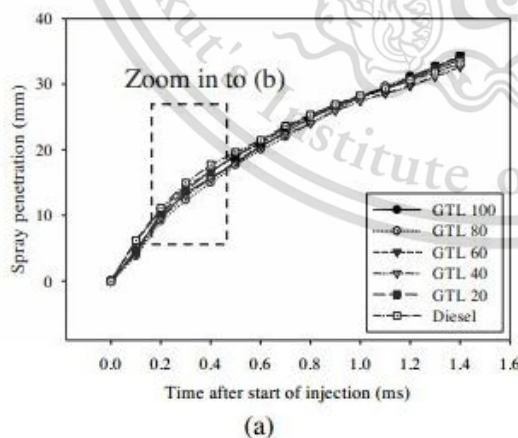


Fig. 3 (a) spray penetration, (b) zoom-in of (a), (c) spray angle and (d) spray velocity at $P_{inj}=400$ bar, $T_{inj} = 1$ ms and $P_{back} =45$ bar

3.2 Spray characteristics at injection pressure of 1,600 bar

3.2.1 Spray penetration

The increase in injection pressure results higher mass flow rate. Figures 4(a) and 4(b) show spray penetration of all test fuels at 1,600 bar injection pressure under same back

pressure of 45 bar and injection duration of 1 ms. From the effect of injection pressure as compared between Fig 3(a) and Fig 4(a), when rail pressure increased from 400 to 1,600 bar, the spray penetration is longer due to increase in fuel quantity, which is in accordance with Shervani-Tabar et al [12]. At higher injection pressure, diesel has higher penetration than other type of fuel blends. The difference is quite clear for longer spray penetration of diesel fuel at long time after start of injection.

3.2.2 Spray angle

Figure 4(c) shows the spray angle of all tested fuels with 1,600 bar injection pressure. The result shows that the higher the injection pressure, the larger the spray angle. For better combustion, larger spray angle is preferred. In this experiment, the result shows the spray angle drops at initial stage and regains quickly. According to fuel type, GTL80 shows better spray angle throughout the period of investigation.

3.2.3 Spray velocity

Figure 4(d) shows the spray velocity of all test fuels. Purpose of velocity measurement was to find possible differences between compared fuels. In this case, spray velocity is higher as the injection pressure increased from 400 to 1600 bar. For higher injection pressure, the spray velocities for all fuel types are nearly same. GTL80 and GTL60 shows better spray velocity.

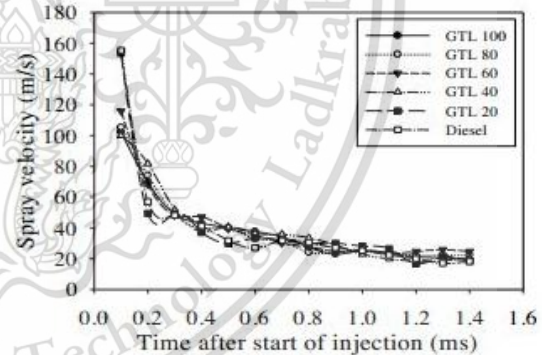
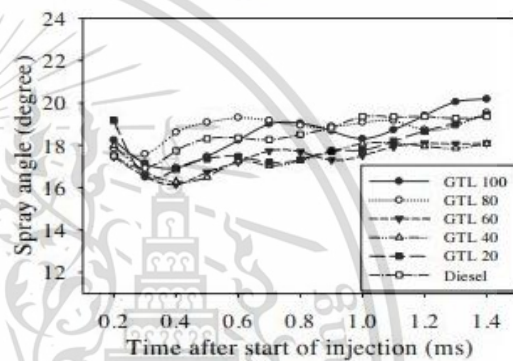
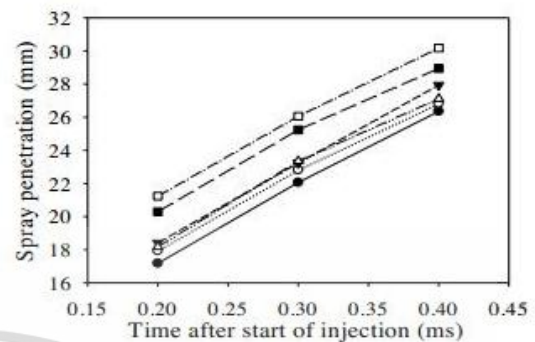
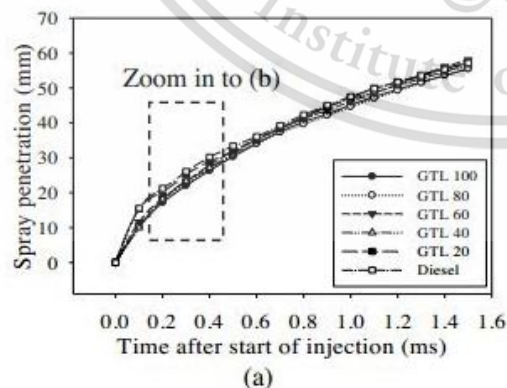


Fig. 4 (a) spray penetration, (b) zoom-in of (a), (c) spray angle and (d) spray velocity at $P_{inj}=1600$ bar, $T_{inj}=1$ ms and $P_{back}=45$ bar.

4. Conclusion

In this paper, fuel spray characteristics between GTL-diesel blended fuels were compared in terms of spray penetration, spray angle and spray velocity under same back pressure and injection pressures under same back pressure and injection duration. The following conclusions were drawn.

- a) For the same test condition, diesel fuel has higher spray penetration than GTL fuel due to higher density. Increasing in GTL fraction in blended fuel shortens the spray penetration.
- b) Spray angle is characterized because larger spray angle is preferred for better combustion efficiency. The result at lower injection pressure shows higher spray angle with increasing GTL fraction in blended fuels at early stages up to 0.7 ms. While at higher injection pressure, difference in spray angle could not be clearly seen throughout the investigated period. GTL blends with diesel shows improvement in spray angle.
- c) Spray velocity is mostly dependent on injection pressure. Initially, GTL has higher spray velocity. The spray velocity difference between different fuels could not be clearly differentiated at the end.

5. Acknowledgement

The author would like to thank Thailand Advanced Institute of Science and Technology and Tokyo Institute of Technology (TAIST-Tokyo Tech) for providing full scholarship, National Metal and Materials Technology center (MTEC) for funding the research work and providing test fuel and Hi-Tech resource for providing hi speed video camera.

6. References

- [1] Li, Y., Tian, G., Zhang, J., Xu, H. Comparative Experimental Study on Microscopic Spray Characteristics of RME, GTL and Diesel. SAE Technical Paper, 2010.
- [2] Chen, P.-C., Wang, W.-C., Roberts, W.L., Fang, T. Spray and atomization of diesel fuel and its alternatives from a single-hole injector using a common rail fuel injection system. *Fuel*. 2013, 103, 850-61.
- [3] Bezergianni, S., Dimitriadis, A. Comparison between different types of renewable diesel. *Renewable and Sustainable Energy Reviews*. 2013, 21, 110-6.
- [4] Sajjad, H., Masjuki, H.H., Varman, M., Kalam, M.A., Arbab, M.I., Imtenan, S., et al. Engine combustion, performance and emission characteristics of gas to liquid (GTL) fuels and its blends with diesel and bio-diesel. *Renewable and Sustainable Energy Reviews*. 2014, 30, 961-86.
- [5] Heywood, J.B. *Internal Combustion Engine Fundamentals*, McGraw-Hill, 1988.
- [6] Tanabe, K., Kohketsu, S., Nakayama, S. Effect of Fuel Injection Rate Control on Reduction of Emissions and Fuel Consumption in a Heavy Duty DI Diesel Engine. SAE Technical Paper, 2005.
- [7] Tinprabath, P., Hespel, C., Chanchaona, S., Foucher, F. Influence of Biodiesel and Diesel Fuel Blends on the Injection Rate and Spray Injection in Non-Vaporizing Conditions. SAE Technical Paper, 2013.
- [8] Dernothe, J., Hespel, C., Houille, S., Foucher, F., Mounaim-Rousselle, C. Influence of Fuel Properties on the Diesel Injection Process in Nonvaporizing Conditions. 2012, 22, 461-92.
- [9] Guohong, G., Chonglin, S., Lidong, L. Spray characteristics of diesel fuel, Fishch-Tropsch diesel fuel and their blend. In: *Electrical and Control Engineering (ICECE)*, 2011 International Conference on, 2011, pp. 4079-82.
- [10] Azimov, U.B., Kim, K.S., Jeong, D.S., Lee, Y.G. Instantaneous 2-D visualization of spray combustion and flame luminosity of GTL and GTL-biodiesel fuel blend under quiescent ambient conditions. *Int.J Automot. Technol.* 2011, 12, 159-71.
- [11] Hulkkonen, T., Hillamo, H., Sarjoavaara, T., Larimi, M. Spray Studies and Diesel Fuel Comparasion In: *Swedish-Finnish Flame Days 2011*, The Swedish and Finnish National Committees of the International Flame Research Foundation, Piteå, Sweden, 2011.
- [12] Shervani-Tabar, M.T., Sheykhvazayefi, M., Ghorbani, M. Numerical study on the effect of the injection pressure on spray penetration length. *Applied Mathematical Modelling*. 2013, 37, 7778-88.

BIOGRAPHY

Name: Santosh Paudel
Nationality: Nepalese
Date of Birth: 20th December 1987
Address: Dhikurpokhari-5, Kaski, Nepal
Marital Status: Single

Education Background

Secondary School: Shree Ne. Ra. Ma. Vi. Sapahi, Bara, Nepal (2003)
10+2: Faculty – Science
 Janapriya Multiple Campus, Pokhara, Kaski, Nepal (2005)
Undergraduate: Faculty- Mechanical Engineering
 Kathmandu University, Dhulikhel, Kavre, Nepal (2009)
Master’s Degree: TAIST-Tokyo Tech
 (International College, KMITL,) Bangkok, Thailand
 (2015)

Proceedings:

1. **Paudel S.,** Srichai P., Saisirirat P., Karin P., Charoenphonphanich C., Chollacoop N., and Kosaka H., “Spray Visualization of GTL -Diesel Fuel blends in High Pressure Chamber”, RMUTI journal special issue I, 2015
2. **Paudel S.,** Srichai P., Saisirirat P., Karin P., Charoenphonphanich C., Chollacoop N., and Kosaka H, “Experimental Study of Physical/Chemical Properties of GTL -Diesel Fuel Blends on Injection Rate”, Burapha University International Conference 2014, July 3-4, 2014, Thailand